EVALUATION OF EMISSION UNCERTAINTIES AND THEIR IMPACTS ON AIR QUALITY MODELING: APPLICATIONS TO BIOMASS BURNING

A Dissertation
Presented to
The Academic Faculty

by

Di Tian

In Partial Fulfillment
of the Requirements for the Degree
Doctor of Philosophy in the
School of Civil and Environmental Engineering

Georgia Institute of Technology
December 2006

EVALUATION OF EMISSION UNCERTAINTIES AND THEIR IMPACT ON AIR QUALITY MODELING: APPLICATION TO BIOMASS BURNING

Approved by:

Dr. Armistead G Russell, Advisor
School of Civil and Environmental Engineering
Georgia Institute of Technology

Dr. Michael Chang
School of Earth and Atmospheric Science
Georgia Institute of Technology

Dr. James A. Mulholland
School of Civil and Environmental Engineering
Georgia Institute of Technology

Dr. Yuhang Wang
School of Earth and Atmospheric Science
Georgia Institute of Technology

Dr. Randall L. Guensler
School of Civil and Environmental Engineering
Georgia Institute of Technology

Date Approved: October 6, 2006

To my husband and family

ACKNOWLEDGEMENTS

I really appreciate enormous support from many individuals during my Ph.D. studies. Professor Ted Russell, my advisor, has continuously imparted knowledge, provided insightful guidance and support. My groupmates and other members in Environmental Engineering program at Tech – Dr. Yongtao Hu, Dr. Daniel Cohan, Sergey Napelenok, Jaemeen Baek, Helena Park, Yan Bo, K.J. Liao, Evan Cobb, Dr. Talat Odman, Michelle Bergin, Dr. Amir Hakami, Dr. Jim Wilkinson, Sangil Lee, Santosh Chandru, Burcak Kaynak, and others - have greatly helped my research and made my experience at Tech a memorable journey. James Boylan, Amit Marmur, and Maudood Khan, both former groupmates and current colleagues at the Georgia Environmental Protection Division presented tremendous support during the critical period of finishing my thesis. I also thank my thesis committee members, Professors Yuhang Wang, Michael Chang, James Mulholland and Randall Guensler, for their efforts, suggestions and support. Special thanks also go to Alan Dozier, Dan Chan, Neal Edmonson and Jim Paul of Georgia Forestry Commission, Tom Pace of U.S. Environmental Protection Agency, Ms. Elisabeth Reinhardt, Mr. Bruce Bayle, Mr. Dale Wade (retired), Dr. Roger Ottmar and Dr. Yongqiang Liu of U.S. Department of Agriculture Forest service for their valuable discussion. Above all, I am blessed by the tremendous love, support, and encouragement of my husband and my family. In particular, thank my sister for taking good care of me in my first year in the US, thank my family in China for understanding of my being far away, and thank my husband for being always supportive. Research for this dissertation was conducted with funding from Environmental Protection Division of the Georgia Department of Natural Resources and U.S. Environmental Protection Agency. All in all, the research presented in this dissertation will not be possible without the support mentioned above.

TABLE OF CONTENTS

LIST OF TABLES

LIST OF FIGURES

Page

CHAPTER 1 INTRODUCTION

Context and Motivation

Air pollution can adversely affect human health (Dockery et al., 1993; Koren, 1995), crops and ecosystems (Fuhrer, 2002), degrade visibility (Malm et al., 2000), and lead to climate change (IPCC, 2001). It has changed from an urban environmental problem to a phenomenon spreading to state, country, and even global scales. In response, a variety of regulations, standards, and policies have been enacted world-wide, e.g. the Clean Air Act in the U.S.A. and the Clean Air for Europe (CAFE).

Addressing air pollution problems requires understanding the root causes of these problems. Emissions of air pollutants and their precursors are of particular interest as those are typically controlled to remediate elevated levels of pollutants. Emissions from major sources have been inventoried and applied in air quality management. However, the same amount of emissions from sources with varying emission characteristics (e.g. locations, time, emitting height, etc.) can have different air quality impacts. In addition, secondary air pollutants such as ozone are not emitted directly, but instead formed from their precursors through a series of complex physical and chemical processes in the atmosphere. Nonlinear relationships between concentrations of secondary species and precursor emissions are observed. Therefore, the amount, alone, of emissions can't be directly used to evaluate the air quality impacts from different sources.

Three-dimensional photochemical air quality models (i.e. source-oriented air quality models), which are capable of simulating air pollutant concentrations and how those levels change in response to different levels of emissions, are usually employed to investigate the root causes. In this approach, physical and chemical processes in the atmosphere are described using the atmospheric diffusion-reaction equation, which is later solved numerically. Different relationships between concentrations and emissions

are expected for different air pollutants due to their unique behaviors in the atmosphere. Impacts of varying meteorological and emission conditions are addressed by detailed meteorological and emission inputs respectively.

Accuracy of simulations from the air quality models and their applications is greatly impacted by uncertainties in model formulation and parameterization, initial and boundary conditions, and meteorological and emission inputs. Among these sources of uncertainty, emissions are regarded as one of the largest (Guenther et al., 2000; NRC, 1991; Placet et al., 2000; Russell and Dennis, 2000; Sawyer et al., 2000). Impacts of emission uncertainties have been evaluated by both sensitivity and uncertainty analysis. Sensitivity analysis of air quality models estimate how model outputs change with inputs and has been applied to evaluate model performance, investigate relationships between outputs and inputs, and identify sensitive input variables. However, estimated sensitivity coefficients of model simulations to emission inputs can partially reveal the impacts of emission uncertainties on air quality modeling, since responses of simulation uncertainties are also impacted by the levels of emission uncertainties. Uncertainty analysis, which takes into account not only the sensitivity coefficients but also quantified emission uncertainties, is usually conducted to estimate overall uncertainties in model simulations.

The magnitude of emissions uncertainties differs by sources and pollutants. For instance, sulfur dioxide (SO_2) emissions estimated by Continuous Emissions Monitoring (CEM) data for electricity generating utilities (EGU) are less uncertain than volatile organic compounds (VOCs) emissions from mobile sources. In addition, emission estimates for sources in the U.S. (especially urban areas) are viewed as being better known than in less developed countries (NARSTO, 2003). Qualitative uncertainties for different pollutants in the North American have been summarized in a recent NARSTO report (NARSTO, 2003). However, evaluating impacts of emission uncertainties on air quality modeling requires quantified emission uncertainties, which are often described

using probability distributions. Emission uncertainties can be quantified by inverse air quality modeling (top-down), propagation of input uncertainties (bottom-up), encoding of expert elicitation, or a mixture of these methods.

Inverse air quality modeling estimates uncertainty factors of emissions by comparing simulation results from air quality modeling and ambient/satellite measurements using various techniques. Such techniques include Kalman filtering, ridge regression, and Bayesian least squares method (Gilliland et al., 2003; Hartley and Prinn, 1993; Mendoza-Dominguez and Russell, 2000; Shim et al., 2005). This method can be used for uncertainties in total emissions, emissions during different periods, within different regions or from different source categories. However, the quality of such results is largely limited by the capability of air quality models and the availability of observation data. Uncertainties in other parts of the models and the inputs can cause uncertainties in such estimates.

Emission uncertainties have also been evaluated by propagation of uncertainties in emission modeling inputs (Chi et al., 2004; Hanna et al., 2005). Input uncertainties are quantified by statistical analysis of measurement data or encoding of expert elicitation. Expert elicitation refers to the method that “experts” are asked to give estimates of uncertainties based on their experience (Morgan and Henrion, 1990). This method is usually applied when relevant data are not available, or there is a gap between available data and desired variables. Quantified input uncertainties are described by probability distributions, and then are propagated through the emission models using either analytical or numerical methods. When emissions models are nearly linear and emission uncertainties are small, an analytical method can be used. Other circumstances require numerical methods, of which the Monte Carlo method is the most popular due to its flexibility.

In addition to estimation of uncertainties in emission modeling inputs, expert elicitation has also been applied to directly estimate emission uncertainties (Bergin et al.,

1999; Hanna et al., 1998; Hanna et al., 2001). As input uncertainties are propagated through emission modeling, analytical or numerical methods can be used to propagate emission uncertainties though air quality models.

Impacts of emission uncertainties can theoretically be quantified for any modeling systems or air pollutants using methods summarized above. However, propagation emission uncertainties through a complicated air quality model using numerical methods is rather computationally expensive, and thus their applications are greatly impeded. In addition, current applications focus on quantification of uncertainties in ozone simulations, and uncertainties in fine particulate matter ($PM_{2.5}$) simulations are rarely quantified. Being one of the major sources for $PM_{2.5}$, uncertainties in emissions from biomass burning are of great interest. Biomass burning is a combustion process that consumes biomass fuels and includes both natural (e.g. wildfires) and man-made (e.g. prescribed forest burning, agriculture field burning, land clearing, wood burning in fireplaces and woodstoves, residential leaf burning, etc). In the United States, biomass burning contributes about 35% of the fine particulate matter ($PM_{2.5}$, i.e. PM with aerodynamic diameter less than 2.5 μm) emissions (US-EPA, 2004). Previous $PM_{2.5}$ source apportionment studies using both receptor models and source-oriented air quality models suggest significant contributions from biomass burning in the southeastern United States (Kim et al., 2003; Kim, 2003; Liu et al., 2005; Park et al., 2006; Zheng et al., 2002; Zheng et al., 2006). However, the discrepencies in estimates of source contributions using different methods are also significant.

Structure and Scope of this Thesis

This thesis evaluates the emission uncertainties associated and their impacts on air quality modeling, with special attention to biomass burning. All simulations are based on the Models-3 modeling system recommended by the US Environmental Protection Agency (http://www.epa.gov/asmdnerl/models3/cmaq.html), with the Community

Multiscale Air Quality Model (CMAQ). Uncertainties in emissions and simulated concentrations of air pollutants provide added information to improve policy-making. These results can also shed light on future research to improve emissions and air quality modeling. Specifically, the chapters are structured as follows.

Chapter 2: Uncertainty analysis of ozone formation and emission control efficiencies using high-order sensitivities.

CMAQ-HDDM-3D can calculate sensitivities at the same time with concentrations. It is applied for ozone sensitivity analysis in the southeastern US during future year 2007 under three summer ozone episodes. Calculated sensitivity coefficients including both first and higher orders are used to develop a simplified air quality model, which is used to propagate emission uncertainties. In essence, the sensitivities define a response surface of how pollutant concentrations change with emissions. Emission uncertainties are summarized based on literature review of other studies. Their impacts on ozone formation and emission control efficiencies are both studied.

Chapter 3: Uncertainties in biomass burning emissions and seasonal $PM_{2.5}$ source contributions in the southeastern United States using CMAQ. Uncertainties in biomass burning emissions, including their amount, temporal and spatial characteristics, and speciation are evaluated first for a January 2002 episode. The results are then compared with results from a receptor model. An updated emission inventory with monthly county-level emissions, improved speciation profiles with higher organic matter components and 90% reduction of emissions from wood burning in fireplaces and woodstoves is developed for March, May and July 2002, representing different typical seasons. Both primary and secondary impacts from biomass burning are identified, as well as source contributions from each individual source.

Chapter 4: Air quality impacts from forest fires under different forest management practice. Air quality impacts with particular interest on $PM_{2.5}$ and O_3 from forest fire emissions under different forest management practices in Georgia are

investigated, including different burning seasons, different fire-return intervals (FRI), and controlling emissions during smoldering. The results can be used to guide forest management practices to reduce air quality impacts from forest fires. They also indicate the uncertainties in simulated air quality impacts that may be due to ignoring impacts from human activities.

Chapter 5: Uncertainties in Prescribed Forest Fires Emission Inventories and Their Impact on Air Quality Modeling. Uncertainties in emission estimates are propagated from the uncertainties of three inputs: acreage burned, fuel consumption and emission factors. These are evaluated using literature review, evaluating and propagating modeling uncertainties and by use of expert elicitation to fill specific knowledge gaps. The Monte Carlo method is further used to propagate the above uncertainties with consideration of different correlations to estimate uncertainties in total emissions, which are then propagated through air quality modeling to get uncertainties in $PM_{2.5}$ concentrations.

Chapter 6: Conclusion. Major findings in this thesis are summarized and recommendations for future research are provided.

References

Bergin, M. S., Noblet, G. S., Petrini, K., Dhieux, J. R., Milford, J. B., and Harley, R. A. (1999). Formal uncertainty analysis of a lagarangian photochemical air pollution model. Environ. Sci. Technol. 33, 1116-1126.

Chi, T. R., Unal, A., Tian, D., and Russell, A. G. (2004). Uncertainty of NONROAD Emissions in Georgia. 13th International Emission Inventory Conference "Working for Clean Air in Clearwater". http://www.epa.gov/ttn/chief/conference/ei13/.

Dockery, D. W., Pope, C. A., Xu, X., Spengler, J. D., Ware, J. H., Fay, M. E., Ferris, B. G., and Speizer, F. E. (1993). An association between air pollution and mortality in six U.S. cities. New England J. Med. 329, 1753-1808.

Fuhrer, J. (2002). Ozone impacts on vegetation. Ozone Science and Engineering 24, 69-74.

Gilliland, A. B., Dennis, R. L., Roselle, S. J., and Pierce, T. E. (2003). Seasonal NH3 emission estimates for the eastern United States based on ammonium wet concentrations and an inverse modeling method. Journal of Geophysical Research-Atmospheres 108.

Guenther, A., Geron, C., Pierce, T., Lamb, B., Harley, P., and Falle, R. (2000). Natural emissions of non-methane volatile organic compounds, carbon monoxide, and oxides of nitrogen from North America. Atmospheric Environment 34, 2205-2230.

Hanna, S. R., Chang, J. C., and Fernau, M. E. (1998). Monte Carlo estimates of uncertainties in predictions by a photochemical grid model (UAM-IV) due to uncertianties in input variables. Atmos. Environ. 32, 3619-3628.

Hanna, S. R., Lu, Z. G., Frey, H. C., Wheeler, N., Vukovich, J., Arunachalam, S., Fernau, M., and Hansen, D. A. (2001). Uncertainties in predicted ozone concentrations due to input uncertainties for the UAM-V photochemical grid model applied to the July 1995 OTAG domain. Atmos. Environ. 35, 891-903.

Hanna, S. R., Russell, A. G., Wilkinson, J. G., Vukovich, J., and Hansen, D. A. (2005). Monte Carlo estimation of uncertainties in BEIS3 emission outputs and their

effects on uncertainties in chemical transport model predictions. J. Geophys. Res. 110, D01302.

Hartley, D., and Prinn, R. (1993). Feasibility of Determining Surface Emissions of Trace Gases using an inverse method in a three-dimensional chemical transport model. J. Geophys. Res. 98, 5183-5198.

IPCC (2001). "Climate Change 2001: The Scientific Basis. Contribution of Working Group I to the Third Assessment Report of the Intergovernmental Panel on Climate Change," Cambridge University Press, Cambridge, United Kingdom and New York, NY, USA.

Kim, E., Hopke, P. K., and Edgerton, E. S. (2003). Source identification of atlanta aerosol by positive matrix factorization. J. Air Waste Manage. Assoc. 53, 731-739.

Kim, E., P.K. Hopke, P. Paatero, and E.S. Edgerton (2003). Incorporation of parametric factors into multilinear receptor model studies of atlanta aerosol. Atmos. Environ. 37, 5009-5021.

Koren, H. S. (1995). Associations between criteria air pollutants and asthma. Environmental Health Perspectives 103.

Liu, W., Wang, Y. H., Russell, A. G., and Edgerton, E. S. (2005). Atmospheric aerosol over two urban-rural pairs in the sourtheastern United States: chemical composition and possible sources. Atmos. Environ. 39, 4453-4470.

Malm, W. C., Pitchford, M. L., Scruggs, M., Sisler, J. F., Ames, R., Copeland, S., Gebhart, K. A., and Day, D. E. (2000). "Spatial and Seasonal Patterns and Temporal Variability of Haze and its Constituents in the United States: Report III." Coop. Inst. for Res. in the Atmos., Colo. State Univ., Fort Collins, CO.

Mendoza-Dominguez, A., and Russell, A. G. (2000). Iterative Inverse Modeling and Direct Sensitivity Analysis of a Photochemical Air Quality Model. Environ. Sci. Technol 34, 4974-4981.

Morgan, M. G., and Henrion, M. (1990). "Uncertainty: A Guide to Dealing with Uncertainty in Quantitative Risk and Policy Analysis," Cambridge University Press.

NARSTO (2003). "Particulate matter science for policy makers."

NARSTO (2005). "Improving Emission Inventories for Effective Air Quality Management Across North America."

NRC (1991). "Committee on Tropospheric Ozone Formation and Measurement. Rethinking the ozone problem in urban and regional air pollution, National Academy Press."

Park, S.-K., Murmur, A., Ke, L., Yan, B., Russell, A. G., and Zheng, M. (2006). Source apportionment of PM2.5: comparison between receptor and air quality models. in submission to Environ. Sci. and Technol.

Placet, M., Mann, C. O., Gilbert, R. O., and Niefer, M. J. (2000). Emissions of ozone precursors from stationary sources: a critical review. Atmospheric Environment 34, 2183-2204.

Russell, A. G., and Dennis, R. (2000). NARSTO critical review of photochemical models and modeling. Atmospheric Environment 34, 2283-2324.

Sawyer, R. F., Harley, R. A., Cadle, S. H., Norbeck, J. M., Slott, R., and Bravo, A. (2000). Mobile sources critical review: 1998 NARSTO assessment. Atmospheric Environment 34, 2161-2181.

Shim, C., Wang, Y., Choi, Y., Palmer, P. I., Abbot, D. S., and Chance, K. (2005). Constraining global isoprene emissions with Global Ozone Monitoring Experiment (GOME) formaldehyde column measurements. J. Geophys. Res. 110.

US-EPA (2004). EPA 2001 modeling platform emission inventory. http://www.epa.gov/ttn/chief/emch/invent/. Accessed on May, 2005.

Zheng, M., Cass, G. R., Schauer, J. J., and Edgerton, E. S. (2002). Source apportionment of PM2.5 in the southeastern United States using solvent-extractable organic compounds as tracers. Environ. Sci. and Technol. 36, 2361-2371.

Zheng, M., Ke, L., Edgerton, E. S., Schauer, J. J., Dong, M., and Russell, A. G. (2006). Spatial distribution of carbonaeous aerosol in the southeastern US using molecular markers and carbon isotope data. in submission to J. of Geophys. Res.

CHAPTER 2 UNCERTAINTY ANALYSIS OF OZONE FORMATION AND EMISSION CONTROL RESPONSES USING HIGH-ORDER SENSITIVITIES

Abstract

Uncertainties in emission inventories are regarded as one of the major sources of uncertainty in air quality modeling. Their impacts on ozone formation and emission control efficiencies during future year 2007 with three different base year episodes have been evaluated using high-order sensitivities calculated by a decoupled direct method implemented in community multiscale air quality model (CMAQ). Large emission inventory uncertainties, e.g. a factor of 1.5 for 95% confidence interval (CI) of stationary point NO_X emission and a factor of 2 for 95% CI of all other emissions, lead to less than 10% uncertainties (as coefficient of variance) in ozone concentrations. Elevated ozone concentrations in Atlanta are impacted by NO_X emissions from Atlanta mobile sources, point sources inside and outside Atlanta, and Atlanta anthropogenic VOC emissions in a decreasing order, with anthropogenic VOC emissions having their primary impacts in the downtown Atlanta area. Uncertainties in Atlanta mobile NO_X emissions have the largest impact on uncertainties in ozone concentrations, with similar impacts of uncertainties in emissions from other source categories at a smaller scale. A large variance in the impacts of emission inventory uncertainties is found within an episode, while the variance between episodes is small. Reducing NO_X emissions from Atlanta mobile source is the most efficient way to control ozone, followed by point NO_X emissions inside and outside of Atlanta and anthropogenic VOC emissions. Mean emission control efficiencies with consideration of emission inventory uncertainties indicate similar ranking, with

---

This chapter will be submitted to Atmospheric Environment. Co-authors are Dan Cohan, Yongtao Hu, Sergey Napelenok, Michael Chang, and Armistead Russell.

significant uncertainties associated with emission control efficiencies. Uncertainties in emissions sometimes even lead to negative emission control efficiencies, i.e. ozone concentrations increase with emission reduction. Better understanding of emissions in Atlanta is required for the development of a reliable control strategy in the Atlanta area.

Introduction

Source-oriented air quality models (AQM) can help us to understand complicated relationships between emission sources and air pollutant concentrations in the atmosphere. They are applied to identify major sources and evaluate emission control responses to different abatement measures. A key input of such endeavors is emission inventories, which are regarded as one of the major sources of uncertainty in air quality modeling (Guenther et al., 2000; Placet et al., 2000; Russell and Dennis, 2000; Sawyer et al., 2000). Understanding uncertainty impacts on air quality modeling can help policy makers in making decisions, as well as suggest means for reducing uncertainty.

Impacts of emission inventory uncertainties on air quality modeling can be assessed by uncertainty propagation, with quantified emission inventory uncertainties. When concentrations of air pollutants change linearly with emissions, an analytical method (i.e. Gaussian method) (Morgan and Henrion, 1990) using first-order sensitivity coefficients can be used. However, secondary pollutants such as ozone have a very non-linear response to its precursor emissions (primarily nitrogen oxides (NO_X) and volatile organic compounds (VOCs)) (Cohan et al., 2005; Hakami et al., 2004; Lin et al., 1988). Analytical methods should consider impact from nonconstant first-order sensitivity coefficients. In addition, uncertainties in emission inventories are usually large, and thus specified by log-normal probability distributions to avoid values without physical meaning (e.g. negative emissions). Due to the nonlinear response and lack of normality, numerical methods (e.g. Monte Carlo, or MC methods) are frequently employed to

propagate emission inventory uncertainties. Previous studies have applied MC methods or variants to evaluate uncertainties in various air quality models, by specifying probability distributions of emissions and other inputs according to expert elicitation, measurements, or a mixture of both (Bergin et al., 1999; Hanna et al., 1998; Hanna et al., 2001). Generally, numerical methods require running air quality models hundreds of times, if not more, and additional simulations are needed to assess uncertainties in emission control efficiencies at various control levels due to the complicated nonlinear response of concentrations to emissions. Because large-scale multidimensional air quality modeling is computationally intensive, systematic uncertainty analysis using MC methods is limited, though a few studies have used such an approach (Bergin et al., 1999; Hanna et al., 1998; Hanna et al., 2001).

Sensitivity analysis of air quality models provides detailed insight into complicated responses. Linear responses can be characterized by first-order sensitivity coefficients, or slopes of the response curve, while supplementary high-order sensitivity coefficients are required to characterize strong nonlinear systems. High-order sensitivity coefficients provide information on the curvature of the response curve. To calculate sensitivities, the decoupled direct method (DDM), a direct sensitivity analysis method, has been implemented in a variety of 3-D AQMs, and is now one of the most widely used sensitivity approaches (Dunker, 1981; Yang et al., 1997). DDM integrates the sensitivity equations decoupled from the model equations and calculates sensitivities at the same time with concentrations (Dunker, 1981; Yang et al., 1997). A recent study has expanded its capability in calculating high-order sensitivities in 3-D AQMs by including high-order sensitivity equations, referred to as High-order Decoupled Direct Methods in Three Dimensions (HDDM-3D) (Hakami et al., 2003). Such high-order sensitivity coefficients have been used in source apportionment and control strategy development and significant improvement in the accuracy of the analysis has been achieved (Cohan et al., 2005; Hakami et al., 2003, 2004).

Here, HDDM-3D is used to calculate first and high-order ozone sensitivities to a variety of emission sources. Sensitivity coefficients are calculated for each grid and time to reflect unique local meteorological and emissions conditions. Such results can then be used as a reduced-form, or simplified AQM (RFAQM). This can be used to propagate emission inventory uncertainties, instead of running the original AQM, via Monte Carlo analysis. Three summer episodes (August 1-15, 1999; August 11-19, 2000, and July 5-17, 2001) are selected using the Classification and Regression Tree (CART) analysis technique with historical meteorological and air quality measurements as inputs (ICF Consulting/Systems Applications International. 2002). These episodes are chosen because their meteorological conditions are expected to be prone to ozone formation and they cover a variety of typical regimes impacting the southeastern United States. The modeling domain covers the southeastern US, with special attention to the Atlanta area, which refers to the Atlanta-Sandy Springs-Gainesville CSA including thirty-two counties with historical ozone problems. Air quality in the future year 2007 is simulated using emissions projected from different base year emissions and meteorological conditions under the three summer episodes. Uncertainties in simulated ozone concentrations and emission control responses with different abatement measures are investigated.

Methods

Air quality during the three summer episodes are simulated with the Community Multiscale Air Quality (CMAQ) model v. 4.3 using SAPRC-99 as the chemical mechanism (Byun and Ching, 1999). The modeling domain covers the southeastern United States at 12-km resolution, and has 13 vertical layers reaching about 15,000 m on top, with about 18 m for the bottom layer. Its initial and boundary conditions are supplied by simulations from a 36-km resolution grid covering the eastern half of the United States. Meteorological conditions for the episodes are simulated with the NCAR's 5th generation Mesoscale Model (MM5). Details are provided elsewhere (Hu et al., 2003;

Tian et al., 2004). Base year emission inventories are based on the final version 2 of the US Environmental Protection Agency (EPA) National Emission Inventory 1999 (http://www.epa.gov/ttn/chief/net/1999inventory.html), with updated NO_X and sulfur dioxide (SO_2) emissions from electricity generating units (EGUs) using hourly continuous emissions monitoring (CEM) data (http://cfpub.epa.gov/gdm), and improved emissions from mobile and partial area sources in Georgia (Unal et al., 2003). These emissions are processed through the Sparse Matrix Operator Kernel Emissions (SMOKE) Modeling System v. 1.5 (Houyoux et al., 2000). Biogenic emissions are calculated based on Biogenic Emissions Land Use Database version 3 (BELD3) using the Biogenic Emission Inventory System version 3 (BEIS3). Results of the fist two days for each episode are discarded as model initialization periods. Model performance is evaluated by comparing model results with observations collected as part of the Aerometric Information Retrieval System (AIRS; archived at http://www.epa.gov/ttn/airs/airsaqs/archived%20data/downloadaqsdata.htm). Four performance metrics: mean bias (MB), root mean square error (RMSE), mean normalized bias (MNB), and mean normalized error (MNE) are calculated.

Potential air quality in future year 2007 is simulated with base year meteorological conditions and future year emissions projected according to

$$Emission_{2007} = Emission_{base} * Factor_{growth} * (1 - Factor_{control}) \quad (1)$$

Where $Factor_{growth}$ refers to the emission growth factor from base year to future year, and is calculated using Economic Growth Analysis System Version (EGAS) 4.0; $Factor_{control}$ is the control efficiency under existing control policies, including the NO_X SIP call, the State Implementation Plan, and VOC RACT (Reasonably Available Control Technology) and MACT (Maximum Achievable Control Technology) controls, etc. (Hu et al., 2004). Biogenic emissions are kept the same as respective base year emissions.

The RFAQM is developed using Taylor expansions and calculated sensitivity coefficients. Given that ozone concentrations are expressed as a function of emissions, i.e. $C = f(x, y)$, ozone concentrations at different emission levels can be calculated from a base case scenario using a multidimensional expansion, e.g. for two source categories x and y

$$\begin{aligned} f(x_0 + \Delta x, y_0 + \Delta y) \approx\ & f(x_0, y_0) + \Delta x f_x^{(1)}(x_0, y_0) + \Delta y f_y^{(1)}(x_0, y_0) \\ & + \frac{(\Delta x)^2}{2!} f_{xx}^{(2)}(x_0, y_0) + \frac{(\Delta y)^2}{2!} f_{yy}^{(2)}(x_0, y_0) + \Delta x \Delta y f_{xy}^{(2)}(x_0, y_0) \\ & + \frac{(\Delta x)^3}{3!} f_{xxx}^{(3)}(x_0, y_0) + \frac{(\Delta y)^3}{3!} f_{yyy}^{(3)}(x_0, y_0) + \frac{(\Delta x)^2 (\Delta y)}{2} f_{xxy}^{(3)}(x_0, y_0) \\ & + \frac{(\Delta x)(\Delta y)^2}{2} f_{xyy}^{(3)}(x_0, y_0) + \ldots \end{aligned} \tag{2}$$

Results from HDDM-3D are semi-normalized sensitivities (S). For example, first-order sensitivity to emission source j with emissions p_j (i.e. $S_j^{(1)}$) is:

$$S_j^{(1)}(\bar{x}, t) = \tilde{P}_j \frac{\partial C(\bar{x}, t)}{\partial p_j} = \tilde{P}_j \frac{\partial C(\bar{x}, t)}{\partial (\varepsilon_j \tilde{P}_j)} = \frac{\partial C(\bar{x}, t)}{\partial \varepsilon_j} \tag{3}$$

Where $\tilde{P}_j$ is the nominal value of p_j (i.e. the value used in the simulation) and ε_j is the scaling variable ($p_j = \varepsilon_j \tilde{P}_j$) with a nominal value of 1. Similarly, the second order sensitivity $S_{j,k}^{(2)}$ is:

$$S_{j,k}^{(2)} = \tilde{P}_j \frac{\partial}{\partial p_j} \left(\tilde{P}_k \frac{\partial C}{\partial p_k} \right) = \frac{\partial^2 C}{\partial \varepsilon_j \varepsilon_k} \tag{4}$$

Here and below, the dependencies of $S_{j,k}^{(2)}$ on $\bar{x}$ and t are no longer explicitly shown. When $j = k$, $S_{j,j}^{(2)}$ is sensitivity of $S_j^{(1)}$ to emission p_j. When $j \neq k$, $S_{j,k}^{(2)}$ refers to sensitivity of $S_j^{(1)}$ to emission p_k, indicating interactions between two different emissions p_j and p_k. All sensitivity coefficients vary in space and time. Although significant nonlinear responses of ozone to emissions have been observed, first- and second-order

sensitivities can accurately capture the response of concentrations to emissions (Cohan et al., 2005; Hakami et al., 2004). The ozone concentrations at different emission levels are then approximated by

$$C \approx C_0 + \sum_{i=1}^{N} \Delta\varepsilon_i S_i^{(1)} + \frac{1}{2}\sum_{i=1}^{N}\sum_{j=1}^{N} \Delta\varepsilon_i \Delta\varepsilon_j S_{i,j}^{(2)} \quad (5)$$

where, C_0 is the ozone concentrations simulated at current emission levels, N refers to the number of emission source categories, $\Delta\varepsilon_i$ refers to scaling factors of emissions from source i.

Uncertainties in ozone simulations are propagated from emission inventory uncertainties in four source categories, including point NO_X emissions and non-point NO_X emissions, and anthropogenic and biogenic VOC emissions. Though any number of source categories can be theoretically considered, more sensitivity coefficients are required to depict the ozone response to emissions with an increasing number of emission source categories. For 10 emission source categories, 65 sensitivity coefficients (up to second-order) technically might be considered according to equation 5. However, as the sources are split up, the nonlinear terms become negligible, except for the major sources. In addition, $S_{j,k}^{(2)}$ become more significant when two sub-source categories have similar spatial distributions (Cohan et al., 2005).

In this study, uncertainties in emissions are quantified following literature reviews, and then propagated through RFAQM using MC methods (Morgan and Henrion, 1990) with more than 20000 random sets of input parameters. Both 95% confidence interval (CI) and coefficients of variance (cov, i.e. standard deviation divided by mean) are used to represent uncertainties in simulated ozone concentrations. Effects of correlations between uncertainties in different emission source categories are also studied.

Impacts of individual emission sources on ozone concentrations and their associated uncertainties are also studied. Preliminary tests show that ozone concentrations in the Atlanta area are mainly sensitive to six anthropogenic sources: NO_X emissions from stationary point sources both in and outside of Atlanta, Atlanta mobile onroad and nonroad sources, and Atlanta VOC emissions from mobile and stationary sources. Individual source contributions are defined as the difference in simulated ozone concentrations with and without emissions from a specific source, i.e. the zero-out source contribution (ZOC) of a source (Cohan et al., 2005). According to RFAQM, ZOC of source j can be estimated using sensitivity coefficients as:

$$ZOC_j \cong C\big|_{p_j=P_j} - C\big|_{(p_j=0;i.e.,\Delta\varepsilon_j=-1)} \approx S_j^{(1)} - \frac{1}{2}S_{j,j}^{(2)} \quad (6)$$

Impacts of source j on uncertainties in simulated ozone concentrations are also quantified using similar methods as ozone uncertainty analysis mentioned above, except that only uncertainty in one source category is considered at a time. To account for the impact from interaction between mobile onroad and nonroad emissions, ZOCs of Atlanta mobile NO_X emissions (ZOC_j) are first calculated and then allocated to onroad and nonroad sub-categories (ZOC_{ji}) according to their respective first order sensitivity coefficients ($S_{ji}^{(1)}$):

$$ZOC_{ji} \approx ZOC_j \times \frac{S_{ji}^{(1)}}{S_j^{(1)}} \quad (7)$$

$$S_j^{(1)} = \sum_{i=1}^{N} S_{ji}^{(1)} \quad (8)$$

Uncertainties in simulated ozone concentrations caused by uncertainties in Atlanta mobile NO_X emissions (cov_j) are also first estimated and then allocated to each sub-source (onroad and nonraod) category according to:

$$\mathrm{cov}_{ji} \approx \mathrm{cov}_j \times \sqrt{\frac{(S_{ji}^{(1)})^2}{\sum_{i=1}^{N}(S_{ji}^{(1)})^2}} \quad (9)$$

Similarly, equations 8-10 are applied to evaluate impacts of Atlanta VOC emissions from mobile and stationary sources.

Emission control responses for different levels of emissions reduction are estimated using RFAQM. When emissions from a source category are reduced by a factor f_{emis}, ozone concentrations change to:

$$C\big|_{p_j=(1-f_{emis})\times\tilde{P}_j} = C_0 + (-f_{emis})S_j^{(1)} + \frac{1}{2}(-f_{emis})^2 S_{jj}^{(2)} \quad (10)$$

The resulting control efficiency (CE) is:

$$CE = 1 - \frac{C\big|_{p_j=(1-f_{emis})\times\tilde{P}_j}}{C\big|_{p_j=\tilde{P}_j}} = 1 - \frac{C_0 + (-f_{emis})S_j^{(1)} + \frac{1}{2}(-f_{emis})^2 S_{jj}^{(2)}}{C_0} = \frac{f_{emis}S_j^{(1)} - \frac{1}{2}f_{emis}^2 S_{jj}^{(2)}}{C_0} \quad (11)$$

Uncertainties in CE are propagated from emission inventory uncertainties using MC methods. For a random value (P_j) of emissions from a source category following specific probability distributions, the corresponding CE with an emission reduction factor f_{emis} is calculated by:

$$CE = 1 - \frac{C\big|_{p_j=(1-f_{emis})\times P_j}}{C\big|_{p_j=P_j}} = 1 - \frac{C_0 + \Delta\varepsilon_{fj}S_j^{(1)} + \frac{1}{2}(\Delta\varepsilon_{fj})^2 S_{jj}^{(2)}}{C_0 + \Delta\varepsilon_j S_j^{(1)} + \frac{1}{2}(\Delta\varepsilon_j)^2 S_{jj}^{(2)}} \quad (12)$$

where the scaling factor for the random emission P_j is $\Delta\varepsilon_j = \frac{P_j}{\tilde{P}_j} - 1$, and changes to

$\Delta\varepsilon_{fj} = \frac{(1-f_{emis})P_j}{\tilde{P}_j} - 1 = \Delta\varepsilon_j(1-f_{emis}) - f_{emis}$ with additional emission reduction factor f_{emis}. In the above analyses, the S_j are not treated as uncertain, and will depend on meteorology and other factors.

Results and Discussion

More than fifty five thousand ozone observation records with ozone concentrations larger than 40 ppbv, have been used to evaluate air quality modeling performance. Simulated ozone concentrations in 1999 and 2000 are slightly low on average: 2.69% and 0.51% respectively. In 2001, they are slightly high: 4.19%. In addition, MNEs are around 20% in all episodes (Table 2-1). Model performance for three base years is well within recommended levels. Air quality in future year 2007 is simulated using the same meteorological inputs. 1999 is the most polluted, and 2001 is the cleanest among all episodes.

Table 2-1 Statistics of ozone performance for three base year episodes (cutoff = 40 ppbv)

Episode	N	MOC (ppbv)	MB (ppbv)	RMSE (ppbv)	MNB (%)	MNE (%)
1999	26032	67.6	-3.10	17.2	-2.69	20.3
2000	14104	63.6	-1.10	14.9	-0.51	19.1
2001	15783	59.1	1.40	12.6	4.19	17.4

N refers to the number of applicable hourly ozone observations in performance evaluation. Mean of observation (MOC) is calculated as $MOC = \frac{1}{N}\sum_{i=1}^{N} C_i^o$. Statistical metrics are calculated as: $MB = \frac{1}{N}\sum_{i=1}^{N}\left(C_i^s - C_i^o\right)$, $RMSE = \sqrt{\frac{1}{N}\sum_{i=1}^{N}\left(C_i^s - C_i^o\right)^2}$, $MNB = \frac{1}{N}\sum_{i=1}^{N}\frac{\left(C_i^s - C_i^o\right)}{C_i^o}\times 100\%$, $MNE = \frac{1}{N}\sum_{i=1}^{N}\frac{\left|C_i^s - C_i^o\right|}{C_i^o}\times 100\%$, where C_i^s is the hourly ozone simulations and C_i^o is the respective observations.

Projected anthropogenic NO_X and VOC emissions during future year 2007 are grouped into four source categories, including stationary point and area sources, and mobile onroad and nonroad sources (Table 2-2). NO_X emissions from stationary point sources with base year 1999 are larger than the other two years (about 400 tons/day more for the whole domain, and 17 tons/day more for the Atlanta area), due to larger base year emissions estimated from CEM data. Differences in mobile onroad emissions with the three base years are due to different meteorological conditions, since the same activity data (vehicle miles traveled, VMT) is used. Different meteorological conditions also lead

to a large difference in biogenic emissions, with 7900 tons/day more biogenic VOC emissions during base year 1999 than 2001 in the whole modeling domain and 510 tons/day for Atlanta. NO_X and VOC emissions from other source categories with three different base years are the same. Among these sources, NO_X emissions are mainly emitted from stationary point and mobile sources while VOC emissions are dominated by biogenic sources. Stationary area and mobile sources are the major anthropogenic VOC sources.

Table 2-2 Daily NO_X and VOC emissions during 2007 projected from different base year emission inventory (tons/day)

Sources	NO_X						VOC					
	Domain			Atlanta			Domain			Atlanta		
	1999	2000	2001	1999	2000	2001	1999	2000	2001	1999	2000	2001
Stationary Point	2590	2190	2206	143	133	126		930			31	
Stationary Area		468			63			3300			226	
Mobile Onroad	2060	2000	2040	282	274	275	1260	1230	1270	143	140	140
Mobile Nonroad		1100			130			645			68	
Biogenic	368	353	330	9.4	8.9	8.4	39900	37400	32000	2100	1950	1590

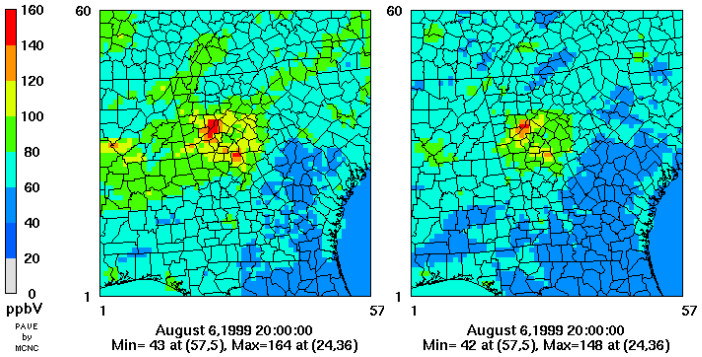

Figure 2-1 Simulated 8-hr ozone concentrations at the time of peak for August 1999 (left) and projected 2007 with base year 1999 (right) in FAQS 12-km grid

Simulated 8-hr ozone concentrations peak on August 6th 1999 with a maximum ozone concentration of 164 ppbv and decrease to 148 ppbv with projected 2007 emissions (Figure 2-1). All 8-hr ozone concentrations above the National Ambient Air Quality Standard (NAAQS) are simulated to fall about 5~20 ppbv in future year 2007

with existing controls. However, there are still regions that would exceed the NAAQS, primarily in the Atlanta area.

Uncertainties in stationary point and non-point NO_X emissions and anthropogenic and biogenic VOC emissions are developed from literature review. Emission inventory uncertainties have been quantified by expert elicitation (Hanna et al., 2001) and more qualitative means (NARSTO, 2003). Hanna used log-normal distributions and 95% CI denoted uncertainties. Uncertainties with a factor of 1.5 were chosen for stationary point source emissions (i.e. their 95% CI was $(\frac{\tilde{P}_j}{1.5}, 1.5\,\tilde{P}_j)$.) and a factor of 2 for all other sources (i.e. their 95% CI was $(\frac{\tilde{P}_j}{2}, 2\,\tilde{P}_j)$.). Recent qualitative summaries of emission inventory uncertainties showed a similar trend between sources (NARSTO, 2003), though a better understanding of NO_X emissions from mobile sources was concluded. Quantitative uncertainty analyses of mobile nonroad emissions by propagating uncertainties in input parameters indicated a factor of 1.6 for their NO_X emissions uncertainties and a factor of 1.5 for their VOC emissions uncertainties (Chi et al., 2004). Both factors of 2.0 and 1.5 are used for uncertainties in mobile source emissions in this study. Uncertainties in non-point NO_X emissions, the sum of emissions from area and mobile sources, depend on both uncertainties in emissions from each individual source and correlations between them. When pure dependence between sources is assumed, uncertainty factors in total non-point NO_X emissions are similar to those for each individual source. However decreased uncertainty factors for such total emissions are expected for a case with pure independence. Since the decreased uncertainty doesn't indicate a better understanding of emissions, the same uncertainty factors as the individual source are applied to non-point NO_X emissions. In addition, uncertainties in biogenic emissions estimated by BEIS3 have been quantified, showing similar results (Hanna et al., 2005). Here, two sets of emission inventory uncertainty factors are

employed, including factors 1.5, 2, 2 and 2 (labeled as uncertainty analysis 2) and factors 1.5, 1.5, 2, 2 (labeled as uncertainty analysis 1.5) for NO_X emissions from stationary point and non-point sources and anthropogenic and biogenic VOC emissions, respectively.

Mean daily peak 8-hr ozone concentrations in downtown Atlanta, Georgia with uncertainty analysis 1.5 are very similar to the simulated nominal values, which are larger than mean concentrations with uncertainty analysis 2 (Figure 2-2). It is due to the positively skewed probability distributions of emission inventory uncertainties. Associated uncertainties (as 95% CI) with uncertainty analysis 2 have a larger range than uncertainty analysis 1.5. The two uncertainty analyses have similar 97.5^{th} percentiles, but uncertainty analysis 2 has a significantly smaller 2.5^{th} percentile. This is because the rate of ozone formation decreases with increased emissions and thus ozone concentrations are less sensitive to emissions at high emission levels.

Simulated ozone concentrations and associated uncertainties during 2007 for all grids within the Atlanta area and times with values larger than 80 ppbv are summarized for three different base year episodes (Table 2-3). Ozone concentrations in 2007 with 1999 meteorology are highest, followed by 2000 and 2001. Uncertainties in ozone concentrations for different base year episodes are similar, being 9.4% (as cov) for uncertainty analysis 2 and 6.3% for uncertainty analysis 1.5. Variance of uncertainties in ozone simulations is small; for example, uncertainties in ozone simulations are 6.5±1.2% (cov: mean±std) using 1999 meteorology. In addition, consideration of correlations between uncertainties in emissions from different source categories doesn't significantly impact uncertainties in simulated ozone concentrations. For uncertainty analysis 2, when correlations between the uncertainties in emissions from the four sources mentioned above increase from 0 to 0.5 (rank correlation coefficients), uncertainties in simulated ozone concentrations change little. In summary, levels of uncertainty decrease significantly from inputs to outputs, i.e. ozone simulations are not very sensitive to

emission inventory uncertainties, though larger uncertainties are expected with increasing emission inventory uncertainties.

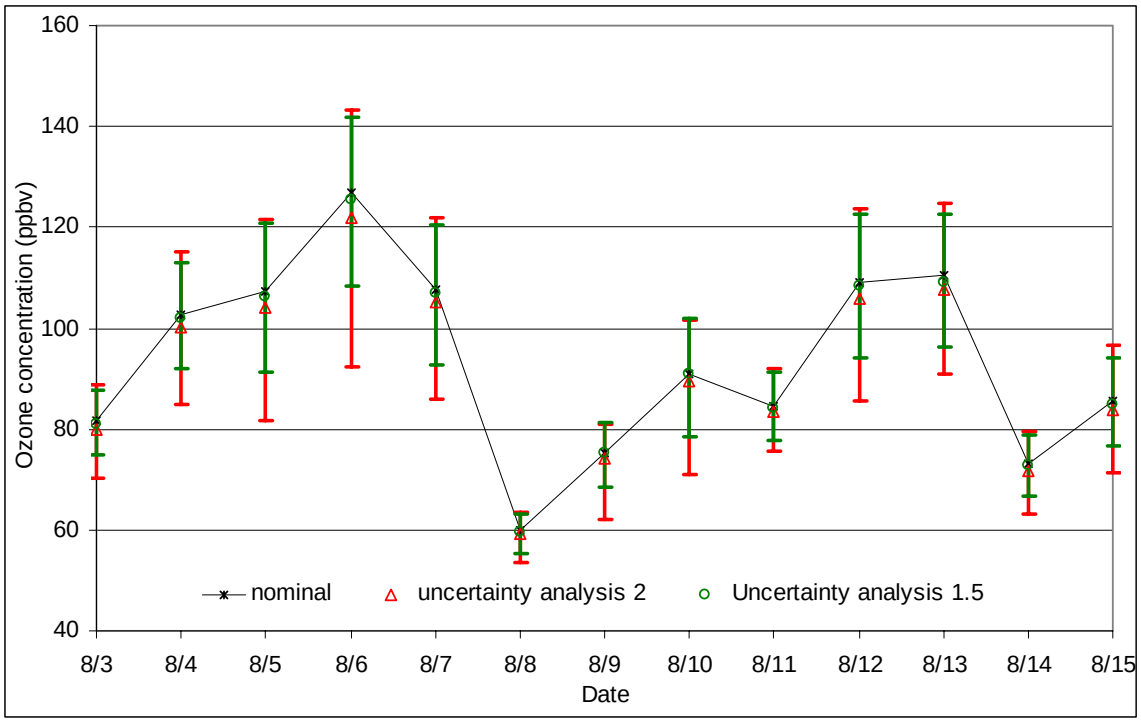

Figure 2-2 Daily peak 8-hr ozone concentrations and associated uncertainties as 95% CI during 2007 with base year 1999 in downtown Atlanta, Georgia
Uncertainty analysis 2 assumes factors of 1.5, 2, 2 and 2 for 95% CI of uncertainties for NO_X emissions from stationary point and non-point sources, anthropogenic and biogenic VOC emissions respectively, while factors of 1.5, 1.5, 2 and 2 are assumed for uncertainty analysis 1.5.

Table 2-3 8-hr ozone concentrations (mean) and associated uncertainties as cov (mean±std) during 2007 with three different base year episodes (cut-off = 80 ppbv)

Base Year	8-hr ozone concentrations	Uncertainties (cov, %)	
	(ppbv)	uncertainties analysis 2.0	uncertainties analysis 1.5
1999	90.4	9.8±1.9	6.5±1.2
2000	87.7	9.2±2.1	6.1±1.2
2001	86.3	9.2±1.4	6.1±0.8

Atlanta mobile onroad NO_X emissions have the largest impact on ozone formation in downtown Atlanta, with a peak contribution of 27 ppbv on August 6th, 1999 (Figure 2-3), followed by mobile nonroad NO_X emissions (peak contribution of 13 ppbv) and

much smaller contributions from other sources. Ozone depletion by Atlanta mobile NO_X emissions has also been found on some days with low ozone concentrations. Variation of daily peak 8-hr ozone and source contributions indicates that impacts from emissions inside of Atlanta increase or decrease together with ozone concentrations, while point NO_X emissions outside of Atlanta have a larger impact when ozone concentrations are lower in downtown Atlanta. Stronger transport can bring emissions from further away into the Atlanta region, but will also diminish pollution. Though absolute ozone concentrations and source contributions during 2007 are different between the three base year episodes with different meteorological conditions, the relative importance of source contributions doesn't change that much. Additional results at a station in suburban Atlanta (about 25 miles north of downtown Atlanta) show similar behavior as in downtown Atlanta, except a smaller impact from anthropogenic VOC emissions and no significant ozone depletion (Figure 2-3).

Scatter plots of source contributions to 8-hr ozone concentrations larger than 80 ppbv for all grids in Atlanta indicate strong correlations between elevated ozone concentrations and mobile emissions in Atlanta (Figure 2-4). A summary of all shows Atlanta mobile onroad NO_X emissions contribute 14.4 ppbv to 8-hr ozone, together with 5.6 ppbv from Atlanta mobile nonroad NO_X emissions, 2.9 ppbv and 2.2 ppbv respectively from stationary point NO_X in and outside Atlanta, 0.8 ppbv from Atlanta mobile VOC emissions and 0.7 ppbv from Atlanta stationary VOC emissions (Table 2-4). Variance of source contributions from mobile NO_X emissions is relatively smaller than other sources within an episode, accompanied by significantly less source contributions with base year 2001. Source contributions from point NO_X emissions have large variations within an episode and between episodes. Significant discrepancies in impacts from anthropogenic VOC emissions within an episode are found.

(a)

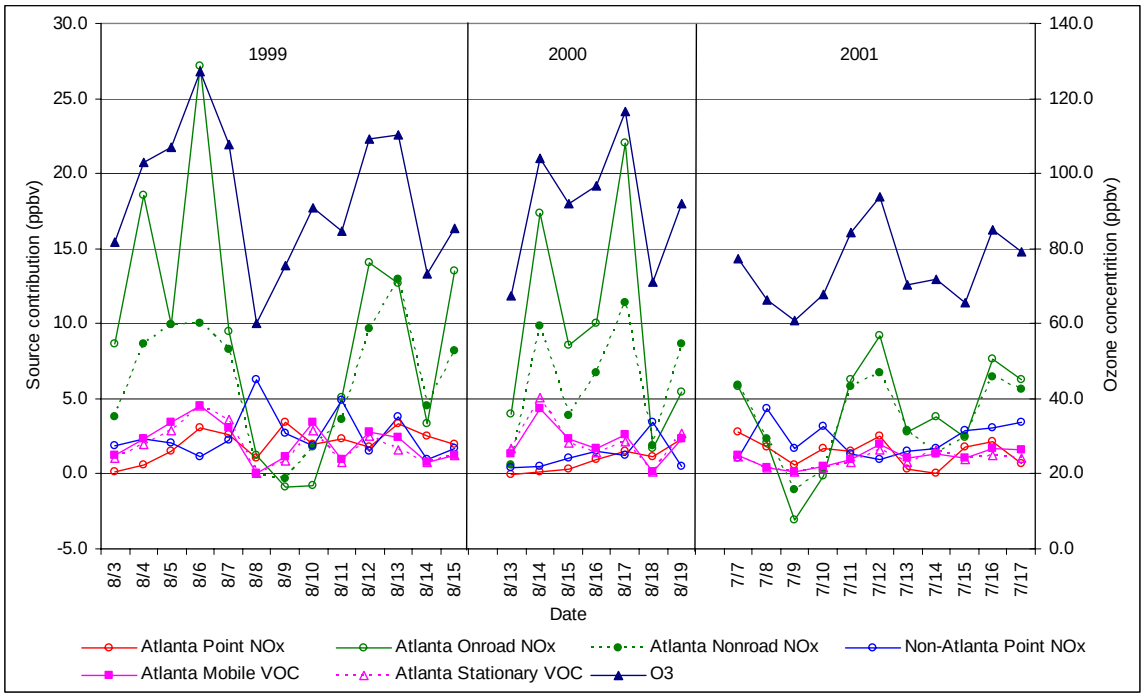

(b)

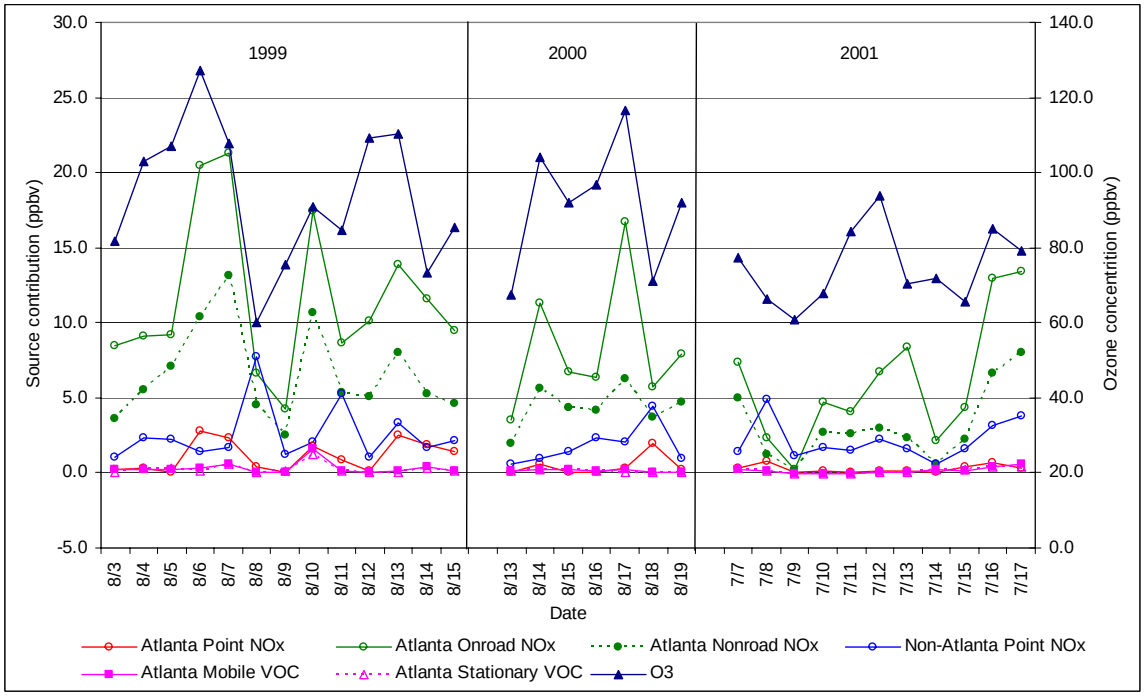

Figure 2-3 Daily peak 8-hr ozone concentrations and source contributions during 2007 under three base year episodes in downtown Atlanta (a) and suburban Atlanta (b). Right axis is for ozone concentrations and left axis is for source contributions.

P-values from linear regression analyses for source contributions and concentrations show strong correlations between elevated ozone to both Atlanta mobile NO_X and VOC emissions and Atlanta stationary VOC emissions under the three meteorologies (Table 2-4). (P-values less than 0.05 indicate correlations between source contributions and elevated ozone concentrations with 95% confidence.) Correlations between elevated ozone concentrations and stationary point NO_X emissions change year to year. For example, significant correlations between ozone concentrations and stationary point NO_X emissions in and outside of Atlanta respectively with base year 2000 and 1999 have been observed, though no correlations have been found for other years. Linear regression also indicates larger source contributions from Atlanta mobile NO_X emissions. When stationary point NO_X emissions are regressed against correlated with elevated ozone concentrations, negative linear regression coefficients are observed, implying their impacts decrease with increasing ozone concentrations, e.g., because of increased dispersion. However, the sensitivities are positive.

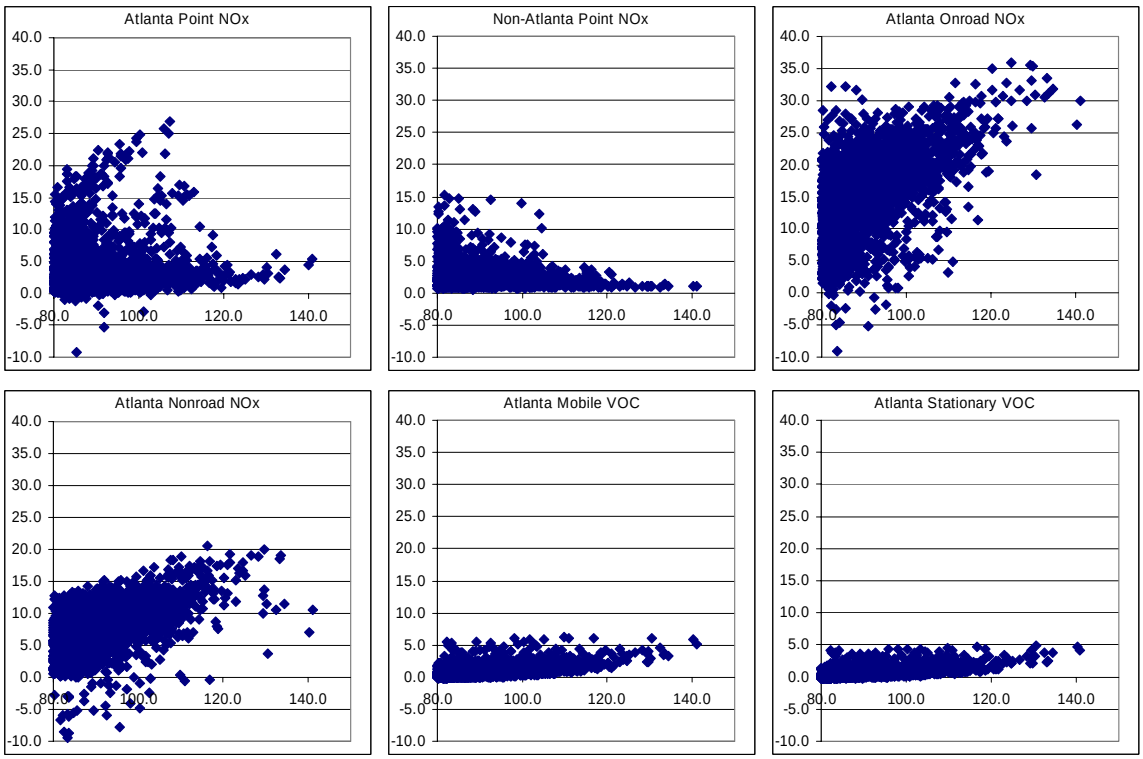

Figure 2-4 Scatter plots of 8-hr ozone source contributions during 2007 with 1999 meteorology for all grids in Atlanta at all time steps (cutoff = 80 ppbv). X axis is ozone concentrations (ppbv) and Y axis is source contributions (ppbv).

Table 2-4 Impacts of emissions from major source categories on ozone concentrations during 2007 for all grids in Atlanta at all time steps (cutoff = 80 ppbv) and their associated uncertainties with different base year episodes

	Base	Stationary Point NO_X		ATL Mobile NO_X		Mobile VOC	Stationary VOC
	Year	ATL	NATL	on-road	non-road	ATL	ATL
ZOC (ppbv)							
mean±std	1999	3.9±3.9	2.5±1.7	14.9±6.3	7.3±3.8	0.8±0.9	0.6±0.7
	2000	2.3±2.8	1.4±0.9	14.5±7.0	5.3±3.3	0.8±0.9	0.6±0.8
	2001	2.6±2.1	2.6±2.0	13.9±7.6	4.2±2.6	0.9±0.6	0.8±0.6
Correlation							
p-value	1999	0.311	0.000	0.000	0.000	0.000	0.000
	2000	0.001	0.412	0.000	0.000	0.000	0.000
	2001	0.170	0.516	0.000	0.000	0.000	0.000
Coefficient	1999	-0.008	-0.038	0.386	0.231	0.052	0.042
	2000	-0.042	-0.003	0.417	0.225	0.045	0.033
	2001	0.025	0.011	0.402	0.276	0.050	0.039
O3 Uncertainty (cov, %)							
mean±std	1999	0.77±0.68	0.52±0.37	5.6±2.0 3.3±1.3	2.9±1.6 1.7±0.84	0.31±0.34	0.18±0.24
	2000	0.48±0.55	0.31±0.20	5.5±1.7 3.2±1.2	2.9±1.9 1.6±0.81	0.45±0.54	0.37±0.47
	2001	0.55±0.42	0.53±0.37	5.4±1.7 3.1±1.3	3.0±1.1 1.7±0.65	0.53±0.40	0.45±0.36

Uncertainties in ozone concentrations from Atlanta mobile NO_X emissions have two values, the upper one assuming a factor of 2 for 95% CI and the lower one with a factor of 1.5. ATL refers to Atlanta and NATL refers to areas outside of Atlanta in the modeling domain.

Uncertainties in NO_X emissions from stationary point sources are assumed to be a factor of 1.5, while a factor of 2 is assumed for uncertainties in anthropogenic VOC emissions from mobile and stationary sources in Atlanta. Factors of 2 and 1.5 have been separately applied to uncertainties in Atlanta mobile NO_X emissions. Uncertainties in ozone concentrations (as cov) caused by uncertainties in Atlanta mobile onroad and nonroad NO_X emissions are 5.5% and 2.9% respectively when a factor of 2 is assumed (Table 2-4). These uncertainties decrease to 3.2% and 1.7% when an uncertainty factor of 1.5 for mobile NO_X is applied. Variation within an episode is less than 40% (as cov) and no significant deviation between episodes is found. They are followed by uncertainties in stationary point NO_X emissions in and outside of Atlanta, which contribute about 1% (cov). Large variation within an episode and between episodes has also been observed. It

is similar to impacts from anthropogenic VOC emissions, though with a smaller contribution to uncertainties in ozone concentrations.

Emission control responses at the time of peak 8-hr ozone in downtown Atlanta are calculated by equation 12 for point NO_X emissions in and outside of Atlanta with 20%, 40%, 60% or 80% emission reduction (Figure 2-5). Similarly, emission control responses for other sources with 20% or 40% emission reduction are estimated. With 20% or 40% emission reductions in all sources, emission control responses for Atlanta mobile onroad NO_X emissions are the highest, followed by nonroad NO_X emissions, stationary VOC emissions, mobile VOC emissions and stationary point NO_X emissions in Atlanta and stationary point NO_X emissions outside of Atlanta. This ranking is also found for average emissions control responses calculated by equation 11 (Table 2-5) for each meteorology, except fields for stationary point NO_X emissions in and outside of Atlanta using 2001. Control responses to Atlanta mobile NO_X emissions are similar for the three episodes, while significantly different control responses are found for other source categories. Different meteorological conditions and corresponding VOC emissions levels explain the difference. Average control responses for anthropogenic VOC emissions in the whole Atlanta area are much smaller than those in downtown Atlanta. This is due to higher biogenics and thus lower sensitivity of ozone concentrations to anthropogenic VOC emissions, outside of downtown Atlanta (Figure 2-3). Overall, reducing 80% of stationary point NO_X emissions and 40% of mobile NO_X emissions will lead to 10-13% reduction in ozone concentrations.

Mean control responses to stationary point NO_X and anthropogenic VOC emissions at the time of peak 8-hr ozone in downtown Atlanta agree well with respective nominal values, accompanied by a relatively larger 95% CI (Figure 2-5). These 95% CIs don’t overlap 0, indicating that ozone concentrations will decrease with emission reductions with 95% confidence. However, if a factor of 2 uncertainty in Atlanta mobile NO_X emission is used, the mean response is less than the nominal value. In this case, the

95% CIs overlap 0 and thus a reduction in Atlanta mobile NO_X emissions might lead to increased ozone concentrations. Using the mean control response also leads to different relative rankings of source categories. A large uncertainty is associated with emission control responses due to emission inventory uncertainties.

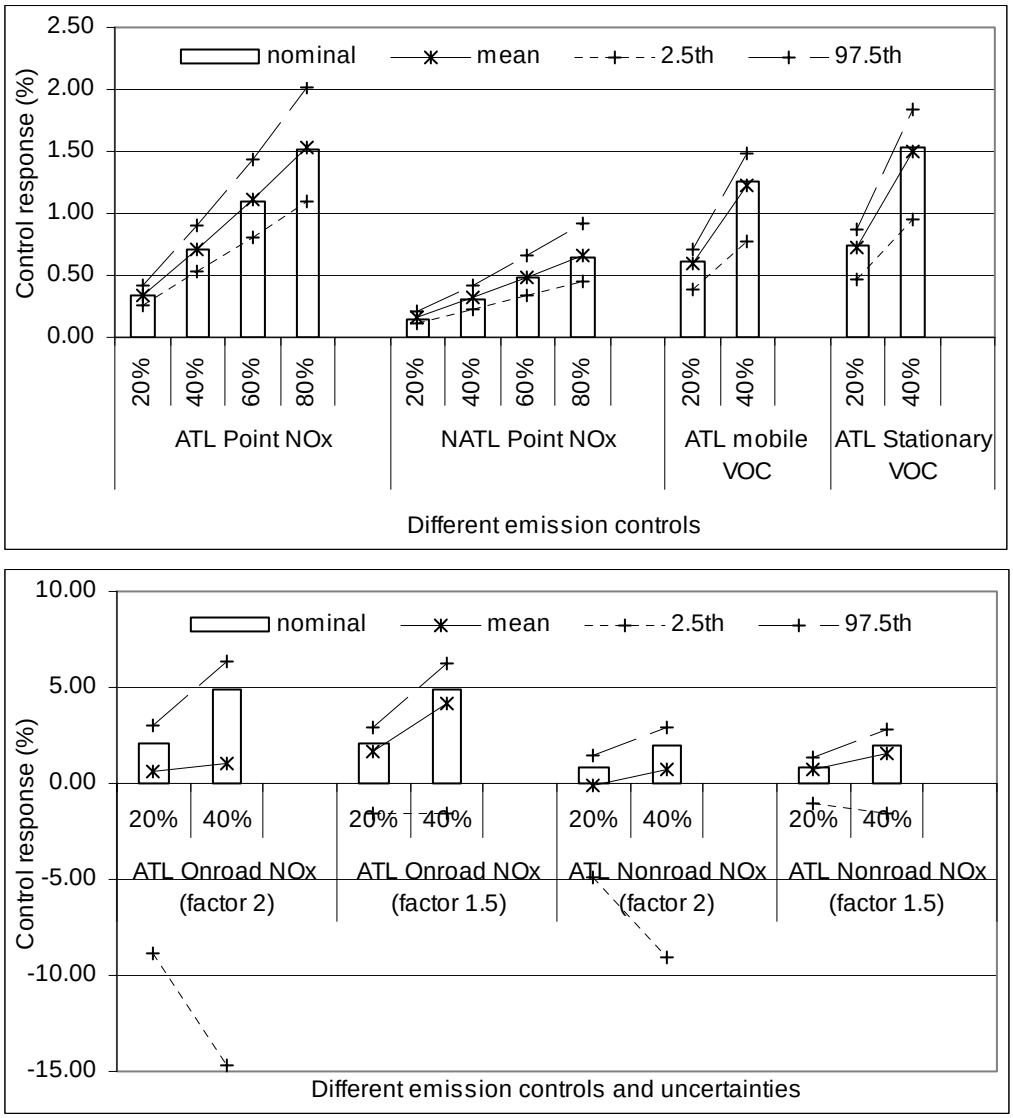

Figure 2-5 Uncertainties in emission control responses due to emission inventory uncertainties at the time of peak 8-hr ozone in downtown Atlanta, Georgia (1999 meteorology and 2007 emisisons)

ATL and NATL refer to emissions inside and outside of Atlanta respectively. Factor 2 and factor 1.5 refer to 95% CI of emission inventory uncertainties. 20%, 40%, 60%, and 80% stand for fraction of emission reduction.

Table 2-5 Emission control responses and their associated uncertainties propagated from emission inventory uncertainties for different base year meteorologies.

Sources		1999			2000			2001		
	Control	Nominal (%)	Mean (%)	% of negative	Nominal (%)	Mean (%)	% of negative	Nominal (%)	Mean (%)	% of negative
Stationary Point NO_X_ATL	20%	0.78	0.78	2.2	0.47	0.47	5.4	0.53	0.53	1.5
	40%	1.6	1.6	1.6	1.0	1.0	5.2	1.1	1.1	1.3
	60%	2.5	2.5	1.3	1.5	1.5	4.7	1.7	1.7	0.84
	80%	3.4	3.5	1.2	2.0	2.1	4.5	2.3	2.3	0.84
Stationary Point NO_X_NATL	20%	0.52	0.52	0	0.30	0.31	0	0.54	0.54	0
	40%	1.1	1.1	0	0.62	0.63	0	1.1	1.1	0
	60%	1.6	1.6	0	0.94	0.96	0	1.7	1.7	0
	80%	2.2	2.2	0	1.3	1.3	0	2.4	2.4	0
Mobile on-road_ATL	20%	2.4	1.6	27	2.3	1.9	30	2.2	1.9	34
Factor 2	40%	5.0	4.4	22	4.8	4.1	25	4.7	4.1	31
Mobile on-road_ATL	20%	2.4	2.2	11	2.3	2.2	12	2.2	2.1	18
Factor 1.5	40%	5.0	4.7	9.3	4.8	4.6	10	4.7	4.5	15
Mobile non-road_ATL	20%	1.1	0.95	29	1.1	0.89	33	1.1	0.85	37
Factor 2	40%	2.3	1.9	27	2.2	1.8	30	2.2	1.8	34
Mobile non-road_ATL	20%	1.1	1.1	13	1.1	1.0	14	1.1	1.0	19
Factor 1.5	40%	2.3	2.2	11	2.2	2.1	12	2.2	2.1	18
Mobile VOC_ATL	20%	0.15	0.15	13	0.16	0.16	14	0.20	0.19	1.3
	40%	0.31	0.31	10	0.33	0.33	12	0.40	0.39	1.1
Stationary VOC_ATL	20%	0.19	0.18	13	0.21	0.20	13	0.25	0.24	1.3
	40%	0.38	0.37	9	0.42	0.41	11	0.50	0.50	0.84

Same notes as in Figure 2-5. % of negative refers to the fraction of simulations having negative control efficiencies.

Mean emission control responses for 8-hr ozone concentrations larger than 80ppb are similar to the respective nominal values for stationary point NO_X and anthropogenic VOC emissions, but less than the nominal values for Atlanta mobile NO_X emissions. The relative ranking of control responses using the mean is the same as using nominal values. Differences between episodes are not obvious, except for stationary point NO_X and Atlanta VOC emissions, driven by the very stagnant conditions during part of 1999. The relative ranking of control efficiencies by mean values across scenarios doesn't change. The fraction of simulations with a 95% CI of control efficiencies overlapping 0, i.e.

possible negative control efficiencies are also calculated (Table 2-5). For example, with an emission uncertainty factor of 2 for Atlanta mobile onroad NO_X emissions, 27% of the simulations have negative control responses. Chances for negative control efficiencies are largest for Atlanta mobile NO_X emissions, followed by Atlanta stationary point NO_X emissions and anthropogenic VOC emissions. Reducting point NO_X emissions outside of Atlanta always lowers ozone concentration (with 95% confidence).

Conclusion

Impacts of emission inventory uncertainties on ozone formation and emission control response using future year 2007 emissions with three different historical meteorologies have been calculated using high-order sensitivities calculated by CMAQ-HDDM-3D. Large emission inventory uncertainties, e.g. a factor of 2 for all emissions except a factor of 1.5 for of stationary point NO_X emission, lead to less than 10% uncertainties (as cov) in ozone concentrations.

Elevated ozone concentrations in Atlanta are impacted by NO_X emissions from Atlanta mobile sources, point sources inside and outside Atlanta, and Atlanta anthropogenic VOC emissions in a decreasing order, with anthropogenic VOC emissions having their primary impacts in the downtown Atlanta area. Linear regression analysis indicates a strong positive correlation between ozone concentrations with source contributions from Atlanta mobile NO_X emissions and anthropogenic VOC emissions. Correlations between ozone concentrations and point NO_X emissions vary significantly from year to year and the responses decrease with increasing ozone concentrations. Uncertainties in Atlanta mobile NO_X emissions have the largest impact on uncertainties in ozone concentrations, with similar impacts of uncertainties in emissions from other source categories at a smaller scale. A large variance in the impacts of emission inventory uncertainties is found within an episode, while the variance between episodes is small.

Reducing NO_X emissions from Atlanta mobile sources gives the greatest response using the nominal values, followed by point NO_X emissions inside and outside of Atlanta and then anthropogenic VOC emissions. Mean emission control responses after consideration of emission inventory uncertainties, indicate similar rankings. Uncertainties in emissions from Atlanta mobile sources suggest that negative emission control responses, i.e. ozone concentrations increase with emission reduction are possible. Better understanding of emissions in Atlanta is required for a reliable control strategy development for Atlanta area.

Considering impacts on air quality modeling due to emission inventory uncertainties provides additional important information to policy makers. In addition, methods proposed in this paper greatly reduce the computational cost for similar uncertainty analyses, which requires running AQM hundreds of times, if not more. They can also be applied to other modeling systems, when high-order sensitivities are available.

Reference

ICF Consulting/Systems Applications International. 2002. "Ozone episode selection analysis for urban areas in northern Georgia and northern Alabama (1995-2001). Prepared for John J. Jansen, Southern Company."

Bergin, M. S., Noblet, G. S., Petrini, K., Dhieux, J. R., Milford, J. B., and Harley, R. A. (1999). Formal uncertainty analysis of a lagarangian photochemical air pollution model. Environ. Sci. Technol. 33, 1116-1126.

Byun, D. W., and Ching, J. K. S. (1999). "Science algorithms of the EPA models-3 Communicty Multiscale Air Quality (CMAQ) modeling system," Rep. No. EPA/600/R-99/030.

Chi, T. R., Unal, A., Tian, D., and Russell, A. G. (2004). Uncertainty of NONROAD Emissions in Georgia. 13th International Emission Inventory Conference "Working for Clean Air in Clearwater". http://www.epa.gov/ttn/chief/conference/ei13/.

Cohan, D. S., Hakami, A., Hu, Y. T., and Russell, A. G. (2005). Nonlinear Response of Ozone to Emissions: Source Apportionment and Sensitivity Analysis. Environ. Sci. Technol. 39, 6379-6748.

Dunker, A. M. (1981). Efficient calculation of sensitivity coeficients for complex atmospheric models. Atmos. Environ. 15, 1155-1161.

Guenther, A., Geron, C., Pierce, T., Lamb, B., Harley, P., and Falle, R. (2000). Natural emissions of non-methane volatile organic compounds, carbon monoxide, and oxides of nitrogen from North America. Atmospheric Environment 34, 2205-2230.

Hakami, A., Odman, M. T., and Russell, A. G. (2003). High-order, direct sensitivity analysis of multidimensional air quality models. Environ. Sci. Technol. 37, 2442-2452.

Hakami, A., Odman, M. T., and Russell, A. G. (2004). Nonlinearity in atmospheric response: A direct sensitivity analysis approach. J. Geophys. Res. 109, D15303.

Hanna, S. R., Chang, J. C., and Fernau, M. E. (1998). Monte Carlo estimates of uncertainties in predictions by a photochemical grid model (UAM-IV) due to uncertianties in input variables. Atmos. Environ. 32, 3619-3628.

Hanna, S. R., Lu, Z. G., Frey, H. C., Wheeler, N., Vukovich, J., Arunachalam, S., Fernau, M., and Hansen, D. A. (2001). Uncertainties in predicted ozone concentrations due to input uncertainties for the UAM-V photochemical grid model applied to the July 1995 OTAG domain. Atmos. Environ. 35, 891-903.

Hanna, S. R., Russell, A. G., Wilkinson, J. G., Vukovich, J., and Hansen, D. A. (2005). Monte Carlo estimation of uncertainties in BEIS3 emission outputs and their effects on uncertainties in chemical transport model predictions. J. Geophys. Res. 110, D01302.

Houyoux, M. R., Vukovich, J. M., Jr., C. J. W., Wheeler, N. J. M., and Kasibhatla, P. (2000). Emission inventory development and processing for the seasonal model for regional air quality. J. Geophys. Res. 105, 9079-9090.

Hu, Y., Cohan, D. S., Odman, M. T., and Russell, A. G. (2004). "Air quality modeling of the August 11-20, 2000 episode for the Fall Line Air Quality Study. Prepared for Environmental Protection Division, Georgia Department of Natural Resources."

Hu, Y., Odman, M. T., and Russell, A. G. (2003). "Meteorological modeling of the first base case episode for the Fall Line Air Quality Study. Prepared for Environmental Protection Division, Georgia Department of Natural Resources."

Lin, X., Trainer, M., and Liu, S. C. (1988). On the nonlinearity of the tropospheric ozone production. J. Geophys. Res. 93, 15879-15888.

Morgan, M. G., and Henrion, M. (1990). "Uncertainty: A Guide to Dealing with Uncertainty in Quantitative Risk and Policy Analysis," Cambridge University Press.

NARSTO (2003). "Particulate matter science for policy makers."

Placet, M., Mann, C. O., Gilbert, R. O., and Niefer, M. J. (2000). Emissions of ozone precursors from stationary sources: a critical review. Atmospheric Environment 34, 2183-2204.

Russell, A. G., and Dennis, R. (2000). NARSTO critical review of photochemical models and modeling. Atmospheric Environment 34, 2283-2324.

Sawyer, R. F., Harley, R. A., Cadle, S. H., Norbeck, J. M., Slott, R., and Bravo, A. (2000). Mobile sources critical review: 1998 NARSTO assessment. Atmospheric Environment 34, 2161-2181.

Tian, D., Hu, Y., and Russell, A. G. (2004). "Meteorological modeling of the 1999 August episode for the Fall-Line Air Quality Study. Prepared for Environmental Protection Division, Georgia Department of Natural Resources."

Unal, A., Tian, D., Hu, Y., and Russell, A. G. (2003). "2000 August Emissions Inventory for Fall Line Air Quality Study (FAQS). Prepared for Environmental Protection Division, Georgia Department of Natural Resources."

Yang, Y.-J., Wilkinson, J. G., and Russell, A. G. (1997). Fast, direct sensitivity analysis of multidimensional photochemical models. Environ. Sci. Technol. 31, 2859-2868.

CHAPTER 3 UNCERTAINTIES IN BIOMASS BURNING EMISSIONS AND SEASONAL $PM_{2.5}$ SOURCE CONTRIBUTIONS IN THE SOUTHEASTERN UNITED STATES USING CMAQ

Abstract

Biomass burning emissions are a major contributor to $PM_{2.5}$ in the southeastern United States and are investigated using source-oriented air quality modeling. Impacts of uncertainties in emissions, including total amount, temporal and spatial characteristics, and speciation on air quality modeling during January are first investigated to identify emission shortcomings. Estimated source contributions from biomass burning are further compared with CMB results at two SEARCH sites (JST and YRK), suggesting a 90% reduction of emissions from wood burning in fireplaces and woodstoves. The improved emissions recommended by the above uncertainty analysis are then developed for March, May and July 2002. Both primary and secondary impacts from biomass burning are identified. Tracers linked to each individual biomass burning source are used to study individual source contributions. About 83% of $PM_{2.5}$ caused by biomass burning is primary (e.g. primary organic aerosol and elemental carbon), and the rest is secondary in origin (e.g. secondary organic aerosol, ammonium and nitrate). Air quality impacts from biomass burning have large temporal and spatial variations, higher in winter (January) and spring (March), and lower in summer (May and July). Biomass burning influences much of the modeling domain and peaks in the southwestern Georgia (a more rural area). Prescribed burning is has the largest air quality impacts among biomass burning sources,

---

This chapter will be submitted to Journal of Geophysical Research. Co-authors are Yongtao Hu, Yuhang Wang, and Armistead Russell.

peaking in March and the southwestern Georgia. Overall impacts from wildfires are much smaller in spite of a sever local impact and peak in May. Emissions from other biomass burning have significant air quality impacts during January and March at much smaller magnitudes, and negligible impacts during May and July. In the Atlanta $PM_{2.5}$ non-attainment area prescribed burning is always the largest biomass burning source, followed by land clearing and wood burning in fireplaces and woodstoves. Understanding the source contribution of biomass burning can help policy-makers design more efficient and effective control strategies. In addition, better knowledge of organic aerosols from primary sources will assist the investigation of secondary organic aerosols.

Introduction

Biomass burning is combustion processes that consume biomass fuels, either though natural processes (e.g. wildfires) or man-made processes (e.g. prescribed burning, agriculture field burning, land clearing, wood burning in fireplace and woodstove, residential leaf burning, etc). During combustion, large amounts of air pollutants, e.g. particulate matter (PM), volatile organic compounds (VOCs), nitrogen oxides (NO_X), ammonia (NH_3), and carbon monoxide (CO) can be emitted. In the United States, biomass burning contributes about 35% of the fine particulate matter ($PM_{2.5}$, i.e. PM with aerodynamic diameter less than 2.5 μm) emissions [*US-EPA*, 2004]. Much of the mass emitted is carbonaceous (70-95%) and carbonaceous material is a substantial component of $PM_{2.5}$ in the United States [*NARSTO*, 2003]. Previous $PM_{2.5}$ source apportionment studies using both receptor models and source-oriented models (SOMs) suggest significant contributions from biomass burning in the southeastern United States [*Kim, et al.*, 2003; *Kim*, 2003; *Liu, et al.*, 2005; *Marmur, et al.*, 2006; *Park, et al.*, 2006; *Zheng, et al.*, 2002; *Zheng, et al.*, 2006]. In addition, a resent study shows that climate change leads to increased wildfire activities in the western United States [*Westerling, et al.*, 2006].

$PM_{2.5}$ air pollution adversely affects human haealth [*Dockery, et al.,* 1993]. It also can degrade visibility [*Malm, et al.*, 2000] and influence global warming [*IPCC,* 2001]. Recent studies suggest that the carbonaceous component in $PM_{2.5}$ has potentially the largest adverse impacts on human health [*Peel, et al.*, 2005]. In response to health concerns, the U.S. Environmental Protection Agency (US EPA) promulgated a National Ambient Air Quality Standard (NAAQS) in 1997 for $PM_{2.5}$ and designated non-attainment areas in December 2004. In addition, visibility reduction due to $PM_{2.5}$ is of concern, and is addressed under the Clean Air Act Amendment and the US EPA's 1999 Regional Haze Rule. Regulators are now faced with identifying effective strategies to lower $PM_{2.5}$ levels and thus must address biomass burning.

Two types of air quality models are usually employed to investigate air quality impacts from biomass burning emissions. Receptor models estimate source contributions with ambient observations and respective source profiles. Generally, different biomass burning sources have similar source profiles, and thus results from receptor models cannot differentiate source contributions from these sources. Furthermore, emissions from biomass burning have large spatial and temporal variations. For example, large-scale wildfires are usually limited to regions with available fuels during dry and hot seasons. Limited observation sites are insufficient to catch area-wide air quality impacts. Source-oriented models, which are capable of simulating air pollutant concentrations based on detailed emissions and meteorological conditions, however, can be used in this type of assessment.

Accuracy of air quality impact estimates found using SOMs is greatly affected by the quality of emission and meteorological inputs and modeling algorithms. Uncertainties in emission inputs are addressed in this study, since such data is suspected of having potentially large uncertainties [*NARSTO,* 2003]. Improved emission estimates with better temporal and spatial characteristics are developed and applied to investigate air quality impacts from biomass burning during January, March, May and July 2002, with

particular focus on the state of Georgia, where biomass burning emissions are large. These months are chosen as they have different levels of biomass burning emissions. During these months, meteorological conditions and physical-chemical processes of pollutants in the atmosphere are quite different as well. Specifically, biomass burning emissions during winter and spring are typically much larger than during summer in Georgia, with emissions from prescribed burning (the largest individual biomass burning source) peaking in March, emissions from fireplaces and woodstoves in January, emissions from wildfires in May, and very low biomass burning emissions in July.

Methods

Air quality modeling

Four months in 2002 (January, March, May and July) are simulated with the Community Multiscale Air Quality (CMAQ) model v. 4.3 using SAPRC-99 as the chemical mechanism, ISORROPIA for aerosol equilibrium, Modified Euler Backward Iterative (MEBI) method for the chemistry solver, the Regional Acid Deposition Model (RADM) for clouds, AERO3 for aerosol dynamics and the Piecewise Parabolic Method (PPM) for horizontal and vertical advections [*Byun and Ching*, 1999]. Results of the fist two days for each month are discarded as model initialization periods. The modeling domain has 19 vertical layers reaching to about 15 km vertically, with a 36 m bottom layer. It covers the southeastern United States at 12-km resolution. Initial and boundary conditions are supplied by simulations on a 36-km resolution grid covering the United States (Unified RPO modeling domain). Meteorological conditions for the episodes are simulated with the NCAR/Penn State 5th generation Mesoscale Model (MM5), described in detail elsewhere [*Grell, et al.*, 1994; *Olerud and Sims*, 2003]. Emission inventories are obtained from VISTAS, and hereafter referred to as VISTAS 2002 [*VISTAS*, 2005], and

then processed through the Carolina Environmental Program's (CEP) Sparse Matrix Operator Kernel Emissions (SMOKE) Modeling System v. 2.1 [*Houyoux, et al.*, 2000].

Simulations from the above modeling are evaluated by comparing model results with observations collected as part of the Interagency Monitoring of Protected Visual Environments (IMPROVE), the SouthEastern Aerosol Research and Characterization (SEARCH), the Assessment of Spatial Aerosol Composition in Atlanta (ASACA) and the Speciation Trends' Network (STN) networks. Organic carbon (OC) observations are converted to organic matter (OM) by multiplying using a factor of 1.4, which has been widely used, though recent studies suggest it is low [*Turpin and Lim*, 2001]. Six performance metrics: including mean bias (MB), mean error (ME), normalized mean bias (NMB), normalized mean error (NME), mean fractional bias (MFB), and mean fractional error (MFE), are calculated [*Boylan, et al.*, 2006].

Uncertainties in biomass burning emissions

Uncertainties in total amount of emissions

Emissions from biomass burning sources are typically calculated as the product of the burned area (A), fuel consumed per area (F_a) and an emission factor (E_f):

$$E = A \times F_a \times E_f \quad (1)$$

Fuel consumption is the amount of biomass consumed during a fire per area burned, and the emission factor is the ratio of the mass of pollutant emitted per unit mass of fuel consumed. Two different emission inventories for wildfires, prescribed and agriculture field burning and land clearing, all specific to Georgia, are employed to study the impact from uncertainties in total amount of emissions. One emission inventory is obtained from the US EPA 2001 modeling platform emission inventory (hereafter referred to as EPA 2001) [*US-EPA*, 2004], and the other is VISTAS 2002 [*VISTAS*, 2005]. They are developed using different estimation methods. In EPA 2001, emissions

from wildfires and prescribed burning are developed by obtaining burned area at state- or regional-level, and then allocated to county-level according to specific spatial surrogates (e.g. acres of forest). Emissions from agriculture field burning are developed by estimating the burned area according to state-level crop production, assuming that 3% of the crop residual is consumed, and emissions from land clearing are based on the area disturbed by residential, non-residential, and road construction. In VISTAS 2002, case-specific burned area for wildfires and county-level burned areas for other types of burning are directly obtained by surveying state and federal agencies, with updated fuel loading and emission factors for wildfires and prescribed burnings.

Uncertainties in temporal and spatial characteristics of emissions

Emissions from biomass burning sources are traditionally inventoried at annual- and county- levels. To develop more spatially and temporally resolved (e.g. gridded and hourly) emissions for air quality modeling, they are processed using spatial surrogates and temporal (monthly, daily, and diurnal) profiles in emission models (e.g. SMOKE in this study). However, biomass burning emissions, especially from wildfires, prescribed and agriculture field burning, and land clearing, are rather stochastic, often intense events and are not well captured by such approaches. For example, wildfires will not uniformly occur across all forests everyday of the fire season. As such, significant temporal and spatial uncertainties are expected in the emissions developed using SMOKE. However, accounting for when and where fires actually occur are important to detailed studies of the impact of biomass burning on ambient $PM_{2.5}$ concentrations.

Emissions from prescribed and agriculture field burning and land clearing are inventoried at the annual and county-level in EPA 2001 and VISTAS 2002, as are emissions from wildfires in EPA 2001. Emissions from wildfires in VISTAS 2002 are treated as point sources with daily emissions and detailed location information for each burning. Source-specific monthly, daily or diurnal temporal profiles are required to

allocate these emissions to hourly level. Generally, monthly temporal allocation factors specific to a source are used to allocate annual total emissions in each county to monthly level. The difference in burning seasons between counties is ignored in the process. The same factors can also alter the relative spatial distributions of emissions during a certain period. Hence, a monthly county-level emission inventory for prescribed and agriculture field burning and land clearing are developed here (hereafter referred to as UPDATED), using detailed burned area data [*GFC*, 2005] and the same fuel loading and emissions factors as in VISTAS 2002. Different model results with VISTAS 2002 and UPDATED emission inventory indicate the influence from detailed monthly-level emissions.

Source-specific daily temporal profiles are obtained from VISTAS [*VISTAS*, 2005]. By default, allocation of emissions from prescribed and agriculture field burning, and land clearing are not day dependent. However, staff at the Georgia Forest Commission, who are responsible for issuing burning permits in Georgia, indicate that these burnings predominantly occur during weekdays [*Commission*, 2005]. In addition, burning occurrence also depends on meteorological and fuel conditions. For example, burning permits are not issued when dispersion is low, or burning can't be successfully conducted after precipitation when fuels are wet [*Hardy, et al.*, 2001]. However, currently available records do not carry the detailed information at the daily level. Simulated air quality impacts with two different daily temporal profiles are compared. One of the profiles equally allocates monthly emissions from prescribed burning to each day, and the other profile allocates such emissions only to weekdays.

Uncertainties in $PM_{2.5}$ speciation

Uncertainties in speciation of primary $PM_{2.5}$ biomass burning emissions into primary OM (POA), elemental carbon (EC), sulfate (SO_4^{2-}), nitrate (NO_3^-), and other unspecified mass using speciation profiles, are essential to the understanding of speciated $PM_{2.5}$. $PM_{2.5}$ speciation profiles for biomass burning emissions are obtained from EPA

[*US-EPA*, 2004], with POA as the major species. Such POA concentrations are currently calculated by multiplying the OC measurements with a factor of 1.2-1.4 to account for the other elements bound to C [*Fine, et al.*, 2002; *Hays, et al.*, 2005]. However, molecular level analyses of POA indicate that the POA/OC ratio for wood burning is about 1.9 [*Turpin and Lim*, 2001]. In addition, these analyses only measure less polar organics and do not account for water-soluble species which comprise 20-80% of organic aerosols [*Saxena and Hildemann*, 1996; *Sullivan and Weber*, 2006]. Since more water-soluble organic compounds have higher ratios of molecular weight to carbon weight than less water-soluble organic compounds, the POA/OC ratio for biomass burning may be larger than 1.9. As such, current speciation profiles tend to underestimate the POA fractions. Here, POA fractions for wildfires, prescribed burning and wood burning in fireplaces and woodstoves are recalculated by subtracting fractions of EC (f_{EC}), SO_4^{2-} ($f_{SO4^{2-}}$), NO_3^- (f_{NO3^-}) and other unspecified mass (f_{other}) from 1:

$$f_{POA} = 1 - f_{EC} - f_{SO4^{2-}} - f_{NO3^-} - f_{other} \quad (2)$$

The f_{EC}, $f_{SO4^{2-}}$, f_{NO3^-}, and f_{other} for wildfires and prescribed burning are updated by recent field and lab measurements [*Andreae and Merlet*, 2001; *Hays, et al.*, 2002; *Lee, et al.*, 2005]. These measurements don't show significant difference between emissions from wildfires and prescribed burning and thus the same speciation profile is employed. Measurements for species other than EC, OC, SO_4^{2-} and NO_3^- (e.g. Potassium and chloride) are considered as other unspecified mass. Similarly, the speciation profile for wood burning in fireplaces and woodstoves is updated by recent lab measurements for dominant tree species in the southern United States [*Fine, et al.*, 2002] and typical woods used for wood-burning [*Mcdonald, et al.*, 2000]. Significant difference in emission characteristics from different crops, e.g. wheat and rice, has been observed in lab measurements [*Hays, et al.*, 2005]. However, information on agriculture burned areas by crops and emission factors for every crop is lacking. In addition, even though land

clearing appears to emit more visible smoke [*Commission*, 2005], there is no available information that can be used to improve its speciation profile. Therefore, US EPA recommended speciation profiles are used for agriculture field burning and land clearing [*US-EPA*, 2004].

Impacts of uncertainties in emissions on air quality modeling are investigated in January 2001, when emissions from various biomass burning sources are significant. These impacts are further evaluated by comparing with observation data and receptor modeling results using Chemical Mass Balance (CMB). The CMB modeling employed both identified individual organic compounds and elemental species (e.g. sulfate, nitrate, ammonium, elemental carbon, organic carbon, and trace metals) [*Chen and Zheng*, 2006; *Zheng, et al.*, 2002]. Relative distributions of organic compounds in source emissions provide additional means to identify source contributions that cannot be uniquely identified by elemental compositions alone.

Seasonal air quality impacts from biomass burning

Improved emissions described in the previous are applied to all episodes. Air quality impacts from biomass burning emissions are obtained by comparinging CMAQ simulations with and without biomass burning emissions. Both primary and secondary impacts are therefore assessed. Source contributions from individual biomass burning sources are computed by tracing POA (the major component) emissions from these sources in CMAQ. These tracer emissions are generated by SMOKE using specific speciations, and then input into CMAQ together with other emissions. These tracers are treated as non-reactive species, and go through similar physical processes as other primary carbonaceous aerosol species [*Baek, et al.*, 2005].

Results and discussion

Impacts of emission uncertainties on air quality modeling

Emissions from wildfires, prescribed and agriculture field burning, and land clearing in Georgia during 2002 estimated in EPA 2001 differ significantly from VISTAS 2002, due to different estimation methods and input data used (Table 3-1). There are around 18,000 tons/year more $PM_{2.5}$ emissions in VISTAS 2002 than EPA 2001. In EPA 2001, emissions are distributed almost equally among the four biomass burning sources. In comparison, the difference among the burning sources in VISTAS 2002 is fairly large, and prescribed burning contributes about 70% of the total emissions from the four sources combined. These emissions are much larger than emissions from other biomass burning sources (e.g. wood burning in fireplaces and woodstoves).

Table 3-1 Summary of biomass burning emissions in Georgia during 2002 (103 tons/year)

		CO	VOC	NO_X	NH_3	SO_2	PM_{10}	$PM_{2.5}$
EPA 2001	Wildfires	130	5.9	2.7	0.56	0.74	12	10.4
	Prescribed burning	110	5.1	2.3	0.47	0.62	10	8.7
	Agriculture burning	2	0.4	-[2]	-	-	11	9.8
	Land clearing	100	7.0	3.0	-	-	10	10
	Sub_total	340	18	8.0	1.0	1.4	43	39
VISTAS2002	Wildfires	100	4.7	2.1	0.45	0.59	9.7	8.3
	Prescribed burning	470	22	10	2.1	2.8	46	40
	Agriculture burning	17	2.6	-	-	-	3.0	3.0
	Land clearing	64	4.4	1.9	-	-	6.5	6.5
	Sub_total	650	34	14	2.6	3.4	65	57
	Fireplaces [1]	53	27	0.6	-	0.13	9.0	9.0
	Other biomass	2	0.4	-	-	-	0.5	0.5
	Sub_total	55	27	0.6	-	0.13	9.6	9.6

[1] Fireplaces refers to the sum of emissions from both fireplaces and woodstoves.
[2] - refers to no emissions or emissions are less then 10 tons/year.

Different temporal and spatial distributions of $PM_{2.5}$ emissions are also expected for simulations with the two different emission inventories, due to the different temporal

and spatial characteristics of each biomass burning source, as well as corresponding $PM_{2.5}$ concentrations. POA emissions in January with EPA 2001 are more intense in the Atlanta area than VISTAS 2002, which have denser emissions in the southwestern Georgia (Figure 3-1). Responsive POA concentrations with EPA 2001 are higher than VISTAS 2002 by 0.7 $\mu g/m^3$ for the Atlanta $PM_{2.5}$ non-attainment area, and less than VISTAS 2002 by 0.6 $\mu g/m^3$ for the whole Georgia (Figure 3-1). Estimates with VISTAS 2002 agree well with the fact that most forest fires in Georgia are conducted under control, i.e. prescribed burning [*Commission*, 2005]. Total annual emissions from biomass burning in UPDATED are same as VISTAS 2002. However, spatial distributions of POA emissions and concentrations are significantly different between the two inventories. These differences can be attributed to the application of county-specific monthly temporal profiles. Simulations with different emission inventories are also compared with the observations. Model performance statistics with VISTAS 2002 are better than those with EPA 2001, whereas they are almost same as those with UPDATED due to the fact that most monitor sites are outside of the affected regions (Table 3-3 and Figure 3-2).

Daily $PM_{2.5}$ concentrations vary significantly from day to day with the same biomass burning emissions as a result of different meteorological conditions. Sensitivity results show that monthly averaged $PM_{2.5}$ concentrations not affected by daily temporal profiles for prescribed burning (not shown). Since the exact dates when the biomass burning occur are rarely known, air quality impacts from biomass burning are analyzed monthly.

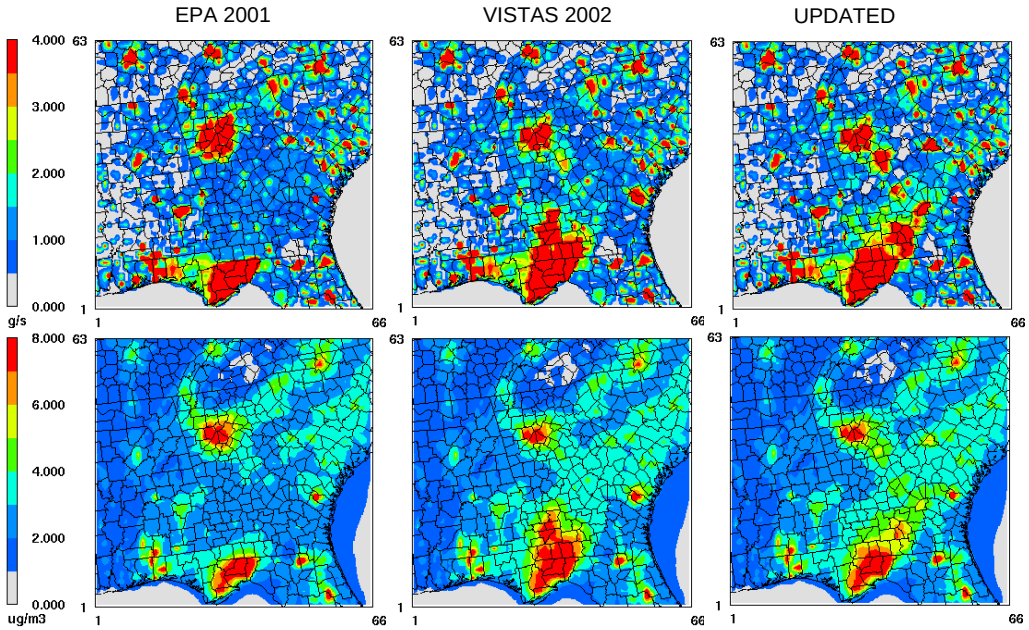

Figure 3-1 Monthly-average POA emissions (first row) and concentrations (second row) using different emission inventories during January 2002

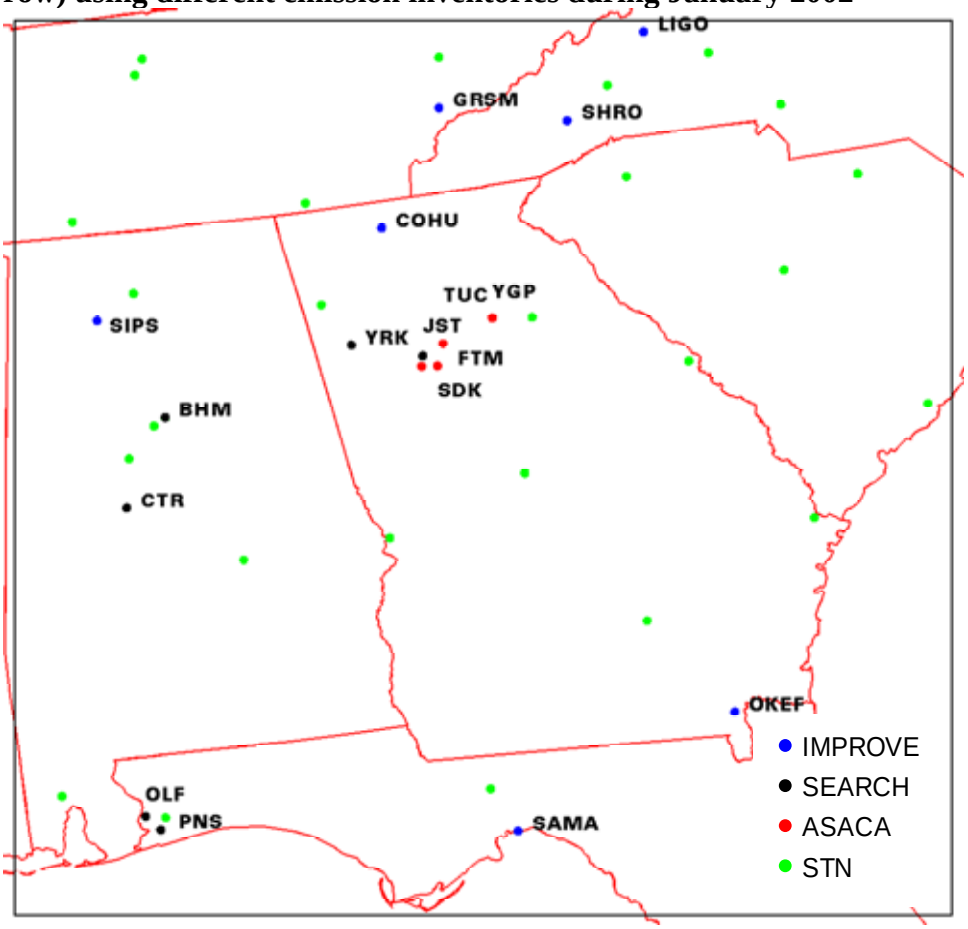

Figure 3-2 Observation sites in the IMPROVE, SEARCH, STN, and ASACA networks

EC and POA are major species for emissions from biomass burning. The EC fraction for emissions from wildfires and prescribed burning is reduced from EPA recommended 0.16 to 0.056, according to recent measurements. The EC fraction for wood burning in fireplaces and woodstoves combustion found by recent measurements is similar to the value recommended by EPA and thus the EPA value is kept same. Updated POA fractions derived using equation (2) increase by 0.13 for wildfires and prescribed burning, and by 0.30 for wood burning in fireplaces and woodstoves (Table 3-2). Given POA and OC ratios are larger than 1.9 for biomass burning emissions according to molecular level analyses, updated OC fractions are less than 0.5. They are much lower than the measurements (0.602-0.788 for forest fires and 0.530-0.718 for residential wood burning based on the measurements mentioned above), indicating that the updated POA fractions do not overestimate POA contributions. The lower OC fractions calculated here could be partially explained by the absorption of organic vapor on quartz fiber filters and accordingly overestimated OC levels in the measurements [*Fine, et al.*, 2002]. Simulations with updated speciation profiles lead to increased POA and decreased EC emissions, as well as corresponding OM and EC concentrations. Model performance of EC is significantly improved; however, model performance of OM deteriorates significantly (Table 3-3).

Table 3-2 $PM_{2.5}$ speciation profiles for biomass burning sources

		POA	EC	SO_4^{2-}	NO_3^-	Other
Wildfire & Prescribed burn	EPA	0.770	0.160	0.020	0.002	0.048
	Updated	0.898	0.056	0.001	0.015	0.030
Fireplace and Woodstove	EPA	0.566	0.108	0.004	0.002	0.321
	Updated	0.865	0.108	0.004	0.003	0.020
Agriculture burn	EPA	0.670	0.040	0.010	0.003	0.277
Land clearing	EPA	0.670	0.040	0.010	0.003	0.277

Table 3-3 EC and OM performance with different emission uncertainties during January 2002 (Means of EC and OM observations are 0.84 µg/m^3 and 4.83 µg/m^3 respectively.)

Species	Uncertainties in emissions	SIM_mean (µg/m^3)	MB (µg/m^3)	ME (µg/m^3)	NMB (%)	NME (%)	MFB (%)	MFE (%)
EC	EPA 2001	1.13	0.29	0.68	34.2	80.4	22.1	58.5
	VISTAS 2002 / UPDATED	1.13	0.29	0.68	34.5	80.6	22.0	58.4
	UPDATED & Speciation	1.03	0.19	0.62	22.7	73.4	13.3	55.3
	UPDATED & Speciation 90% reduction	0.86	0.01	0.49	1.5	58.1	3.9	50.2
OM	EPA 2001	6.02	1.19	3.05	24.6	63.1	18.3	54.9
	VISTAS 2002 / UPDATED	5.90	1.07	2.94	22.2	60.9	16.3	53.6
	UPDATED & Speciation	6.83	2.00	3.63	41.4	75.2	26.3	57.9
	UPDATED & Speciation 90% reduction	5.34	0.51	2.42	10.5	50.0	11.9	48.9

[1] EPA 2001 refers to the simulation with EPA 2001 emission inventory.
[2] VISTAS 2002 / UPDATED refers to the simulation with VISTAS 2002 or UPDATED emission inventories.
[3] UPDATED & Speciation refers to the simulation with UPDATED emission inventory and updated speciation profiles.
[4] UPDATED & Speciation & 90% reduction refers to the simulation with UPDATED emission inventory and updated speciation profiles, as well as 90% emission reduction of wood burning in fireplaces and woodstoves.

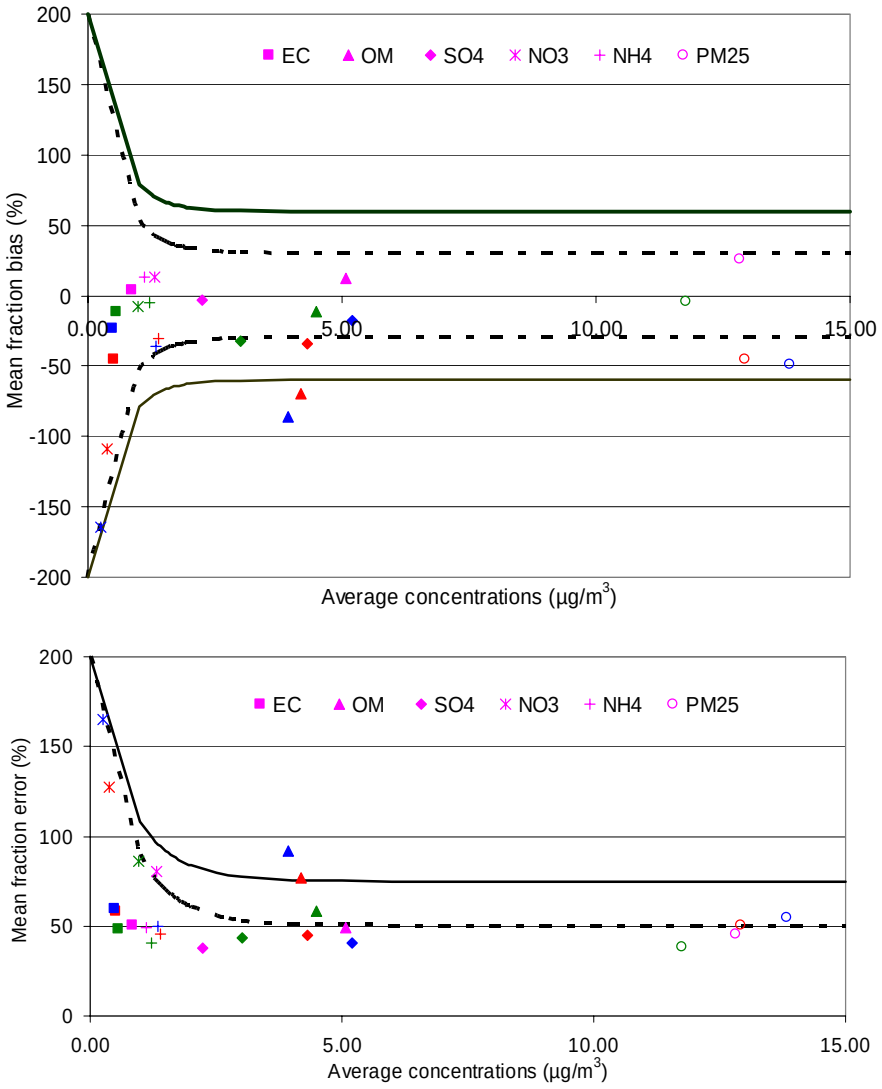

Figure 3-3 Air quality modeling performance of total and speciated $PM_{2.5}$ during four months in 2002. (Solid and dashed lines are suggested criteria from Boylan, 2005) January (purple), March (green), May (red), July (blue)

Table 3-4 Air quality modeling performance of total and speciated $PM_{2.5}$ during January, March, May and July 2002

Month	Species	NOBS (#)	OBS_mean (µg/m³)	SIM_mean (µg/m³)	MB (µg/m³)	ME (µg/m³)	NMB (%)	NME (%)	MFB (%)	MFE (%)
January	EC	260	0.84	0.86	0.01	0.49	1.5	58.1	3.9	50.2
	OM	260	4.83	5.34	0.51	2.42	10.5	50.0	11.9	48.9
	SO_4^{2-}	255	2.29	2.20	-0.10	0.85	-4.3	37.0	-3.4	37.5
	NO_3^-	253	0.97	1.66	0.70	0.97	72.0	100.5	12.9	80.2
	NH_4^+	249	1.00	1.24	0.24	0.54	23.7	54.1	13.3	49.3
	$PM_{2.5}$	253	10.89	14.75	3.86	5.79	35.5	53.2	26.0	45.5
March	EC	266	0.58	0.55	-0.03	0.27	-5.6	46.1	-11.3	48.5
	OM	266	4.31	4.68	0.38	2.56	8.7	59.5	-11.4	58.3
	SO_4^{2-}	285	3.54	2.49	-1.05	1.28	-29.5	36.3	-32.4	43.3
	NO_3^-	284	0.75	1.19	0.44	0.82	58.3	109.3	-8.0	86.1
	NH_4^+	283	1.23	1.20	-0.03	0.47	-2.7	37.8	-5.4	40.8
	$PM_{2.5}$	279	11.64	11.88	0.24	4.40	2.1	37.8	-4.5	38.5
May	EC	253	0.62	0.40	-0.22	0.30	-35.0	48.5	-44.7	58.5
	OM	253	5.66	2.74	-2.92	3.17	-51.6	56.0	-69.9	77.1
	SO_4^{2-}	263	4.96	3.65	-1.31	1.83	-26.5	36.9	-34.5	45.0
	NO_3^-	256	0.54	0.23	-0.31	0.44	-57.2	81.8	-108.6	127.2
	NH_4^+	235	1.58	1.21	-0.37	0.59	-23.3	37.6	-30.9	45.8
	$PM_{2.5}$	252	15.71	10.15	-5.56	6.32	-35.4	40.2	-45.0	50.4
July	EC	333	0.54	0.42	-0.13	0.29	-22.9	52.3	-23.2	60.0
	OM	334	5.63	2.23	-3.40	3.58	-60.3	63.5	-86.2	91.5
	SO_4^{2-}	352	5.61	4.78	-0.83	2.18	-14.8	38.8	-18.1	40.4
	NO_3^-	346	0.43	0.06	-0.37	0.38	-86.9	87.7	-164.1	165.3
	NH_4^+	335	1.60	1.09	-0.51	0.68	-31.7	42.7	-35.6	49.5
	$PM_{2.5}$	342	16.97	10.67	-6.29	7.34	-37.1	43.2	-48.4	54.9

(a) January

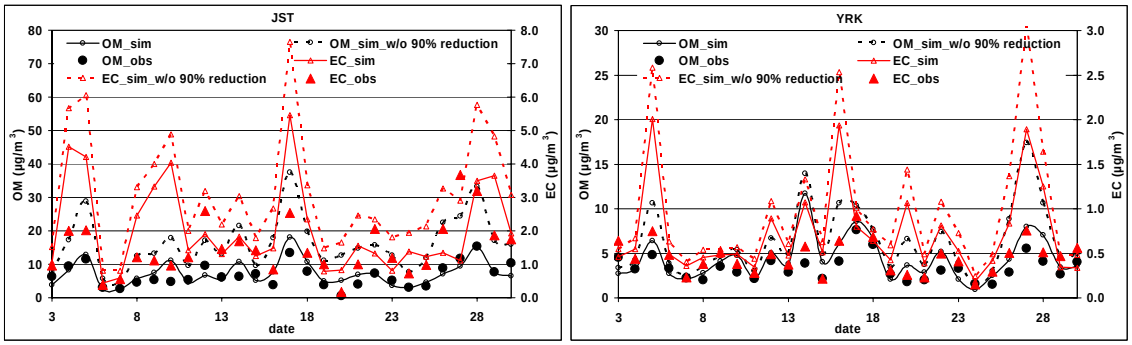

(b) March

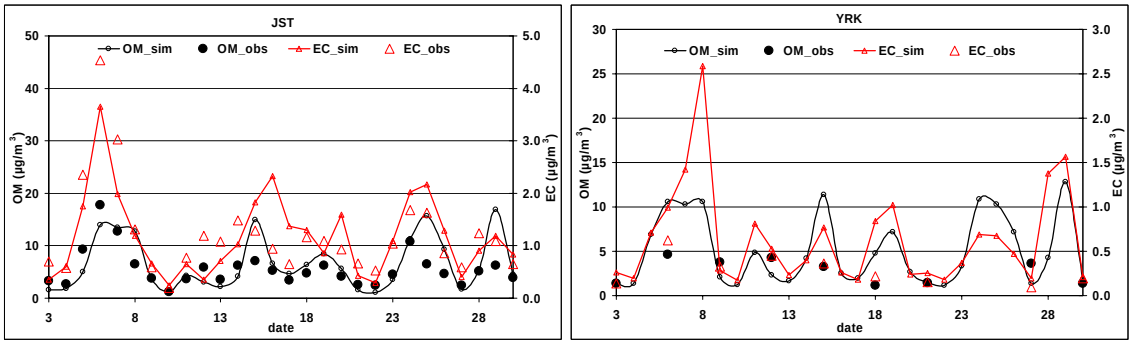

(c) May

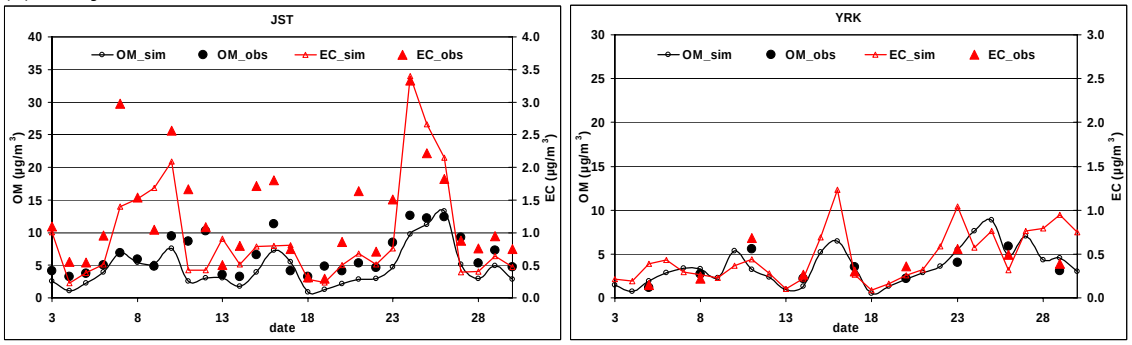

(d) July

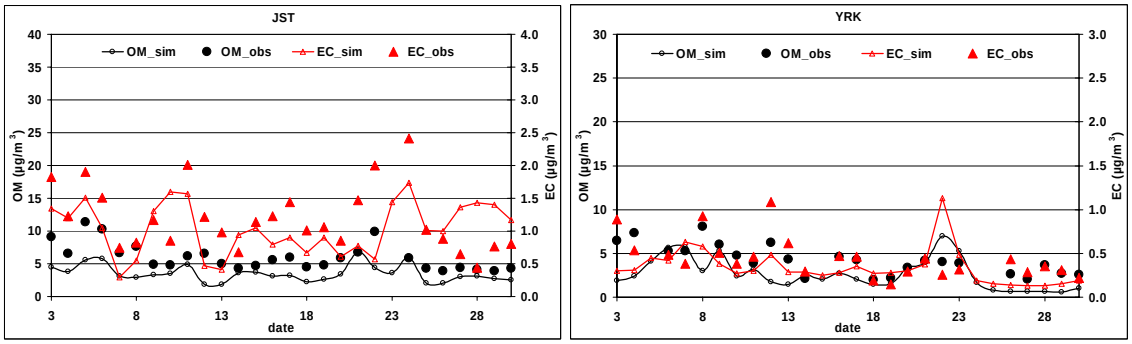

Figure 3-4 Comparison of EC and OM simulations with observations in 2002. JST refers to a SEARCH station at Jefferson Street, Atlanta, Georgia. YRK refers to a SEARCH station at Yorkville, Georgia. OM(EC)_sim: simulated OM(EC) concentrations. OM(EC)_obs: observed OM(EC) concentrations. w/o 90% reduction refers to simulations without 90% reduction of emissions from wood burning in fireplaces and woodstoves.

Time series of simulated and observed daily OM and EC during January at the two SEARCH sites: one urban station located in Jefferson Street, Atlanta, Georgia (JST) and one rural station in Yorkville, Georgia (YRK) show that simulated values fairly follow the observations (Figure 3-4). However, simulated OM and EC are consistently overestimated, indicating a possible high bias in emissions. Estimated $PM_{2.5}$ source contributions from biomass burning during January illustrate that biomass burning contributes to 50-70% of OM and 30-40% of EC at JST and YRK. As such, emissions from biomass burning are suspected as the reason for overestimation. We adjust emissions according to findings using CMB modeling. The CMB analysis of measurements at JST and YRK suggest that wood burning contributed 1.59 $\mu g/m^3$ at JST and 0.450 $\mu g/m^3$ at YRK during January (as $PM_{2.5}$), in comparison with simulated 13.2 $\mu g/m^3$ at JST and 4.2 $\mu g/m^3$ at YRK. Assuming the results from CMB are relatively accurate, a reduction of emissions from biomass burning by 88% is suggested. Even though the recommended emission reduction improves agreement between simulations and observations at JST and YRK, overall model performance likely gets worse due to the fact that simulations of OM and EC at other sites are not always overestimated and reduction of biomass burning emissions can lower these simulations.

Source contributions from individual biomass burning show that emissions from wood burning in fireplaces and woodstoves have the largest air quality impact at JST and YRK, contributing around 90% of POA from all biomass burning at JST and 70% at YRK during January 2002. It is resulted from concentrated emissions in the Atlanta area, despite small annual emissions in Georgia (Table 3-1). Their impacts at other observation sites are relatively small and adjusting their emissions will not significantly change simulated $PM_{2.5}$ at those sites. Furthermore, emissions from fireplace and woodstoves have relatively large uncertainties because of estimation methods and data used. Therefore, the emissions from wood burning in fireplaces and woodstoves are regarded as the major overestimated individual biomass burning source and are reduced by 90%

here. The reduction improves model performance at JST and YRK (Figure 3-4) as well as the overall model performance (Table 3-3), though discrepancies between simulations and observations still remain due to other sources of uncertainties that are not investigated here.

Seasonal source contributions from biomass burning

The updated emissions, including monthly county-level emission inventory from prescribed and agriculture field burning and land clearing (UPDATED), 90% reduction of emission from wood burning in fireplaces and woodstoves and the improved speciation profiles, are applied in other episodes (March, May and July 2002). Overall performance of simulated $PM_{2.5}$ species during these episodes are well within recent performance criteria [*Boylan, et al.*, 2006], except for OM during May and July (Table 3-4 and Figure 3-3). Underestimation in OM is common in the current CMAQ model, and it is likely due to underestimation of secondary organic aerosol (SOA) formation from biogenic sesquiterpene and isoprene emissions, and polymerization of SOA into nonvolatile particles [*Morris, et al.*, 2005]. Time series at JST and YRK show that simulated daily OM and EC follow observations pretty well (Figure 3-4), despite obvious underestimation of OM during May and July. Simulations at OKEF (an IMPROVE site in the southern Georgia) do not capture the peak observed on May 5th, 2002, when the station was directly impacted by a nearby wildfire in Okeefenokee Swamps. The adjacent modeling grid, however, are impacted with simulated levels consistent with the observed.

Simulated $PM_{2.5}$ source contributions from biomass burning usually coincide with peak $PM_{2.5}$ concentrations and have large temporal and spatial variations, with January and March being impacted the most and negligible impacts during May and July (Figure 3-5). Biomass burning emissions respectively contribute 3.0, 5.1, 0.8, and 0.3 $\mu g/m^3$ of $PM_{2.5}$, constituting 25%, 40%, 9% and 4% of total $PM_{2.5}$ during January, March, May and July for the whole modeling domain (Table 3-5). Analyses using receptor models, e.g

Positive Matrix Factorization (PMF) and Chemical Mass Balance (CMB), indicated similar seasonal trends [*Liu, et al.*, 2005; *Zheng, et al.*, 2002]. $PM_{2.5}$ source contributions from biomass burning during January and March are concentrated in the southwestern Georgia, where large amounts of prescribed burning are conducted. $PM_{2.5}$ concentrations caused by biomass burning in the Atlanta $PM_{2.5}$ non-attainment are 1.5 and 2.6 $\mu g/m^3$, respectively, in January and March. Large local impacts from a wildfire in Okeefenokee Swamp during May are obvioius.

About 90% of $PM_{2.5}$ concentrations caused by biomass burning are carbonaceous, including about 85%, 7.5% and 7.5% of POA, SOA and EC, respectively (Table 3-5). Since this modeling does not account SOA formation from terpene (a major SOA precursor) emissions from biomass burning, SOA caused by biomass burning is mainly due to a shift in the gas-aerosol phase partitioning from increased POA emissions. In addition, recent studies [*Andreae and Merlet*, 2001; *Lee, et al.*, 2005; *Mcdonald, et al.*, 2000] suggest that approximately 6% of VOC emissions from biomass burning are terpenes. An additional simulation with consideration of the 6% terpene emissions shows an increase less than 0.1% in SOA, likely due to much larger biogenic terpene emissions. In addition, NH_3 emissions from biomass burning also lead to increased NH_4^+, contributing about additional 2% of $PM_{2.5}$. Extra NH_3 and NO_X emissions from biomass burning lead to increased NO_3^- as well (about 4% of $PM_{2.5}$). No significant increase in SO_4^{2-} levels is observed, as indicated in a recent study in Texas [*Buzcu, et al.*, 2006]. Secondary impacts are spatially similar to primary emissions (Figure 3-6), and are limited to close proximity of the sources. Larger impacts of NH_4^+ and NO_3^- are also located in the northeastern region of modeling domain, where high NH_4^+ and NO_3^- concentrations are observed and high sensitivities to NH_3 and NO_X emissions might also exist.

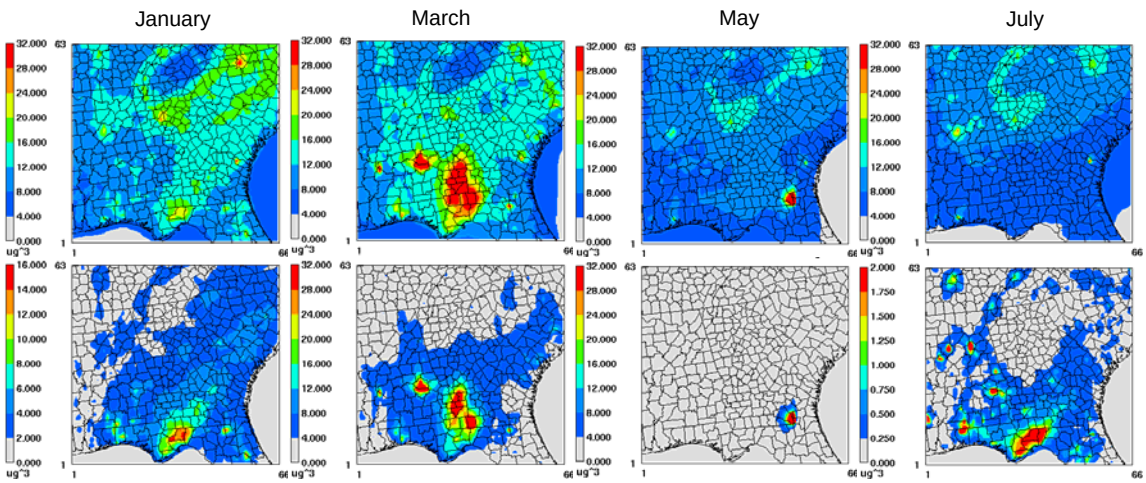

Figure 3-5 Monthly average $PM_{2.5}$ concentrations (first row) and source contributions from all biomass burning (second row) during January, March, May and July 2002. (Note different scales used.)

Table 3-5 Monthly-average source contributions (µg/m^3) from biomass burning during January, March, May and July 2002

		All sources						Biomass Burning					
		$PM_{2.5}$	POA	SOA	EC	NH_4^+	NO_3^-	$PM_{2.5}$	POA	SOA	EC	NH_4^+	NO_3^-
January	Nonatt[1]	16.2	3.1	2.1	1.0	1.5	2.6	2.3	1.5	0.2	0.1	0.1	0.1
	Domain[2]	11.8	3.0	1.8	0.5	1.0	1.4	3.0	2.0	0.3	0.2	0.1	0.2
	JST	21.7	5.3	2.1	2.0	2.0	3.5	2.9	2.0	0.2	0.2	0.1	0.2
	YRK	13.8	2.5	1.9	0.7	1.4	2.2	1.9	1.3	0.1	0.1	0.1	0.2
March	Nonatt	14.9	3.7	2.2	0.7	1.4	1.7	3.9	2.6	0.4	0.2	0.1	0.2
	Domain	12.7	4.3	1.6	0.5	1.1	1.2	5.1	3.7	0.4	0.2	0.1	0.2
	JST	17.1	4.4	2.2	1.2	1.6	2.0	3.6	2.6	0.3	0.2	0.1	0.2
	YRK	13.4	3.1	2.0	0.6	1.3	1.6	3.0	2.2	0.3	0.1	0.1	0.1
May	Nonatt	12.6	1.2	2.7	0.5	1.5	0.5	0.4	0.2	0.1	-	-	-
	Domain	8.4	1.1	1.4	0.2	1.0	0.2	0.8	0.6	0.1	-	-	-
	JST	14.6	2.0	2.6	0.9	1.7	0.7	0.3	0.1	0.1	-	-	-
	YRK	12.2	1.0	2.6	0.5	1.5	0.4	0.3	0.2	0.1	-	-	-
July	Nonatt	13.1	0.9	1.8	0.5	1.6	0.1	0.1	0.1	-	-	-	-
	Domain	8.0	0.6	0.8	0.2	0.9		0.3	0.2	0.1	-	-	-
	JST	15.3	1.8	1.8	1.0	1.9	0.2	0.1	0.1	-	-	-	-
	YRK	12.3	0.7	2.0	0.3	1.5	0.1	0.1	0.1	-	-	-	-

[1] Nonatt refers to source contributions averaged over all grids within the Atlanta PM2.5 nonattainment area.
[2] Domain refers to source contributions averaged over all modeling grids.
[3] – refers to values less than 0.1.

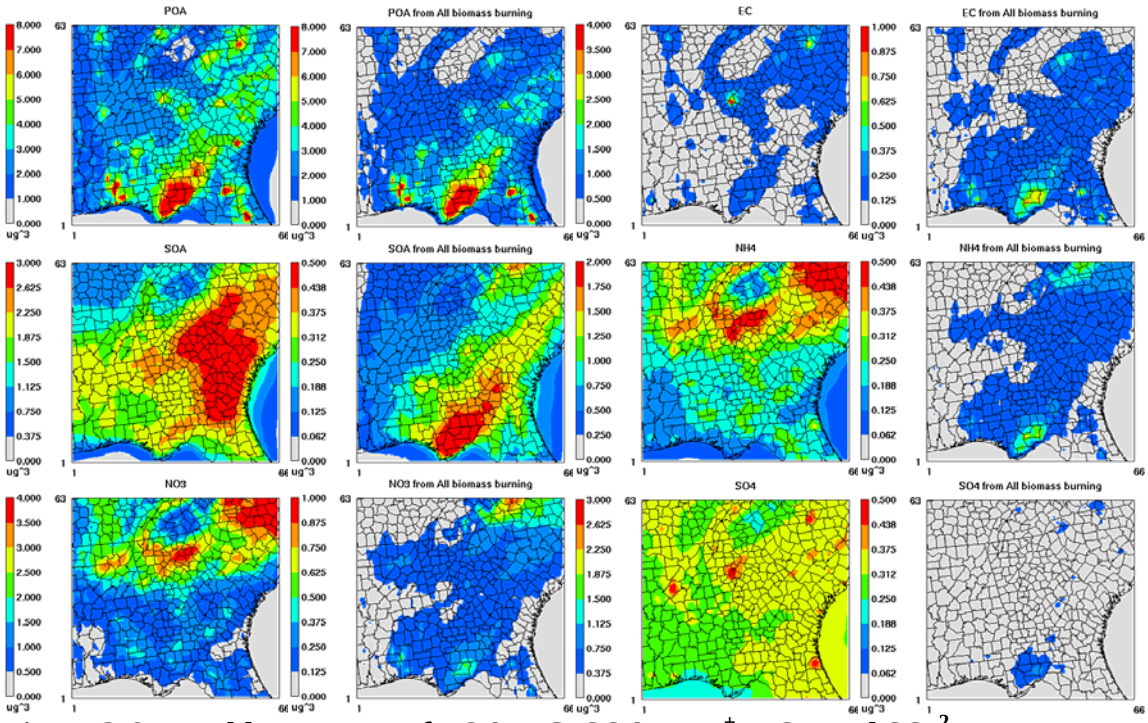

Figure 3-6 Monthly averages of POA, EC, SOA, NH_4^+, NO_3^- and SO_4^{2-} concentrations and source contributions from all biomass burning during January 2002. (Note different scales used.)

As in emissions, prescribed burning has the largest impacts among biomass burning sources (Table 3-6 and Figure 3-7). Significant temporal and spatial variations are also observed. Source contributions from prescribed burning peak in March, followed by January, May and July. They concentrate in the southwest of Georgia, influencing much of the region. Wood burning in fireplaces and woodstoves has the largest impact in January and is centered in the Atlanta area which is characterized with high population densities. Similarly, source contributions from agriculture burning spatially follow the distribution of agricultural lands and peak in March. Source contributions from land clearing and wildfires are more spatially sporadic. Specifically, prescribed burning is always the largest single biomass burning source in the $PM_{2.5}$ non-attainment area, followed by land clearing and wood burning in fireplaces and woodstoves.

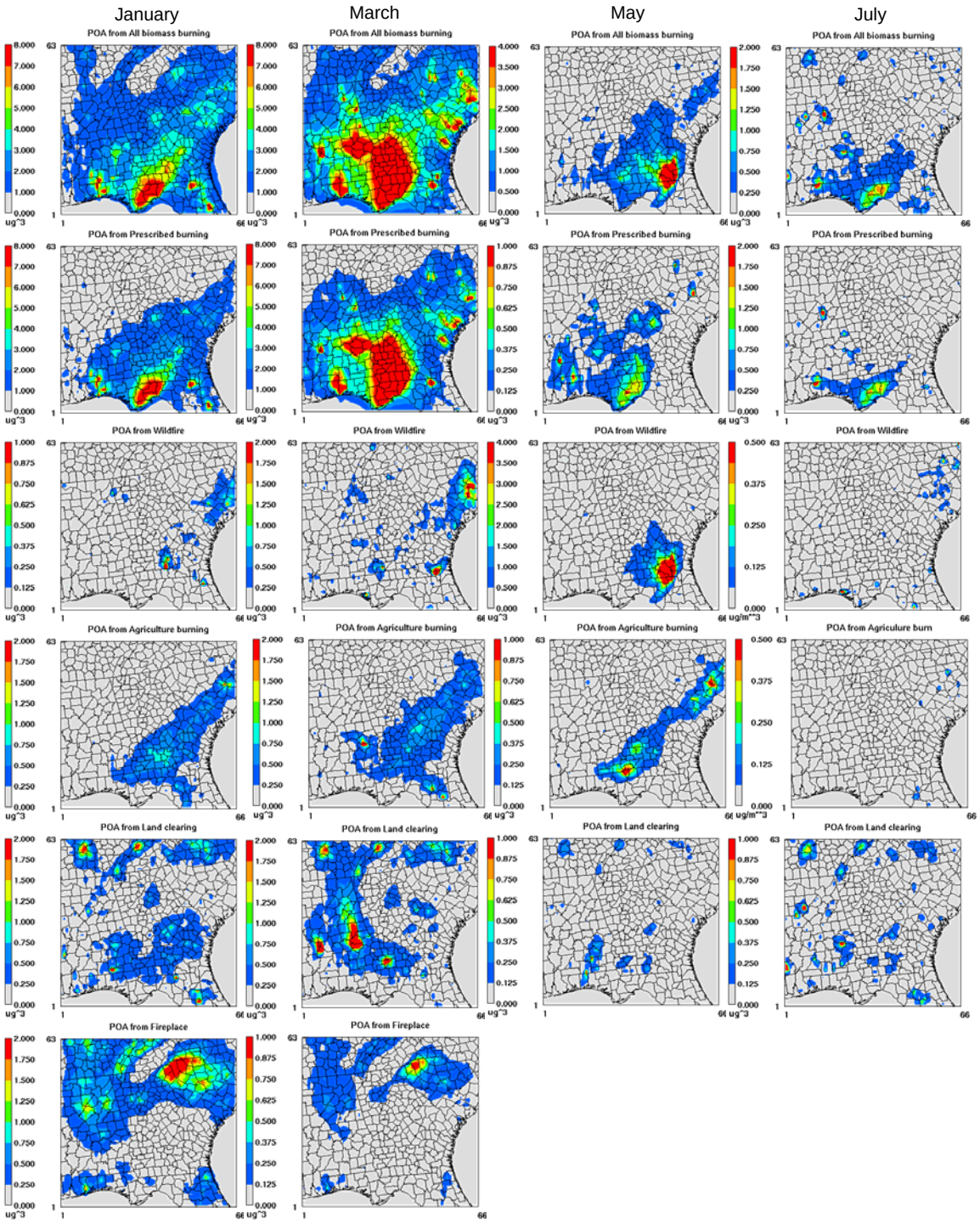

Figure 3-7 Monthly average POA contributions from all biomass burning sources and individual biomass burning sources during January, March, May and July 2002. Impacts from fireplaces and woodstoves combustion emissions during May and July are negligible. (Note different scales used.)

Table 3-6 Monthly-average POA source contribution (μg/m^3) from individual biomass burning sources during January, March, May and July 2002

		All Biomass Burning	Wildfire	Prescribed	Agriculture	Land	Fireplace
January	Nonatt	1.5	-	0.8	-	0.2	0.4
	Domain	2.0	-	1.2	0.1	0.2	0.4
	JST	2.0	-	0.7	-	0.2	1.1
	YRK	1.3	0.2	0.5	-	0.1	0.4
March	Nonatt	2.6	0.1	2.0	0.1	0.2	0.1
	Domain	3.7	0.1	2.9	0.2	0.3	0.1
	JST	2.6	0.1	1.8	0.1	0.2	0.3
	YRK	2.2	0.4	1.4	0.1	0.2	0.1
May	Nonatt	0.2	0.1	0.1	-	-	-
	Domain	0.6	0.4	0.1	0.1	-	-
	JST	0.1	-	-	-	-	-
	YRK	0.2	0.1	-	-	-	-
July	Nonatt	0.1	-	-	-	-	-
	Domain	0.2	-	0.1	-	0.1	-
	JST	0.1	-	-	-	-	-
	YRK	0.1	-	-	-	-	-

Conclusion

Total and speciated $PM_{2.5}$ are simulated for January, March, May and July 2002 over the southeastern US. Impacts of uncertainties in emissions, including total amount, temporal and spatial characteristics, and speciation on air quality modeling during January are investigated. Though model performance evaluated by observations is similar with different emission inventories, significant different spatial distributions of $PM_{2.5}$ emissions and resulted $PM_{2.5}$ concentrations have been observed. Simulations with updated speciation profiles lead to increased POA and decreased EC emissions and concentrations. Model performance for EC is improved, along with deteriorated OM performance. Estimated source contributions are further compared with CMB results, suggesting a 90% reduction of emissions from wood burning in fireplaces and woodstoves.

About 83% of $PM_{2.5}$ caused by biomass burning is POA and EC, and the rest is secondary in origin (e.g. SOA, NH_4^+ and NO_3^-). SOA formed from biomass burning emissions is mainly due to a shift in the gas-aerosol phase partitioning from increased POA emissions. Both primary and secondary impacts are limited to areas in close proximity of emissions. Seasonal source contributions from biomass burning using the updated emissions have large temporal and spatial variations, higher in winter (January) and spring (March), and lower in summer (May and July).

Biomass burning influences much of the modeling domain and peaks in the southwestern Georgia (a more rural area). Prescribed burning is has the largest air quality impacts among biomass burning sources, peaking in March and the southwestern Georgia. Overall impacts from wildfires are much smaller in spite of a sever local impact and peak in May. Emissions from other biomass burning have significant air quality impacts during January and March at much smaller magnitudes, and negligible impacts during May and July. In the Atlanta $PM_{2.5}$ non-attainment area prescribed burning is always the largest biomass burning source, followed by land clearing and wood burning in fireplaces and woodstoves.

References

Andreae, M. O., and Merlet, P. (2001). Emission of trace gases and aerosols from biomass burning. Global Biogeochemical Cycles 15, 955-966.

Baek, J., Park, S. K., Hu, Y. T., and Russell, A. G. (2005). Source apportionment of fine organic aerosol using CMAQ tracters=. In "4th annual CMAS Model-3's users conference", Chapel Hill, NC.

Boylan, J. W., Odman, M. T., Wilkinson, J. G., and Russell, A. G. (2006). Integrated assessment modeling of atmospheric pollutants in the Southern Appalachian Mountains: Part II. Fine particulate matter and visibility. J. Air Waste Manage. Assoc. 56, 12-22.

Buzcu, B., Yue, Z. W., Fraser, M. P., Nopmongcol, U., and Allen, D. T. (2006). Secondary particle formation and evidence of heterogeneous chemistry during a wood smoke episode in Texas. Journal of Geophysical Research-Atmospheres 111.

Byun, D. W., and Ching, J. K. S. (1999). "Science algorithms of the EPA models-3 Communicty Multiscale Air Quality (CMAQ) modeling system," Rep. No. EPA/600/R-99/030.

Chen, Y., and Zheng, M. (2006). Variation of PM2.5 sources in the southeastern US (in preparation).

Dockery, D. W., Pope, C. A., Xu, X., Spengler, J. D., Ware, J. H., Fay, M. E., Ferris, B. G., and Speizer, F. E. (1993). An association between air pollution and mortality in six U.S. cities. New England J. Med. 329, 1753-1808.

Fine, P. M., Cass, G. R., and Simoneit, B. R. T. (2002). Chemical characterization of fine particle emissions from the fireplace combustion of woods grown in the southern united states. Environ. Sci. and Technol. 36, 1442-1451.

GFC. Georgia Forestry Commission. (2005). Status of issuing burning permit in Georgia. Macon, GA.

Grell, G., J., D., and Stauffer, D. (1994). "A description Penn State/NCAR Mesoscale Model (MM5), NCAR/TN-398+STR."

Hardy, C. C., Ottmar, R. D., Peterson, J. L., Core, J. E., and Seamon, P. (2001). "SMOKE Management Guide for Prescribed and Wildland Fire: 2001 Edition," Rep. No. PMS 420-2. NFES 1279. National Wildfire Coodination Group, Boise, ID.

Hays, M. D., Fine, P. M., Geron, C. D., Kleeman, M. J., and Brian, K. G. (2005). Open burning of agriculture biomass: Physical and chemical properties of particle-phase emissions. Atmos. Environ. 39, 6747-6764.

Hays, M. D., Geron, C. D., Linna, K. J., and Smith, N. D. (2002). Speciation of gas-phase and fine particle emissions from burning of foliar fuels. Environ. Sci. and Technol. 36, 2281-2295.

Houyoux, M. R., Vukovich, J. M., Jr., C. J. W., Wheeler, N. J. M., and Kasibhatla, P. (2000). Emission inventory development and processing for the seasonal model for regional air quality. J. Geophys. Res. 105, 9079-9090.

IPCC (2001). "Climate Change 2001: The Scientific Basis. Contribution of Working Group I to the Third Assessment Report of the Intergovernmental Panel on Climate Change," Cambridge University Press, Cambridge, United Kingdom and New York, NY, USA.

Kim, E., Hopke, P. K., and Edgerton, E. S. (2003). Source identification of atlanta aerosol by positive matrix factorization. J. Air Waste Manage. Assoc. 53, 731-739.

Kim, E., P.K. Hopke, P. Paatero, and E.S. Edgerton (2003). Incorporation of parametric factors into multilinear receptor model studies of atlanta aerosol. Atmos. Environ. 37, 5009-5021.

Lee, S., Baumann, K., Schauer, J. J., Sheesley, R. J., Naeher, L. P., Meinardi, S., Blake, D. R., Edgerton, E. S., Russell, A. G., and Clements, M. (2005). Gaseous and Particulate Emissions from Prescribed Burning in Georgia. Environ. Sci. Technol. 39, 9049-9056.

Liu, W., Wang, Y. H., Russell, A. G., and Edgerton, E. S. (2005). Atmospheric aerosol over two urban-rural pairs in the sourtheastern United States: chemical composition and possible sources. Atmos. Environ. 39, 4453-4470.

Malm, W. C., Pitchford, M. L., Scruggs, M., Sisler, J. F., Ames, R., Copeland, S., Gebhart, K. A., and Day, D. E. (2000). "Spatial and Seasonal Patterns and Temporal Variability of Haze and its Constituents in the United States: Report III." Coop. Inst. for Res. in the Atmos., Colo. State Univ., Fort Collins, Colo.

Marmur, A., Park, S.-K., Mulholland, J. A., Tolbert, P. E., and Russell, A. G. (2006). Source apportionment of PM2.5 in the southeastern United States using receptor and emissions-based models: Conceptual differences and implications for time-series health studies. Atmospheric Environment 40, 2533-2551.

Mcdonald, J. D., Zielinska, B., Fujita, E. M., Sagebiel, J. C., Chow, J. C., and Watson, J. G. (2000). Fine particle and gaseous emission rates from residential wood combustion. Environ. Sci. and Technol. 34, 2080-2091.

Morris, R. E., McNally, D. E., and Tesche, T. W. (2005). Preliminary evaluation of the community multiscale air, quality model for 2002 over the southeastern United States. J. Air Waste Manage. Assoc. 55, 1694-1708.

NARSTO (2003). "Particulate matter science for policy makers."

Olerud, D. T., and Sims, A. (2003). "MM5 sensitivity Modeling in Support of VISTAS (Visibility Improvement – State and Tribal Association), VISTAS task 2e deliverable."

Park, S.-K., Murmur, A., Ke, L., Yan, B., Russell, A. G., and Zheng, M. (2006). Source apportionment of PM2.5: comparison between receptor and air quality models. in submission to Environ. Sci. and Technol.

Peel, J. L., Tolbert, P. G., Klein, M., Metzger, K. B., Flanders, W. D., Todd, K., Mulholland, J. A., Ryan, P. B., and Frumkin, H. (2005). Ambient Air Pollution and Respiratory Emergency Department Visits. Epidemiology 16, 164-174.

Saxena, P., and Hildemann, L. (1996). Water-soluble organics in atmospheric particles: A critical review of the literature and application of thermodynamics to identify candidate compounds. J. Atmos. Chem 24, 57-109.

Sullivan, A. P., and Weber, R. J. (2006). Chemical characterization of the ambient organic aerosol soluble in water: 2. Isolation of acid, neutral, and basic fractions by modified size-exclusion chromatography. Journal of Geophysical Research-Atmospheres 111.

Turpin, B. J., and Lim, H. J. (2001). Species contributions to PM2.5 mass concentrations: Revisiting common assumptions for estimating organic mass. Aerosol Sci. Technol. 35, 602-610.

US-EPA (2004). EPA 2001 modeling platform emission inventory. http://www.epa.gov/ttn/chief/emch/invent/. Accessed in May 2005.

US-EPA (2004). Titles and Documentation for PM Profiles. http://www.epa.gov/ttn/chief/emch/speciation/. Accessed in May 2005.

VISTAS (2005). VISTAS 2002 emission inventories.

Westerling, A. L., Hidalgo, H. G., Cayan, D. R., and Swetnam, T. W. (2006). Warming and Earlier Spring Increase Western U.S. Forest Wildfire Activity. Science 313, 940-943.

Zheng, M., Cass, G. R., Schauer, J. J., and Edgerton, E. S. (2002). Source apportionment of PM2.5 in the southeastern United States using solvent-extractable organic compounds as tracers. Environ. Sci. and Technol. 36, 2361-2371.

Zheng, M., Ke, L., Edgerton, E. S., Schauer, J. J., Dong, M., and Russell, A. G. (2006). Spatial distribution of carbonaeous aerosol in the southeastern US using molecular markers and carbon isotope data. in submission to J. of Geophys. Res.

CHAPTER 4 AIR QUALITY IMPACTS FROM FOREST FIRES UNDER DIFFERENT FOREST MANAGEMENT PRACTICES: IMPLICATIONS TO MODELING UNCERTAINTIES

Abstract

Large amounts of air pollutants are emitted during forest fires. Such emissions are modulated by different forest management practices. The impacts of these practices on fire emissions and subsequently on regional air quality are studied using source-oriented air quality modeling. Forest management practices considered here include changing burning seasons and fire-return intervals (FRI), and controlling emissions during smoldering. Air quality impacts from forest fires during different burning seasons are different. The same forest fire emissions lead to the largest impacts on $PM_{2.5}$ levels in January, followed by March, May and July, largely due to greater ventilation and stronger removal processes in the warmer periods. In contrast, their impacts on O_3 levels in the Atlanta area peak in May, followed by March, July and January. Longer FRIs lead to severe individual forest fires; however, they also reduce overall air quality impacts. FRIs are therefore an important factor to optimize air quality-ecosystem management. Furthermore, 30% or 55% of emissions from prescribed forest fires are estimated to be released during the smoldering stage, according to two different methods. These emissions lead to respectively 61% or 81% of $PM_{2.5}$ source contributions from forest fires for the entire Georgia. The larger air quality impacts per unit emissions during smoldering are due to better dispersion for flaming emissions.

This chapter will be submitted to Environmental Science and Technology. Co-authors are Armistead Russell, Yuhang Wang, and Yongqiang Liu.

Introduction

Forest fires are essential and natural processes to maintain forest health (Brown and Smith, 2000; NWCG, 1998). However, inadvertent fires can also cause ecosystem damage and property loss, and threaten human health and safety. This leads to fire suppression efforts during the early twentieth century. In turn, fire suppression changes ecosystem balance, reduces growth and vigor of trees, increases insect and disease mortality, and leads to wildfires of higher intensity due to fuel accumulation (Brown and Smith, 2000; NWCG, 1998; US-EPA, 1998). Current forest management intentionally ignites forest fires (i.e. prescribed fires), which are conducted within limits of certain meteorological and fuel conditions to minimize the adverse impacts from fires. Prescribed fires are planned for conditions that are not likely to lead to their becoming uncontrolled, and when feasible they are often planned to reduce impacts on populated areas. They are typically limited in extent, spatially and temporally. Therefore, increased application of prescribed forest fires is expected. In addition, a resent study shows that climate change leads to increased wildfire activities in the western U.S. (Westerling et al., 2006). Appropriate management practices, including prescribed forest fires, are increasingly required to reduce wildfire hazards.

Large amounts of air pollutants, e.g., particulate matter (PM), volatile organic compounds (VOCs), nitrogen oxides (NO_X), carbon monoxide (CO) and ammonia (NH_3) can be emitted during forest fires. They contribute about 20% of the fine particulate matter ($PM_{2.5}$) in the United States (US-EPA, 2004.). These emissions can lead to violations of ozone (O_3) and $PM_{2.5}$ National Ambient Air Quality Standard (NAAQS), and impair visibility (Sandberg et al., 2002). Both field measurements and numerical modeling have been used to study their air quality impacts (Buzcu et al., 2006; Phuleria et al., 2005; Sapkota et al., 2005). In 1998, the US EPA issued the Interim Air Quality Policy on Wildland and Prescribed Fires (US-EPA, 1998) to address how best to achieve national clean air goals while improving ecosystem health through increased use of fire.

The fire smoke management guide developed by the US Forest Service in 2001 (Hardy et al., 2001) provides suggestions on reducing air quality impacts from forest fire emissions.

Unlike wildfires which are often caused by lightning and naturally occur under specific meteorological and forest fuel conditions, forest managers conduct prescribed fires by varying the time, frequency and intensity of fires to meet operations, ecosystem health and air quality requirements. Prescribed fires are usually conducted during seasons different from those for wildfires (Brown and Smith, 2000). Different forest management goals can also lead to choosing alternative burning seasons, and hence different meteorological conditions and air quality impacts. Fire frequencies can influence fuel consumptions and emissions of a fire, resulting in different air quality impacts. Additionally, intensities of fires can be controlled by different firing techniques (e.g. heading, backing, strip-heading and flanking fires), meteorological and fuel conditions. Techniques are also used to reduce emissions of prescribed fires during smoldering combustion stage, which are large and controllable. Even though different air quality impacts from forest fires under different forest management practices are expected, they are rarely quantified. To address this issue, a source-oriented air quality model, capable of simulating air pollutant concentrations using detailed emissions and meteorological data, is employed.

Historical air quality conditions are first reproduced using the existing forest fire emission patterns together with emissions from other sources as inputs. Emissions from forest fires are then modified to characterize the effects of various management practices. Practices evaluated here include changing burning seasons and fire-return intervals (FRIs), and controlling emissions during smoldering stage. Corresponding air quality impacts are modeled using the specific emissions. Georgia, where forests cover more than 66% of the total land and prescribed fires have been widely used, is chosen for the case study. More than 92 percent of Georgia forestland is owned by industry or private parties. The US Forest Service (USFS) managed national forests lie mostly in the north

and a few tracts in middle Georgia, and the Fish and Wildlife Service (FWS) manages the Okeefenokee Swamps in the south (GFC, 2005). On average, 0.86 million acres of forests are burned by prescribed fires every year according to the records between 1994 and 2005 kept by Georgia Forestry Commission (GFC, 2005), emitting 43 thousand tons of $PM_{2.5}$ a year estimated by the method used in the VISTAS emission inventory (Barnard and Brewer, 2004). These fires mainly burn in the southern pine forests, and consume understory fuels, such as grass, live shrubs and needles, without significantly damaging trees (Brown and Smith, 2000; Carter and Foster, 2004; GFC, 2005).

Understanding air quality impacts from forest fires under different forest management practices is becoming critical to non-attainment designation, control strategy development, and effective air quality and ecosystem managements. Meanwhile, it provides information on uncertainties in air quality modeling that result from lack of consideration of impacts from different forest management practices.

Methods

Historical air quality conditions during 2002 are simulated using the Community Multiscale Air Quality (CMAQ) model v. 4.3 (Byun and Ching, 1999), with meteorological conditions simulated with the NCAR's 5^{th} generation Mesoscale Model (MM5) (Grell et al., 1995; Olerud and Sims, 2003) and emissions with the Sparse Matrix Operator Kernel Emissions (SMOKE) Modeling System v. 2.1 (Houyoux et al., 2000). Modeling performance is evaluated by comparing simulations with observations collected as part of the Interagency Monitoring of Protected Visual Environments (IMPROVE) (VISTA, 2005), the SouthEastern Aerosol Research and Characterization (SEARCH) (Hansen et al., 2003), the Assessment of Spatial Aerosol Composition in Atlanta (ASACA) (Butler et al., 2003) and the Speciation Trends' Network (STN) (US-EPA, 2005) networks. Detailed modeling setup and performance can be found elsewhere (Tian et al., 2006).

Burning season

Different seasons can be chosen for different forest management purposes. In Georgia, burning during the dormant season is the most common. More than 74% of prescribed fires are scheduled between December and March, especially in March (37% of the annual total) (GFC, 2005). Air quality impacts during different seasons from the same forest fire emissions are expected to change due to varying meteorological and photochemical conditions. To represent different forest fire seasons, four months in 2002, including January, March, May and July, are selected. March is the most popular month for current prescribed fires. January is also in the dormant season, with about one third of burning activities in March. Different air quality impacts in January and March can be used to illustrate the benefit of spreading forest fires into other months during the dormant season. Natural forest fires are mainly ignited by lightning and occur in Georgia during May and June when lightning frequency is high and summer thunderstorms haven't provided moisture to the forests (Bentley and Stallins, 2005; Brown and Smith, 2000; US-EPA, 1998). Therefore, corresponding air quality impacts in May are also studied. Finally, air quality impacts from forest fires in July are investigated with particular interest in how such emissions might affect pollutant concentrations during the summer ozone season. Fall is not considered, because it is neither a naturally preferred season nor practical for prescribed forest fires due to wet and large amounts of available fuels for fires. Emissions of prescribed fires originally calculated for March 2002 are individually input into CMAQ for the four different months, together with the applicable emissions from other sources pertaining to the specific month.

Fire-return intervals

Emissions from forest fires are calculated as the product of the burned area (A), fuel consumed per area (F_a) and an emission factor (E_f) (Battye and Battye, 2002):

$$E = A \times F_a \times E_f \quad (1)$$

A is determined from current forest fire records (GFC, 2005), F_a is the amount of biomass consumed during a forest fire per area, and E_f is the ratio of the mass of pollutant emitted per unit mass of fuel consumed.

For a forest fire with a burned area A, its emissions change proportionally to F_a, which increases with longer FRIs. This is referred to as an "individual" or "short-term" impact. Prescribed fires are currently burnt in short intervals of 2~5 years (Brown and Smith, 2000; Carter and Foster, 2004), and would be too severe to control if FRIs are longer than 5 years (Brown and Smith, 2000). Here, F_a s with 2-, 3-, 4- and 5-year FRIs are estimated using a fire behavior model, the First Order Fire Effects Model (FOFEM) v 5.21 (Reinhardt, 2004) with pre-burn fuel characteristics as inputs, such as relative abundance of particular fuelbed components and the condition of the fuel. Separate F_a s are calculated for different forest types in Georgia at various ages, and are used to calculate aggregate relative ratios of F_a s with different FRIs. These ratios are then combined with the F_a (4 tons/acre) used in the most recent emission inventory for prescribed forest fires in Georgia (Barnard and Brewer, 2004), which is taken as that for a 3.5-year FRI, in order to estimate F_a for each FRI.

In comparison, the "overall" or "long-term" impact is defined as air quality impacts from burning forests applicable to prescribed fires in a year. Since FRIs influence not only F_a but also yearly burned acreage (A), overall emissions don't simply increase with FRIs as a single fire does. For example, in Georgia, the total forest area under managements using fires is approximately 3 million acres. If a 2-year FRI were used, 1.5 million acres would be burned each year, and if a 5-year FRI were employed, 0.6 million acres would be burned. Here, annual emissions from prescribed forest fires with different FRIs ranging from 2 to 5 years in Georgia are calculated with respective A and F_a.

Flaming and smoldering

Emissions during flaming and smoldering combustion stages of forest fires have different patterns and dispersion behaviors in the atmosphere (Sandberg and Dost, 1990; Sandberg et al., 2002). Generally, flaming combustion is more complete with less air pollutant emissions per fuel consumed, while smoldering combustion is relatively incomplete with larger emissions. As such, many techniques have been recommended to reduce emissions during the smoldering stage, including back fires, pre-processing fuels with a large potential to smolder using mechanical methods, keeping high moisture in large woody fuels, burning before precipitation, and rapid mop-up, etc. Practically, it is hard to differentiate emissions in these two stages, since they sometimes occur at the same time.

Separate forest fire emissions during the two combustion stages are estimated using their respective fractions of total emissions. The fractions are calculated by two different methods. One method is based on the diurnal profile for prescribed forest fires emissions used in SMOKE (US-EPA, 2004.). The profile shows the hourly emission fractions. According to the guide for prescribed forest fires in southern forests (Hardy et al., 2001; USFS, 1976) and personal communication with forest management experts at Georgia Forestry Commission (GFC, 2005), the flaming stage of prescribed forest fires is assumed to occur between 10:00 and 17:00, and the rest of time is designated as smoldering. Therefore, fractions of emissions during each combustion stage are calculated by adding the hourly emission fractions in the relevant time periods. The other method uses specific F_a values in combination with applicable emission factors for each combustion stage (Battye and Battye, 2002; Lee et al., 2005). Two fire behavior models, Fire Emission Production Simulator (FEPS) v1.0 (Anderson et al., 2004), and Fire Characteristic Classification System (FCCS) (Ottmar, 2005), are employed to estimate separate F_a values during flaming, short-term smoldering and Residual Smoldering

Combustion (RSC). Here, combustion stages are defined according to whether emissions are influenced by the strong convection associated with a flame front (Sandberg and Dost, 1990; Ward et al., 1993). Therefore, F_a values calculated during both flaming and short-term smoldering in the two models are treated as F_a values during flaming, while F_a values during RSC as F_a values during smoldering.

Air quality impacts from emissions during the two combustion stages are simulated using CMAQ during March 2002, when current prescribed forest fires are largest in Georgia. The difference of simulations with and without specific emissions shows respective source contributions. Such information can be used to evaluate effectiveness of controlling emissions during smoldering stage. Emissions during flaming stage are allocated into the period between 10:00 and 17:00 due to the fact as mentioned above, according to the diurnal profile for prescribed forest fires emissions used in SMOKE (US-EPA, 2004.). Similarly, emissions during smoldering stage are allocated to the rest of time.

Results and Discussion

Burning season

Difference of simulated $PM_{2.5}$ concentrations with and without forest fire emissions is calculated to illustrate air quality impacts from forest fires. Source contributions in the entire Georgia and Atlanta $PM_{2.5}$ non-attainment area (including twenty two counties designated by EPA on December 17, 2004) are characterized by monthly averages of all simulations for all grids within the respective areas. Seasonal air quality impacts from existing prescribed forest fire emissions are first evaluated. In 2002, estimated source contributions from the existing fires peak in March, contributing 4.8 $\mu g/m^3$ of $PM_{2.5}$ for the entire Georgia, followed by January with 1.5 $\mu g/m^3$. Their contributions in the Atlanta $PM_{2.5}$ non-attainment area are smaller, being 1.9 $\mu g/m^3$ in

March and 0.7 μg/m^3 in January. Source contributions of fires are negligible during May and July.

We apply the forest fire emissions originally calculated for March 2002 to January, May and July 2002 in order to evaluate air quality impacts during different burning seasons. The impacted regions and strength for $PM_{2.5}$ diminish from January to July (Figure 4-2). Such emissions lead to average $PM_{2.5}$ increases of 7.3 μg/m^3 in January, 4.8 μg/m^3 in March, 3.4 μg/m^3 in May, and 3.0 μg/m^3 in July for the entire Georgia. The decreased burning impacts during summer seasons are due to stronger removal processes in that period, e.g. wet deposition, and dispersion by storms. Impacts on $PM_{2.5}$ in the Atlanta non-attainment area decrease to 2.0 μg/m^3 in January, 1.9 μg/m^3 in March, 1.3 μg/m^3 in May and 0.9 μg/m^3 in July. In addition, it is interesting to note that the seasonal change of $PM_{2.5}$ source contributions in Okefeenookee swamp, located in the south of Georgia, differs from the regional average. Here, the forest fires contribute 3.7 μg/m^3 of $PM_{2.5}$ in January, 1.4 μg/m^3 in March, 0.6 μg/m^3 in May, and 1.1 μg/m^3 in July. This local difference can be partially explained by change of wind direction, and should be addressed in control strategy development. Simulated $PM_{2.5}$ concentrations without prescribed forest fire emissions in Georgia (Figure 4-1) show the same seasonal trend, decreasing from January to July. Even though same daily emissions from forest fires are applied in each specific month, both estimated daily $PM_{2.5}$ concentrations and source impacts vary significantly from day to day, with an obvious decreasing trend from January to July. Violations of the proposed future daily $PM_{2.5}$ standard (35 μg/m^3) are also observed. When averaged over the entire Georgia, these potential exceedences are mainly caused by forest fire emissions which contribute more than 40% of the total $PM_{2.5}$, whereas forest fire emissions have smaller impacts on the Atlanta $PM_{2.5}$ non-attainment area (about 10%). These days have poor dispersion, and should be avoided in burning practice (Figure 4-7).

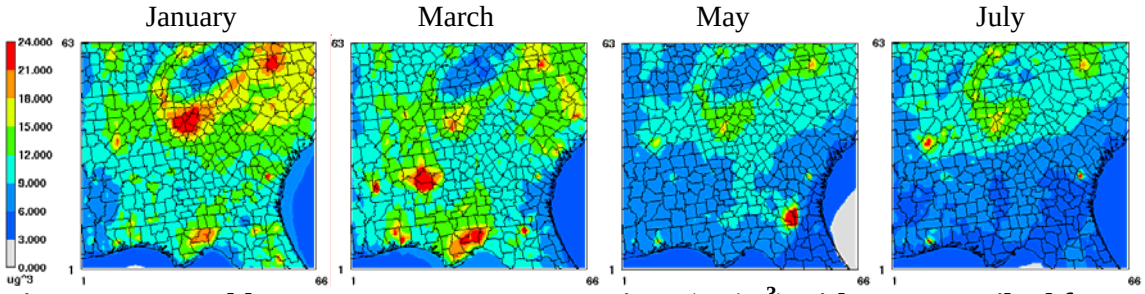

Figure 4-1 Monthly average $PM_{2.5}$ concentrations (µg/m^3) without prescribed forest fire emissions in Georgia during January, March, May and July 2002

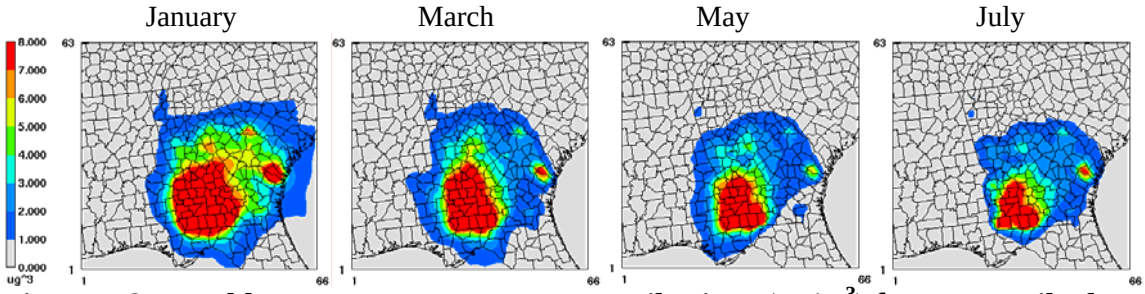

Figure 4-2 Monthly average $PM_{2.5}$ source contributions (µg/m^3) from prescribed forest fires in Georgia for using the March emissions applied to January, March, May and July 2002

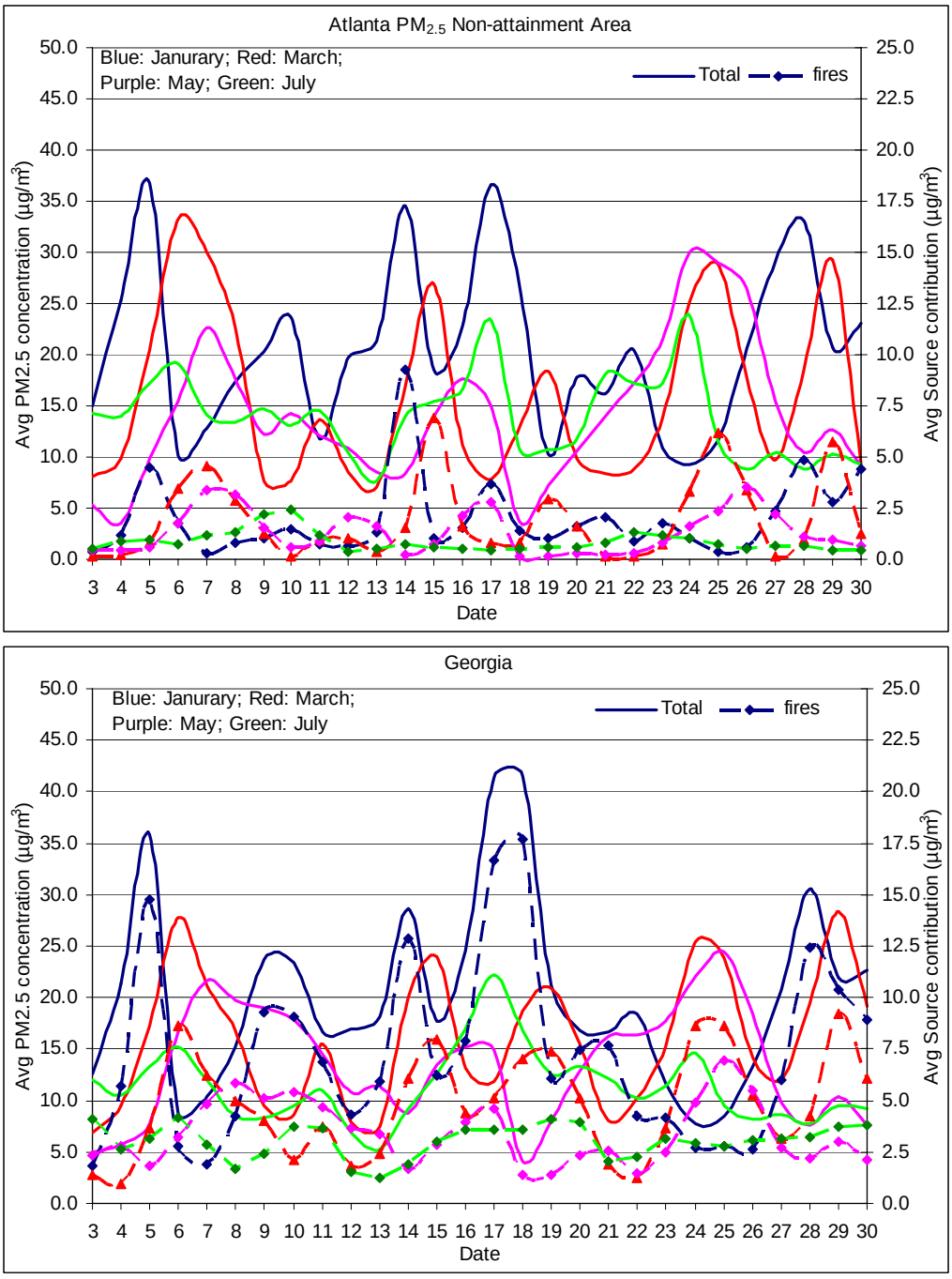

Figure 4-3 Average Daily $PM_{2.5}$ concentrations (µg/m^3) and source contributions (µg/m^3) for using the March prescribed forest fire emissions applied to January, March, May and July 2002

Impacts of forest fires on O_3 formation are also of concern, especially when these fires occur during summer ozone episodes. Generally, the peaks or averages of simulated daily maximum 8-hour O_3 concentrations within a month are found to increase from

January to July and agree well with observations (Figure 4-4 and Figure 4-6). In 2002, existing forest fires significantly impact O_3 concentrations in March, with negligible O_3 contributions in other months. Prescribed fires lead to an increase of 1 ppbv in the peak, daily maximum 8-hr O_3 concentrations during March in the Atlanta metropolitan area (including thirty two counties), a region with historical O_3 problems. During May and July, current practice leads to very low prescribed fire emissions and correspondingly little impact on O_3.

When the forest fire emissions originally calculated for March are applied to the other months (January, May and July), additional NO_X and VOC emissions lead to significant increases of ozone concentrations during May and July (Figure 4-5 and Figure 4-7). Although this impact peaks in the origin of emissions, special attention is paid to the Atlanta metropolitan area. Monthly averages of daily maximum 8-hour O_3 concentrations caused by forest fire emissions are highest in May (0.40 ppbv), followed by March (0.30 ppbv), July (0.27 ppbv), and January (<0.01 ppbv). Such forest fires also lead to 2.4 ppbv for monthly peaks of daily maximum 8-hour O_3 concentrations in May, 1.0 ppbv in March, 0.48 ppbv in July and 0.18 ppbv in January. Though O_3 formation potentials in July are the highest, O_3 formed by additional forest fires emissions are less in July compared with May and March. It is likely due to reduced O_3 sensitivities with increasing emissions and less transported NO_X emissions from fires to the Atlanta area in summer. Slightly negative O_3 source contributions in January are observed when excess NO_X emissions from fires deplete O_3. Since exceedence of the O_3 NAAQS has been rarely observed during January and March in the Atlanta area, impacts of burning forest fires in January and March on O_3 are of less concern. However, planning fires in May requires evaluation of their O_3 impacts.

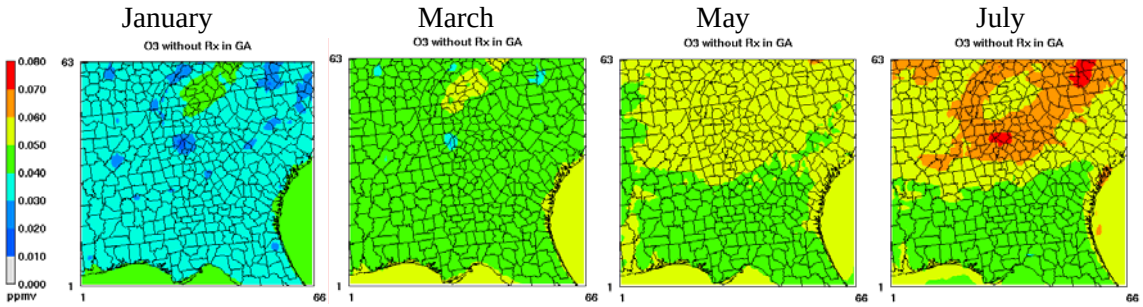

Figure 4-4 Averages of daily maximum 8-hr O_3 concentrations (ppmv) in Georgia within a month during January, March, May and July 2002

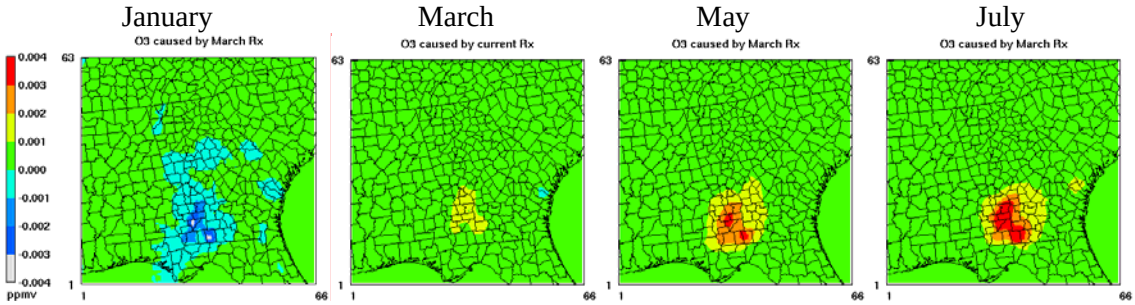

Figure 4-5 Monthly averages of daily maximum 8-hr O_3 source contributions (ppmv) from prescribed forest fires in Georgia during January, March, May and July 2002

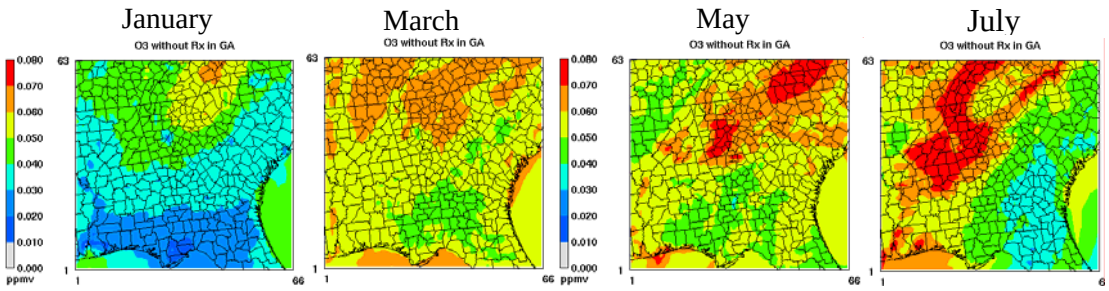

Figure 4-6 Peaks of daily maximum 8-hr O_3 concentrations (ppmv) in Georgia within a month during January, March, May and July 2002

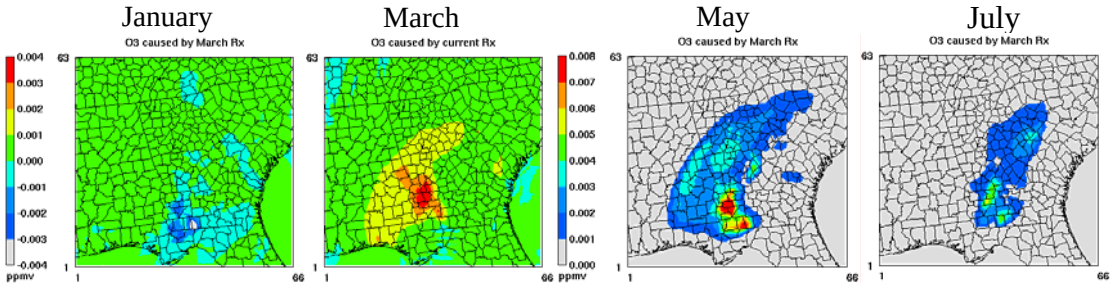

Figure 4-7 Monthly peaks of daily maximum 8-hr O_3 source contributions (ppmv) from prescribed forest fires in Georgia during January, March, May and July 2002

Complex relationships between air quality and forest fires make choosing the optimal fire season difficult. Previously, forest fires had been viewed as a source of O_3 pollution during summer and addressed by different policies (e.g. burning bans during the summer O_3 season). However, the benefit is reduced due to relatively higher $PM_{2.5}$ impacts during other periods. To reduce $PM_{2.5}$ impacts, burning during the summer is found to be preferable. In order to meet requirements from varying air quality and ecosystem management goals, a comprehensive analysis should be carried out, considering air quality impacts of both O_3 and $PM_{2.5}$ at the same time and other associated impacts, including human health, visibility, climate change, and ecosystem health.

Fire-return intervals

Forest fires with longer FRIs usually consume more fuels. Fuel consumptions (F_a s) at different forest ages calculated by FOFEM have similar ratios among different forest types and are further averaged to estimate the ratios of F_a s with various FRIs. Given that F_a with a 2~5-year (i.e. 3.5-year) FRI is 4 tons/acre, F_a s with 2-, 3-, 4- and 5-year FRIs are respectively 2.9, 3.8, 4.3, and 5.0 tons/acre. Emissions from an individual forest fire with a 5-year FRI are approximately 72% larger than those from a fire with the same acreage if a 2-year FRI is employed. On the other hand, annual emissions with a 5-year FRI are 32% less than those with a 2-year FRI, as less forest area is burned each year when a larger FRI is used. Less burned area offsets the increase of F_a per fire (Figure 4-8 and Table 4-1). On average, 56 thousand tons of $PM_{2.5}$ are emitted a year for forest fires in Georgia with a 2-year FRI, while only 38 thousand tons are expected using a 5-year FRI.

The corresponding air quality impacts of fire emissions with different FRIs on $PM_{2.5}$ are almost linear to the emissions, as they mainly impact primary species.

Therefore, air quality impacts on $PM_{2.5}$ from individual and overall forest fires with different FRIs follow the respective emission trends (Figure 4-8). The opposing impact trends pose a critical problem in forest and air quality managements to choose an optimized FRI. Generally, a longer FRI is preferred in respect to reduce "long-term" air quality impacts, while a shorter FRI should be adopted to avoid intense "short-term" and local impacts. Specifically, a longer FRI can lower forest fire impacts on annual average $PM_{2.5}$ levels, however, increase chances of higher daily $PM_{2.5}$ levels. This leads to a conflict in regard to air quality management. In addition, the locations of forest fires can be considered in policy decisions. If forest fires are close to a sensitive area, short FRIs might be adopted to avoid significant short-term deterioration of air quality though sacrificing long-term air quality. On the flip-side, longer FRIs might be employed in relatively remote regions to minimize long-term air quality impacts, with less concern about higher local episodic air quality impacts. Moreover, the feasibility of adopting longer FRIs in forest management should also be considered because of the increased risk of fires escaping with a longer FRI.

Understanding the change of forest fires emissions with different FRIs is also important to evaluate uncertainties in air quality modeling without consideration of detailed FRIs of forest fires, since these FRIs are rarely known. For example, annual emissions from forest fires in Georgia estimated using an average FRI (e.g. a 2~5 FRI) are 23% less than those if a 2-year FRI were assumes and 13% more than those if a 5-year FRI were assumed. As discussed in the previous section, forest fires contribute 1.9 $\mu g/m^3$ of $PM_{2.5}$ during March 2002 in the Atlanta $PM_{2.5}$ non-attainment area. Given that such emissions can be roughly 20% more or less due to the unknown FRIs, uncertainties in $PM_{2.5}$ concentrations are approximately 0.38 $\mu g/m^3$.

Table 4-1 Typical annual burned area, fuel consumption and emissions from prescribed forest fires with different FRI in Georgia

FRI (year)	A (million acres)	F_a (tons/acre)	Emissions (10^3 tons)						
			CO	VOC	NO_X	NH_3	SO_2	PM_{10}	$PM_{2.5}$
2~5	0.86	4	519	24	11	2.3	3.1	51	43
2	1.51	2.9	668	31	14	3.0	4.0	65	56
3	1.00	3.8	579	27	12	2.6	3.5	56	48
4	0.75	4.3	485	23	10	2.2	2.9	47	40
5	0.60	5.0	455	21	10	2.0	2.7	44	38

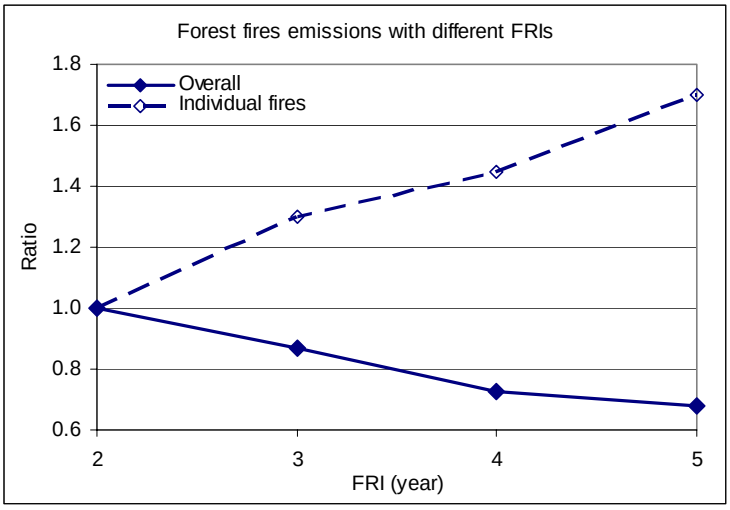

Figure 4-8 Emissions from individual and overall prescribed forest fires with different FRIs

Flaming and smoldering

We apply two methods to estimate emission fractions during both flaming and smoldering stages. The method using the diurnal temporal profile for prescribed forest fires shows that 30% of emissions from prescribed forest fires are released during the smoldering stage and the rest from the flaming stage. The method using specific F_a values and emissions factors for each combustion stage finds 60% of CO, 55% of VOC, 20% of NO_X, 70% of NH_3, 70% of SO_2, and 55% of $PM_{2.5}$ and PM_{10} emissions in the smoldering stage. Explicitly, F_a values estimated by FEPS and FCCS for typical forest types in Georgia indicate that approximately 38% of fuels are consumed during the

smoldering stage. Fuel consumptions during smoldering stage were reported to be 38-44% in the Brazilian Amazon (Kauffman et al., 1998) and over 50% in temperate and boreal fires (Bertschi et al., 2003). Prescribed forest fires in Georgia mainly consume surface fuels; large woody and below ground fuels are usually not consumed during smoldering stage. Therefore, less fuel is consumed during smoldering in Georgia, supporting the estimates by FEPS and FCCS. Even though estimated fractions of fuel consumption during flaming stage are larger than those during smoldering stage, respective emission factors are much higher during smoldering stage for all pollutants except NO_X, leading to larger emission fractions during smoldering stage (except NO_X).

Air quality impacts from forest fires emissions during both combustion stages on $PM_{2.5}$ are discussed here, since March 2002 is not a typical O_3 season though their impacts on O_3 levels have also been observed. $PM_{2.5}$ source contributions from forest fires are mainly caused by corresponding $PM_{2.5}$ emissions (Tian et al., 2006), which are 560 tons/day in Georgia during March 2002. The specific diurnal temporal profiles for flaming and smoldering stages (Figure 4-9) are calculated from the profile used in SMOKE (US-EPA, 2004.), showing the hourly emission rates. Simulations with the estimated emission fractions during both combustion stages by the temporal profile indicate that total forest fires lead to 4.8 $\mu g/m^3$ of $PM_{2.5}$ (monthly average) for the entire Georgia, with 60% of such $PM_{2.5}$ caused by emissions during the smoldering stage. In the Atlanta $PM_{2.5}$ non-attainment area, these fires lead to 1.9 $\mu g/m^3$ of $PM_{2.5}$, with 53% from emissions during the smoldering stage. Larger $PM_{2.5}$ emission fractions during smoldering estimated by the separate F_a values and emissions factors increase estimated $PM_{2.5}$ source contributions from forest fires, with 1.8 $\mu g/m^3$ more $PM_{2.5}$ for the entire Georgia and 0.6 $\mu g/m^3$ more for the Atlanta $PM_{2.5}$ non-attainment area. Such larger fractions also lead to increased portions of $PM_{2.5}$ source contributions from forest fires during the smoldering stage: 81% for the entire Georgia and 76% for the Atlanta $PM_{2.5}$ non-attainment area. Large difference in estimated air quality impacts from forest fires

during different combustion stages suggests the need to improve our understanding of emissions during different stages.

Though there are uncertainties in our understanding of air quality impacts from forest fires, it is obvious that air quality impacts per unit emissions during smoldering are larger than those during flaming. This is due to more effective dispersion of fire emissions at day-time than night, when smoldering fires occur. If techniques as mentioned above are applied to reduce emissions during the smoldering stage, air quality impacts from forest fires can be significantly reduced. Due to an almost linear relationship between forest fire emissions and corresponding impacts on $PM_{2.5}$, 50% reduction in smoldering emissions can lead to approximately 1.5 or 2.7 $\mu g/m^3$ reduction in $PM_{2.5}$ source contributions estimated using the two different emission fractions for the entire Georgia. Similarly, such reduction can cause approximately 0.5 or 1.0 $\mu g/m^3$ reduction in $PM_{2.5}$ source contributions in the Atlanta $PM_{2.5}$ non-attainment area.

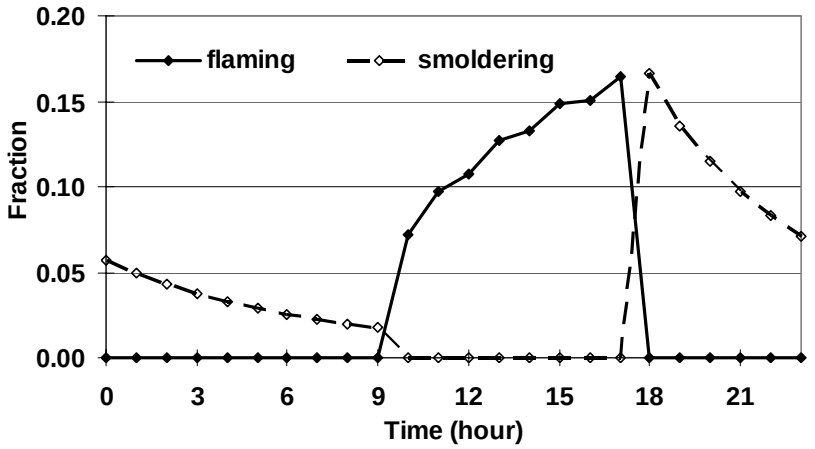

Figure 4-9 Diurnal temporal profiles for prescribed forest fires emissions during flaming and smoldering stages

Table 4-2 Separate $PM_{2.5}$ emissions from prescribed forest fires in Georgia during flaming and smoldering and corresponding $PM_{2.5}$ source contributions for March 2002

	Temporal Profile			Specific Fa and Ef		
	Total	Flaming	Smoldering	Total	Flaming	Smoldering
Emissions (tons/day)	560	390	170	560	250	310
Source contribution ($\mu g/m^3$)						
Atlanta nonattainment	1.9	0.90	1.0	2.5	0.60	1.9
Georgia	4.8	1.9	2.9	6.6	1.2	5.4

Air quality impacts from forest fires when employing different forest management practices, including changing burning season and fire-return intervals (FRIs), and controlling emissions during smoldering, are investigated using source-oriented air quality modeling. Impacts from other forest management practices can also be studied using the methods proposed in this paper.

References

Anderson, G. K., Sandberg, D. V., and Norheim, R. A. (2004). "Fire Emission Production Simulator (FEPS) User's Guide v1.0."

Barnard, W. R., and Brewer, P. (2004). Development of Managed Burning and Wildland Fire Emission Estiamtes for VISTAS. In "13th International Emission Inventory Conference "Working for Clean Air in Clearwater"", Clearwater, FL.

Battye, W., and Battye, R. (2002). "Development of Emissions Inventory Methods for Wildland Fires. Final Report prepared for U.S. EPA." EC/R Incorporated, Research Triangle Park, NC.

Bentley, M. L., and Stallins, J. A. (2005). Climatology of Cloud-to-ground Lightning in Georgia, USA,1992-2003. INTERNATIONAL JOURNAL OF CLIMATOLOGY, 1979–1996.

Bertschi, I., Yokelson, R. J., Ward, D. E., Babbitt, R. E., Susott, R. A., Goode, J. G., and Hao, W. M. (2003). Trace gas and particle emissions from fires in large diameter and belowground biomass fuels. J. Geophys. Res. 108.

Brown, J. K., and Smith, J. K. (2000). "Wildland Fire in Ecosystems: Effects of Fire on Flora," Rep. No. General Technical Report RMRS-GRT-42-volume 2. United States Department of Agriculture, Forest Service, Rocky Mountain Research Station, Ogden, UT.

Butler, A. J., Andrew, M. S., and Russell, A. G. (2003). Daily sampling of PM2.5 in Atlanta: results of the first year of the assessment of spatial aerosol compositon in Atlanta Study. Journal of Geophysical Research-Atmospheres 108 (D1).

Buzcu, B., Yue, Z. W., Fraser, M. P., Nopmongcol, U., and Allen, D. T. (2006). Secondary particle formation and evidence of heterogeneous chemistry during a wood smoke episode in Texas. Journal of Geophysical Research-Atmospheres 111.

Byun, D. W., and Ching, J. K. S. (1999). "Science algorithms of the EPA models-3 Communicty Multiscale Air Quality (CMAQ) modeling system," Rep. No. EPA/600/R-99/030.

Carter, M. C., and Foster, C. D. (2004). Prescribed burning and productivity in southern pine forests: a review. Forest Ecology and Management 191, 93-109.

GFC (2005). Forest Coverage and Mainly Burned Forest Types from Georgia Forestry Commission. Georgia Forestry Commission, Macon, GA.

GFC (2005). Forest fires burned area records from Georgia Forestry Commission. Georgia Forestry Commission, Macon, GA.

GFC (2005). Time for Prescribed Forest Fires from Georgia Forestry Commission. Georgia Forestry Commission, Macon, GA.

Grell, G. A., Dudhia, J., and Stauffer, D. R. (1995). "A Description of the Fifth-Generation Penn State/NCAR Mesoscale Model (MM5)."

Hansen, D. A., Edgerton, E. S., Hartsell, B. E., Jansen, J. J., Kandasamy, N., Hidy, G. M., and Blanchard, C. L. (2003). The southeastern aerosol research and characterization study: Part 1-overview. Journal of the Air & Waste Management Association 53, 1460-1471.

Hardy, C. C., Ottmar, R. D., Peterson, J. L., Core, J. E., and Seamon, P. (2001). "SMOKE Management Guide for Prescribed and Wildland Fire: 2001 Edition," Rep. No. PMS 420-2. NFES 1279. National Wildfire Coodination Group, Boise, ID.

Houyoux, M. R., Vukovich, J. M., Jr., C. J. W., Wheeler, N. J. M., and Kasibhatla, P. (2000). Emission inventory development and processing for the seasonal model for regional air quality. J. Geophys. Res. 105, 9079-9090.

Kauffman, J. B., Cummings, D. L., and Ward, D. E. (1998). Fire in the Brazilian Amazon, 2, Biomass, nutrient pools and losses in cattle pastures. Oecologia 113, 415-427.

Lee, S., Baumann, K., Schauer, J. J., Sheesley, R. J., Naeher, L. P., Blake, D. R., Edgerton, E. S., Russell, A. G., and Clements, M. (2005). Gaseous and Particulate Emissions from Prescribed Burning in Georgia. Environmental Science & Technology (submitted).

NWCG (1998). "Managing Wildland Fire: Balancing America's Natural Heritage and the Public Interest."

Olerud, D. T., and Sims, A. (2003). "MM5 sensitivity Modeling in Support of VISTAS (Visibility Improvement – State and Tribal Association), VISTAS task 2e deliverable."

Ottmar, R. (2005). Fuel Characteristics Classification System.

Phuleria, H. C., Fine, P. M., Zhu, Y. F., and Sioutas, C. (2005). Air quality impacts of the October 2003 Southern California wildfires. Journal of Geophysical Research-Atmospheres 110.

Reinhardt, E. (2004). Using FOFEM 5.0 to Estimate Tree Motality, Fuel Consumption, Smoke Production and Soil Heating From Wildland Fire. http://fire.org/fofem/download/FOFEM5Using.pdf.

Sandberg, D., and Dost, F. N. (1990). "Effects of Prescribed Fire on Air Quality and Human Health," Oregon State Universtiy Press.

Sandberg, D., Ottmar, R., Peterson, J., and Core, J. (2002). "Wildland Fire in Ecosystems: Effects of Fire on Air," Rep. No. General Technical Report RMRS-GTR-42-volume 5. United States Department of Agriculture, Forest Service, Rocky Mountain Research Station, Ogden, UT.

Sapkota, A., Symons, J. M., Kleissl, J., Wang, L., Parlange, M. B., Ondov, J., Breysse, P. N., Diette, G. B., Eggleston, P. A., and Buckley, T. J. (2005). Impact of the 2002 Canadian forest fires on particulate matter air quality in Baltimore City. Environmental Science & Technology 39, 24-32.

Tian, D., Hu, Y., Wang, Y., and Russell, A. (2006). Impacts of Biomass Burning Emissions on Ambient PM2.5 in the Southeastern United States using CMAQ. In preparation.

US-EPA (1998). "Interim Air Quality Policy on Wildland and Prescribed Fires."

US-EPA (2004.). EPA 2001 modeling platform emission inventory. http://www.epa.gov/ttn/chief/emch/invent/. Accessed in May 2005.

US-EPA (2005). Technology transfer network, air quality system. http://www.epa.gov/ttn/airs/airsaqs/. Accessed in May 2005.

USFS (1976). "Southern Forestry Smoke Management Guidebook," Rep. No. General Technical Report SE-10. United States Department of Agriculture, Forest Service, Southeast Forest Experiment Station, Asheville, N.C.

VISTA (2005). Interagency monitoring of protected visual environment. http://vista.cira.colostate.edu/improve/.

Ward, D. E., Peterson, J., and Hao, W. M. (1993). An inventory of particulate matter and air toxic emissions from prescribed fires in the USA for 1989. In "Air and Waste Management Association's 86th Annual Meeting and Exposition". Air and Waste Management Association, Denver, Colorado, USA.

Westerling, A. L., Hidalgo, H. G., Cayan, D. R., and Swetnam, T. W. (2006). Warming and Earlier Spring Increase Western U.S. Forest Wildfire Activity. Science 313, 940-943.

CHAPTER 5 UNCERTAINTIES IN PRESCRIBED FOREST FIRES EMISSION INVENTORIES AND THEIR IMPACT ON AIR QUALITY MODELING

Abstract

Prescribed forest fires emit particulate matter, nitrogen oxides (NO_X), volatile organic compounds (VOCs) and other pollutants into the atmosphere. Due to the limitation of the detailed information on prescribed forest fires (e.g. burned area and fuel consumption), and the temporal and spatial variability, there are large uncertainties associated with current emission inventories for prescribed forest fires. This study aims to evaluate emission uncertainties and their impacts on air quality modeling. Emissions during flaming and smoldering are separately evaluated using specific fuel consumption and emission factors. Four physiographic regions are adopted to describe spatial variance. Uncertainties in burned area, fuel consumption and emission factors are first quantified by literature review, evaluating and propagating modeling uncertainties and by use of expert elicitation to fill specific knowledge gap. Monte Carlo method is further used to propagate the above uncertainties with consideration of different correlations to estimate uncertainties in total emissions, which are then propagated through air quality modeling to get uncertainties in $PM_{2.5}$ concentrations. It is estimated that 48 ± 8.2 thousand tons of $PM_{2.5}$ are emitted by prescribed forest fires in Georgia during 2002. These emissions contribute 7.7 μg/m3 of $PM_{2.5}$ to Georgia and 2.1 $\mu g/m^3$ of $PM_{2.5}$ to non-attainment area during March 2002. The uncertainties in prescribed forest fire emissions lead to 7.3%

This chapter will be submitted to Journal of Air and Waste Management. Co-authors are Armistead Russell, Elisabeth Reinhardt, Yuhang Wang, and Yongqiang Liu.

uncertainties (as coefficient of variance) in simulated $PM_{2.5}$ concentrations within GA, with 2.4% in $PM_{2.5}$ non-attainment area. Therefore, the results from source-oriented air quality modeling with emissions developed using detailed data as in this study are reliable enough and can be used as an important basis for effective air quality management.

Introduction

Fires are essential processes to maintain health in many ecosystems. For example, they influence plant succession, fuel accumulation and decay, nutrient cycles and energy flows, control insects and disease, improve wildlife habitat and forage production, increase water yield, maintain natural succession of land communities, and reduce the need for pesticides and herbicides. However, they can cause ecosystem damage and property loss, and threaten human health and safety. Prescribed fires, which are ignited by management actions and conducted within the limits of fire plans can achieve the benefits of and minimize the adverse impact from fires at the same time. In 1999, there were 2,240,105 acres treated by prescribed fires on Federal lands (NIFC, 2005).

Prescribed fires can emit air pollutants (e.g. particulate matter, volatile organic compounds, nitrogen oxides, carbon monoxide, etc), though their impacts on air quality are rarely studied, particularly in comparison to wildfires (GCVTC, 1996; Phuleria et al., 2005; Sapkota et al., 2005). In 1998, the US EPA issued the Interim Air Quality Policy on Wildland and Prescribed Fires (USEPA, 1998) to address how best to achieve national clean air goals while improving wildland ecosystems health through the increased use of fire. This policy assumes that properly managed prescribed fires can improve the health of wildland ecosystems and reduce the health and safety risks associated with wildfires while meeting clean air and public health goals through careful planning and cooperation among land mangers, air quality regulators, and local communities. The fire smoke management guide developed by the US Forest Service in 2001 (Hardy et al., 2001)

emphasizes actual emission reductions, rather than minimizing smoke impacts by meteorological dispersion as in the 1976 guide (USFS, 1976). Developing effective policies that address the role of prescribed fires in both ecosystem and air quality management requires improved knowledge of the impact on air quality from prescribed fires.

Characterizing effects of prescribed fires on air quality is hampered by the dearth of monitors in rural areas. Source-oriented models, which simulate the physical and chemical process of air pollutants, can be used as a substitute. A first challenge of this approach is to accurately characterize fire emissions. At present, forest fire emissions are typically found by taking the product of the burned area (A), fuel consumed per area (F_a) and an emission factor (E_f):

$$E = A \times F_a \times E_f \quad (1)$$

Fuel consumption is the amount of biomass consumed during a prescribed fire per area, and the emission factor is the ratio of the mass of pollutant per unit mass of fuel consumed. In most cases, available prescribed burn records only give the burn area and the lack of other information makes prescribed fire emission estimation an uncertain endeavor. Currently available emission inventories, [e.g. USEPA National Emission Inventory 1999 version 1.5 and version 3.0, USEPA short term improvements to wildland fires emission inventory, and the Visibility Improvement State and Tribal Association of the Southeast (VISTAS) wildland fires emission inventory] mainly use state-average fuel consumption and emission factors (Table 5.1). Significant differences between these factors suggest potentially large uncertainties in these emission inventories. Meanwhile, characteristics of prescribed forest fires changes over time and space, being dependent upon fuel availability, weather, topography and the way the fire is applied. Fuel availability is primarily determined by the moisture content and fuel size, with additional impact from spatial arrangement and compactness of fuel. In addition, regions are broadly defined, and the mix of vegetation burned within a given area may vary

considerably from regional averages. As such, the amount and nature of pollutants vary widely. Past study suggests that variations in fuel characteristics can contribute up to 83 percent of the error associated in predicting emissions, followed by 30 percent from fuel consumption, and 16 percent from emission factors (Sandberg et al., 2002). Given the potentially large errors in emissions estimates, the large and increasing amount of prescribed forest fires, and the fraction of organic carbon in PM, there is strong reason to quantify uncertainties and their impact on air quality modeling. Here, we conduct an uncertainty analysis of prescribed forest fires emissions, with particular emphasis to emissions and air quality impacts in Georgia, where forest coverage is high and prescribed forest fires have been widely used, and many areas are out of attainment with the $PM_{2.5}$ and O_3 National Ambient Air Quality Standard.

Table 5-1 state-average fuel consumptions (tons/acre) and emission factors (lbs/ton of fuel consumed) used in prescribed forest fire emission inventories of Georgia

	Fuel consumption	Emission Factors							References
		CO	VOC	NO_X	NH_3	SO_2	PM_{10}	$PM_{2.5}$	
EPA NEI99 v1.5	7.1	268	12.8	5.0		0.15	37.6	33.8	(USEPA, 2002)
EPA NEI99 v3.0	9.9	289	13.6	6.2	1.3	1.7	28.1	24.1	(USEPA, 2003a)
EPA Short term	8.0	289	13.6	6.2	1.3	1.7	28.1	24.1	(USEPA, 2003b)
VISTAS	4.0	302	14.2	6.5	1.4	1.8	29.4	25.2	(Barnard and Brewer, 2004)

Methods

Conducting prescribed forest fires in Georgia requires burning permits from the Georgia Forestry Commission (GFC), which are recorded and used to estimate burned area. Burning permits are recorded monthly at the county-level. An exception is military bases, which maintain supplemental data. These records are used, along with regional-average fuel consumptions and emission factors (Table 5.1), to develop an initial inventory of prescribed forest fires emissions.

Emissions during flaming and smoldering stages of prescribe fires have different pattern and dispersion behavior in the atmosphere (Sandberg and Dost, 1990). Generally, flaming combustion mainly consumes fuels with high surface to volume ratios, such as grasses, litter, shrubs, and small diameter woody fuels, and is more complete with less air pollutant emissions per mass of fuel consumed. The major products are CO_2, water vapor and NO_X, and most of these emissions are entrained in a convection column caused by the high thermal energy released in this phase. On the contrary, smoldering combustion is more prevalent in certain fuel types such as duff, organic soils, and rotten logs, with large amounts of incomplete combustion product emissions such as CO, VOC, and PM. Practically, it is hard to differentiate emissions in these two phases, since they sometimes occur at the same time, thus a definition based on whether emissions are influenced by the strong convection associated with a flame front is adopted in this paper (Wade and Lunsford 1989, Sandberg and Dost 1990). Separate fuel consumptions during flaming and smoldering are combined with the applicable, different emission factors for each combustion stage to estimate emissions:

$$E = E_{\text{flaming}} + E_{\text{smoldering}} = A \times (F_{af} \times E_{ff} + F_{as} \times E_{fs}) \quad (2)$$

Where F_{af} and F_{as} are fuel consumption, and E_{ff} and E_{fs} are emissions factors during flaming and smoldering, respectively.

Uncertainties in prescribed forest fire emission estimates are assessed by propagating uncertainties in A, F_{af}, F_{as}, E_{ff} and E_{fs} using Monte Carlo analysis (Morgan and Henrion, 1990). Approaches used to quantify uncertainties in A, F_{af}, F_{as}, E_{ff} and E_{fs} include literature review, evaluating and propagating modeling uncertainties (e.g., in model inputs), and by use of limited expert elicitation to fill specific knowledge gaps (Morgan and Henrion, 1990). Monte Carlo analysis is also applied to quantify F_a uncertainties. These emissions and their associated uncertainties are then input into a source-oriented air quality model to study their impacts on air quality model simulations.

Burned area uncertainties

Individual estimates of fire size based on burning permits tend to be biased systematically high. For example, geographic features, non-uniform fuelbeds, or a change in the weather will often cause a fire to create a mosaic of burned, partially burned and unburned areas, although the entire landscape within the fire perimeter is often reported as burned (Sandberg et al., 2002). It is likely that the burned area estimated from the permit is some fraction of the permitted area. Uncertainties associated with the burned area in different seasons are obtained by expert elicitation (Table 5-3). Three experts at Georgia Forestry Commission, who issue burning permits in Georgia, conduct prescribed burns, predict air quality impacts from prescribed burns, manage field operations, and understand Georgia forest characteristics, were gathered. Goals of this research and summaries of related information based on literature review were provided to them. Active discussions between these experts led to a consensus on the estimates of uncertainties. These estimates were then summarized by the authors and reviewed again by these experts.

Fuel consumption uncertainties

Fuel consumption can be obtained through measurements of pre- and post-burn fuel loading for each fire. However, these data are rarely available or don't provide separate F_{af} and F_{as}. Three fire behavior models, the First Order Fire Effects Model (FOFEM) v5.21 (Reinhardt, 2004), Fire Emission Production Simulator (FEPS) v1.0 (Anderson et al., 2004), and Fire Characteristic Classification System (FCCS) (Ottmar, 2005) are employed to estimate fuel consumption using pre-burn fuel characteristics, such as relative abundance of particular fuelbed components and the condition of the fuel. FEPS and FCCS give separate fuel consumptions during flaming, short-term smoldering and residual smoldering combustion (RSC), while FEFOM only offers fuel consumptions during flaming and short-term smoldering. According to the definition of flaming and

smoldering in this study, fuel consumption during both flaming and short-term smoldering are treated as F_{af}, and fuel consumption during RSC as F_{as}. Initially, each model is applied using default pre-burn fuel loadings specific to that model. Such defaults typically represent parameters for the major forest types. In addition, since moderate fuel moisture content is critical to ensure sufficient fire intensity of prescribed fires and protect forest roots, simultaneously, moderate fuel moisture is assumed in the simulations with the fire behavior models.

Eight default forest cover types for loblolly pine (usually coexists with shortleaf pine) and slash pine (usually coexists with longleaf pine) (SAF 070, SAF 080, SAF 081a, SAF 081b, SAF 083, SAF 084, SRM 809) are selected for use in FOFEM based on their abundance in prescribed fire applications. Estimated fuel consumption of each cover type are averaged for loblolly pine and slash pine, which is further weighted by their relative abundance in Georgia pine forests (63% loblolly pine vs 37% slash pine: Biogenic Emissions Landuse Database version 3 available at http://www.epa.gov/ttn/chief/emch/biogenic) to get the average fuel consumption for Georgia. FEPS provides default fuel loadings to National Fire Danger Rating System (NFDRS) fuel model. NFDRS D (Southern rough), and P (Southern pine plantation) fuel models are used and their corresponding fuel consumption results are then weighted by their coverage in Georgia to obtain the state average (42% D model vs 58% P model: http://www.fs.fed.us/land/wfas/nfdr_map.htm). Two default fuelbeds for loblolly (242) and slash pine (191) were employed for FCCS. Fuel consumption characteristics are also weighted by the abundance of loblolly and slash pine as for FOFEM. These separate fuel consumptions (F_{af} and F_{as}) from FCC and FEPS are also used to calculate fraction of fuel consumption during smoldering (f_s).

Uncertainties in fuel consumption are quantitatively evaluated using FOFEM, assuming the uncertainties are mainly from uncertainties in pre-burn fuel characteristics. FOFEM is chosen over other models due to its flexibility to change the inputs and

capability of batch mode execution. In addition, four physiographic regions, i.e. mountain, piedmont, upper coastal, and lower coastal (Figure 5-2) are adopted to account for the spatial variability of fuel characteristics. In each region, vegetation varies depending on soil type, elevation, moisture, etc. Uncertainty in each fuel characteristic input is obtained through expert elicitation as described above. Those judgments are the combination of expert experience and previous limited field measurements (Brown and Smith, 2000; McNab and Edwards, 1976; McNab et al., 1978; Schoch and Binkley, 1986; USFS, 1976). Expert judgment considers a range of additional factors and the following conclusions were reached: 1) main vegetation cover types burned in Georgia are loblolly pine, slash pine, longleaf pine, and shortleaf pine, in decreasing order, and they burned at about 2~5 year intervals (Brown and Smith, 2000; Carter and Foster, 2004; GFC, 2005). 2) All of Georgia prescribed fires fall within the understory fire regime, which indicates that fires mainly consume understory fuel components (e.g. litter and duff) and approximately 80 percent or more of the above ground dominant vegetation survives fires (Brown and Smith, 2000). 3) Though slash burns are usually more severe than general prescribed fires, there is little reason to separately study them since their burned area is less than 5 percent of the total prescribed burned area (GFC, 2005).

Expert judgment is used to develop uncertainty distributions in each FOFEM input variable. Monte Carlo is then applied to propagate these uncertainties through FOFEM to get the uncertainties in fuel consumption (Morgan and Henrion, 1990). Three thousand independent, random input sets were generated. Unfortunately, FOFEM doesn't estimate fuel consumption during smoldering (F_{as}). The estimated f_s above is then used to extrapolate F_{as} from F_{af} by:

$$F_{as} = \frac{f_s}{(1 - f_s)} F_{af} \qquad (3)$$

When uncertainties in F_{as} are propagated from the uncertainties in F_{af} and f_s according to equation 3 using Monte Carlo method, larger uncertainties in F_{as} for lower coastal area

are observed, which is inconsistent with practical situations. Therefore, the uncertainty factors for F_{as} are assumed the same as those for F_{af} in this study.

Emission factor uncertainties

Emissions from forest fires have been characterized by researchers since about 1970 to estimate emission factors for criteria pollutants and many hazardous air pollutants using a carbon-balance method (Battye and Battye, 2002; Ward et al., 1993). Emissions factors are a function of the composition of the fuel and the physical and chemical processes during combustion. Emission factors for pollutants that contain only carbon, oxygen, and hydrogen (Type I) are controlled by the combustion process, while emission factors for pollutants with minor elements, such as nitrogen, sulfur, and the halogens (Type II), are determined by both factors. Uncertainties in emission factors are quantified according to both literature review and specific field measurements for prescribed forest fires in Georgia conducted in 2004 (Lee et al., 2005). Type I pollutants should have similar results obtained from these two methods, and the recent field measurements in the Southeast are viewed as more representative for Type II pollutants in Georgia forests because results from literature reviews are based on field measurements from the western US and laboratory studies (Battye and Battye, 2002).

CO and $PM_{2.5}$ (Type I) emission factors are parameterized as a function of combustion efficiency (CE, Table 5-7 (Battye and Battye, 2002)), an indicator for the completeness of combustion. CEs from the field measurement in Georgia are 0.94±0.02 and 0.84±0.06 (mean ± standard deviation) during flaming and smoldering respectively, and used to calculate these emission factors. Their associated uncertainties from both the uncertainties in CE and the parameter uncertainties in the equations are considered. Therefore, uncertainties in the emission factors are quantified by traditional propagation:

$$UC_{ef}^2 = UC_{ce}^2 + UC_{parameter}^2 \quad (4)$$

UC_{ef} refers to the uncertainties in emission factors, while UC_{ce} and $UC_{parameter}$ refer to uncertainties in the CE and the parameters respectively. Uncertainties in CE (UC_{CE}) are defined by the standard deviation in the field measurements conducted in Georgia and are then propagated using the Gaussian method (Morgan and Henrion, 1990) to estimate UC_{ce}:

$$UC_{ce}^2 = (\frac{\partial f}{\partial CE})^2 UC_{CE}^2 \quad (5)$$

Where f refers to the empirical equations for CO or $PM_{2.5}$ emission factors (Table 5-7). $UC_{parameter}$ is estimated by the coefficient of variance (cov) of the empirical equations:

$$UC_{parameter} = \text{cov} \times f(CE_{mean}) \quad (6)$$

CE_{mean} refers to the mean of CE and $f(CE_{mean})$ is the emission factor calculated with CE_{mean}. cov is defined as standard deviation divided by mean, and given to describe the parameter uncertainties in the equations. Both the CO emission factor and its associated uncertainty estimated by the field measurement in Georgia agree with the results estimated by the above method, as does the $PM_{2.5}$ emission factor uncertainty, though the $PM_{2.5}$ emission factor itself is biased low. VOC and PM_{10} emission factors are functions of CO and $PM_{2.5}$ emission factors respectively, and their associated uncertainties are determined by the same method described above. NH_3 and SO_2 emission factors (Type II) and their associated uncertainties are determined by field measurements in Georgia. Their uncertainty distributions are based on standard deviations of the measured NH_3 and SO_2 emission factors which are calculated from seven measurements at various locations. The NO_X emission factor and its associated uncertainty are obtained from literature review (Battye and Battye, 2002).

Emission uncertainties

Uncertainties in individual emission estimate (i.e. emission in each county during a month) are propagated from uncertainties in A, F_{af}, F_{as}, E_{ff}, and E_{fs} using the Monte

Carlo method (Morgan and Henrion, 1990) assuming independence between A, F_a and E_f during each combustion phase. Five thousand independent random input sets were generated. Mean and cov are calculated for the outputs with these input samples. Uncertainties in total emissions during both combustion phases are impacted by the correlation between F_{af} and F_{as} ($cor\_F_{af}\&F_{as}$), and correlation between E_{ff} and E_{fs} ($cor\_E_{ff}\&E_{fs}$). Spearman's rank correlations are adopted to describe the correlations for generating the random number matrix (Kendall, 1987). As different fuel components are consumed, and different combustion behavior, during flaming and smoldering, certain but not strong correlations (i.e. rank correlation coefficient ranges from 0.1~0.5) between F_{af} and F_{as}, and between E_{ff} and E_{fs} are used. Emission estimates for Thomas County, GA, during March are used to illustrate the impacts from different correlations. Thomas County is a heavily forested area and March is the month with the greatest prescribed burning activity. This study assumes rank correlation coefficients for $cor\_F_{af}\&F_{as}$ and $cor\_E_{ff}\&E_{fs}$ are 0 for the following analysis on the uncertainties in total emissions during both combustion phases. (explained later in the results section).

Monthly total emissions from all counties in Georgia were calculated by

$$E_{monthly} = \sum_i E_i = \sum_i A_i \times (F_{af_i} \times E_{ff_i} + F_{as_i} \times E_{fs_i}) \quad (7)$$

Where i refers to each of the 159 counties in Georgia. Usually, mean of $E_{monthly}$ is estimated by summing the mean of E_i, and its associated uncertainty is calculated by

$$UC^2_{E_{monthly}} = \sum_i UC^2_{E_i} \quad (8)$$

UC_{Ei} refers to the standard deviation of E_i. The above method (EQN) assumes independence between individual estimates and uncertainties have a normal distribution. Monte Carlo is further employed to directly propagate the input uncertainties (including uncertainties in A_i, F_{afi}, F_{asi}, E_{ffi} and E_{fsi}) to obtain $UC_{Emonthly}$. For individual fire estimate i, as described above, independence between A, F_a, and E_f is assumed. Two extreme cases are then considered for correlation between individual estimates: perfect

independence (IND) and dependence (DEP). IND assumes independence of A, F_a and E_f between individual estimates i and j, while DEP assumes perfect dependence of A, F_a and E_f. In all cases, IND should give the lowest bound, and DEP should give the upper bound of uncertainties. Finally, correlations between individual fire estimates (e.g. i and j) are accounted by defining correlations of A, F_a and E_f between i and j. A has a low correlation between individual estimates (rank correlation coefficients 0~0.4), F_a in the same physiographic regions (intra-region) has relatively high correlations (rank correlation coefficients 0.5~1), F_a in different physiographic regions (inter-region) had relatively low correlations (rank correlation coefficients 0~0.4), and E_f has high correlations (rank correlation coefficients 0.5~1). Tests with different correlations are conducted for monthly total emission estimates during March and the results suggest rank correlation coefficients of 0.1, 0.7, 0.1, and 0.7 respectively being used for A, intra-region F_a, inter-region F_a, and E_f (explained later in the results section). These correlations are then applied to calculate the uncertainties in monthly and annual total emissions within Georgia or by physiographic regions during 2002.

Impact on air quality

Air quality impacts from prescribed forest fires are investigated using the Community Multiscale Air Quality (CMAQ) model v. 4.3, with the Carolina Environmental Program's (CEP) Sparse Matrix Operator Kernel Emissions (SMOKE) Modeling System v. 2.1 (Houyoux et al., 2000) as the emission processor. Modeling configurations and evaluation using observations are described in detail elsewhere (Tian et al., 2006). March 2002 is chosen as the modeling episode due to the largest amount of monthly emissions in Georgia, and impacts on $PM_{2.5}$ (monthly average $PM_{2.5}$ is calculated to eliminate the impact from uncertainties in temporal profiles.) are evaluated. Though elevated ozone has been observed with extensive forest fire emissions, ozone impact is not considered in this study, as March is not in the ozone season (so there is

litter observational data) for Georgia and ozone precursor (VOC and NO_X) emissions from forest fire emissions are significantly smaller than other sources.

$PM_{2.5}$ sensitivities to emissions from forest fires are calculated from two simulations, with and without forest fire emissions. Results show that $PM_{2.5}$ forest fire emissions contribute more than 99% of $PM_{2.5}$ caused by forest fire emissions, and impact from other pollutant emissions can be ignored. The $PM_{2.5}$ sensitivities to $PM_{2.5}$ emissions are then used to propagate uncertainties in $PM_{2.5}$ forest fire emissions using the Gaussian method (Morgan and Henrion, 1990) to estimate uncertainties in $PM_{2.5}$ concentration. Uncertainties in total emissions within Georgia ($UC_{E_{GA}}$) are used, instead of uncertainties in emissions from each county (UC_{Ei}) due to computational cost. Since UC_{Ei}s are similar within a physiographic region and no significant difference of uncertainties in $PM_{2.5}$ emissions between regions has been found (Uncertainties in the mountain are significantly different from other regions, but less than 1% forest fires occur in this region. Explained later in the results section), adopting $UC_{E_{GA}}$ should not impact the results of uncertainties in $PM_{2.5}$ concentrations. The difference between uncertainties during flaming and smoldering phase is also small and thus not separately considered. Therefore, the uncertainties in $PM_{2.5}$ concentrations are estimated by

$$UC_{PM_{2.5}} = S_{E_{GA}} UC_{E_{GA}} = SS_{E_{GA}} \mathrm{cov}_{E_{GA}} \quad (9)$$

Where, $UC_{PM_{2.5}}$ refers to standard deviation of $PM_{2.5}$ concentration; E_{GA} is the total $PM_{2.5}$ emission from Georgia with associated uncertainty $UC_{E_{GA}}$ (as standard deviation) and $\mathrm{cov}_{E_{GA}}$; $S_{E_{GA}}$ is the $PM_{2.5}$ sensitivity to E_{GA}; and $SS_{E_{GA}}$ is the semi-normalized sensitivity. $\mathrm{cov}_{E_{GA}}$ is estimated as detailed above and $SS_{E_{GA}}$ is calculated using CMAQ.

Results and Discussion

In 2002, approximately 820,000 acres of forests in Georgia were burned using prescribed fires, mainly during winter and spring months (Figure 5-1), peaking in March, which alone, had 43% of the total. These fires emit about 41~ 98 thousand tons of $PM_{2.5}$ and significant amount of other pollutants (Table 5-2). More than a factor of two difference between emission estimates using different state-average fuel consumption and emission factors indicates potential large uncertainties in current emission inventories. Uncertainties in input parameters are first illustrated, following by emission uncertainties propagated from the input uncertainties. Their impact on air quality modeling is also discussed as well.

Table 5-2 Emission estimates (10^3 tons) from state-average fuel consumption and emission factors in Georgia during 2002

	CO	VOC	NO_X	NH_3	SO_2	PM_{10}	$PM_{2.5}$
EPA NEI99 v1.5	780	37	14		0.4	110	98
EPA NEI99 v3.0	1200	55	25	5.3	6.9	110	97
EPA Short term	940	44	20	4.2	5.5	92	79
VISTAS	490	23	11	2.3	2.9	48	41

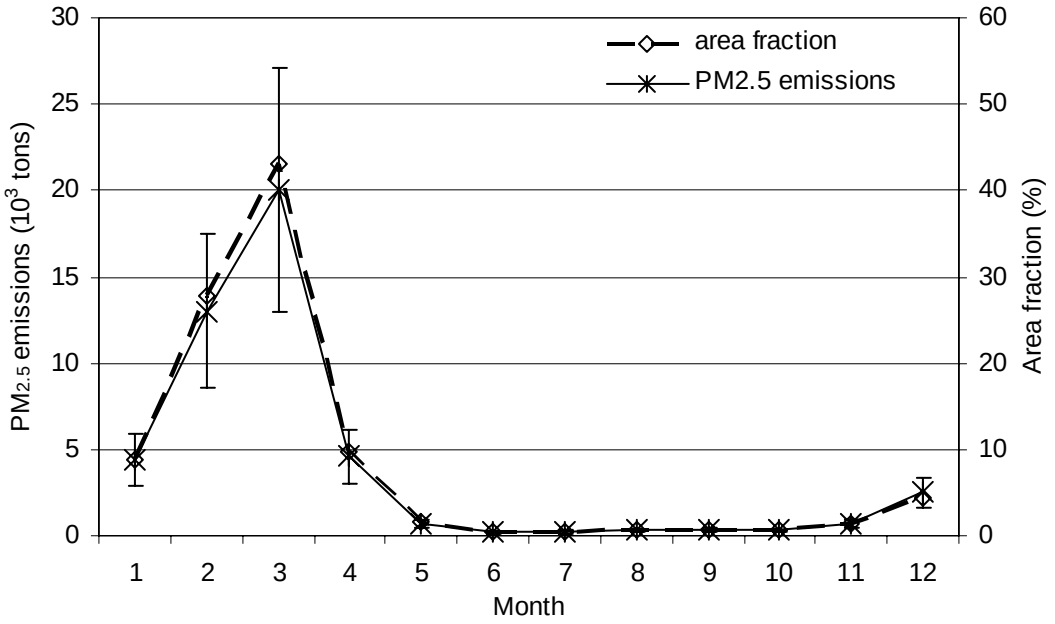

Figure 5-1 Monthly fraction (%) of burning permit area and total $PM_{2.5}$ emissions for prescribed forest fires in Georgia during 2002. Error bars refer to 95% confidence interval.

Uncertainties in burned area

Fires tend to burn more completely during winter due to the fuel being dry, followed by spring/fall and then summer, when the fuel is the moistest. Uncertainties are also highest during summer for the same reason (Table 5-3). Normal distribution is assumed for burned area, with mean being 90% and 95% confidential interval ranging from 85% to 95% of burning permit area during winter. Uncertainties for other seasons can be inferred from information in Table 5-3.

Table 5-3 Uncertainties[1] in burned area estimates (A) from burning permits

Season	Duration	Mean fraction (%)[2]	UC (%) [2,3]
Spring/Fall	Mar - Apr, Sep - Nov	85	5
Summer	May - Aug	80	10
Winter	Dec - Feb	90	5

[1] Normal distribution is assumed.
[2] Mean of burn area estimate (A_mean) is a fraction of burning permit area (Permit_Area) and is expressed in percent, e.g. A_mean equals to 0.9 × Permit_Area during winter.
[3] UC refers to 95% confidential interval, between (A_mean - UC × A_mean) and (A_mean + UC × A_mean).

Fuel consumption uncertainties

Similar estimates of fuel consumption during flaming and short-term smoldering by FOFEM and FCCS, which use different algorithms, give confidence in the emission estimates, though the estimates by FEPS are about 50% more during flaming and three times more during short-term smoldering (Table 5-4). This disagreement is mainly caused by the default fuel characteristic inputs used in FEPS which are not representative of the forests in Georgia that utilize prescribed fires (Anderson et al., 2004). Further comparison with the fuel consumption used in the VISTAS fire emission inventory (Table 5-1), which represents current best understanding of southern forests from forest managers (Barnard and Brewer, 2004), indicates that estimates by FCCS and FOFEM have better agreement. FOFEM is further used to propagate uncertainties in pre-burn fuel characteristics.

Log-normal distributions are adopted to describe the uncertainties in the FOFEM input variables. Pre-burn fuel loadings are categorized by litter, duff, herbaceous, shrub, 1-hr wood, 10-hr wood, 100-hr wood and 1000-hr wood in FOFEM (Reinhardt, 2004), with n-hr wood referring to different size of wood fuel. They increase from mountain to lower coastal regions, consistent with the trend of moisture content and heat. Meanwhile, uncertainties associated with the pre-burn fuel loadings decrease due to larger variability

of the fuel distribution within mountains (Figure 5.2 and Table 5.5). Uncertainties associated with shrub fuel are the largest. Though south and coastal areas in Georgia tends to be moister, fuel moisture is assumed the same among the four regions and only varies with fuel components, since the prescribed forest fires are usually conducted within certain limits. These FOFEM input uncertainties are propagated using Monte Carlo method, resulting in uncertainty distributions of F_{af} by four regions (Table 5-6), which show that the lower coastal has the largest F_{af} (7.3 tons/acre) and smallest uncertainties (factor of 1.3), while the mountain region is opposite (2.6 tons/acre and factor of 1.9). F_{af} estimated for mountain and piedmont regions are comparable to the state-average estimates by FOFEM using default fuel characteristics (3.2 tons/acre).

f_s is about 39% and 37% respectively from FEPS and FCCS (Table 5-4). Similar results have been reported by studies on biomass burning in other regions, e.g 38~44% biomass is consumed during smoldering in the Brazilian Amazon (Kauffman et al 1998) and over 50% of the biomass in temperate and boreal fires (Bertschi et al., 2003). Same f_s (0.38) is used to extrapolate F_{as} from F_{af} for all regions. F_{as} ranges from 1.6 tons/acre (in the mountain region) to 4.5 tons/acre (in the lower coastal region). As mentioned above, same uncertainty factors as for F_{af} are applied to F_{as}.

Table 5-4 Separate fuel consumption (tons/acre) during flaming and smoldering from three fire behavior models

	Flaming			Smoldering	Total[1,2]	Smoldering Fraction (%)
	Flaming	Short-term Smoldering	Sub-Total			
FOFEM	2.3	0.9	3.2			
FEPS	3.2	3.2	6.4	4.1	10.5	0.39
FCCS	2	0.7	2.7	1.6	4.3	0.37

[1] Total is not equal to the sum of flaming and smoldering value due to round off.
[2] Total is the sum of flaming and smoldering.

Table 5-5 Uncertainties in FOFEM input Variables [1]

	Mountain		Piedmont		Upper Coastal		Lower Coastal	
	Mode[3]	UC [4] (factor)	Mode[3]	UC [4] (factor)	Mode[3]	UC [4] (factor)	Mode[3]	UC [4] (factor)
Fuel loading (tons/acre)[2]								
Litter	0.35	3	0.4	1.5	0.5	1.5	1	1.6
1-hr wood	1.5	2	1.5	2	2	1.5	1	1.5
10-hr wood			0.5	1.4	0.7	1.3	1.5	1.4
100-hr wood					0.2	1.5	0.5	1.2
1000-hr wood	0.2	1.5	0.2	1.5	0.2	1.5	1	1.5
Duff	3	2	3	2	4	1.5	5	1.7
Herbaceous			0.3	1.5	0.4	1.3	0.6	1.5
Shrub	0.2	10	0.1	10	0.2	10	3	1.7
Fuel moisture (%)								
10-hr wood	12	1.6	12	1.6	12	1.6	12	1.6
1000-hr wood	20	1.3	20	1.3	20	1.3	20	1.3
Duff	75	1.5	75	1.5	75	1.5	75	1.5
Other								
1000-hr percent rotten (%)	10	1.6	10	1.6	10	1.6	10	1.6
Duff depth (inches)	0.7	3	1	1.2	1.5	1.4	2.5	2.8

[1] Log-normal distribution is assumed.
[2] Litter, 1-hr wood, 10-hr wood, 100-hr wood, 1000-hr wood, duff, herbaceous and shrub are the fuel components that are consumed during prescribed forest fires.
[3] Mode refers to the nominal value. Its unit is shown in the column of variables.
[4] UC refers to uncertainty range (includes 95% of data) between (Mode / Factor) and (Mode × factor).

Table 5-6 Uncertainties[1] in prescribed forest fire fuel consumption (tons/acre) using FOFEM for the four regions in Georgia

Region	Fraction (%)[2]	Flaming		Smoldering	
		Mode[3]	UC (factor)[4]	Mode[3]	UC (factor)[4]
Mountain	1	2.6	1.9	1.6	1.9
Piedmont	12	3.1	1.6	1.9	1.6
Upper Coast	42	4.3	1.4	2.6	1.4
Lower Coast	44	7.3	1.3	4.5	1.3

[1] Log-normal distribution is assumed.
[2] Fraction refers to fraction of prescribed forest fires in specific region.
[3] Mode refers to the nominal value.
[4] UC refers to uncertainty range (includes 95% of data) between (Mode / Factor) and (Mode x factor).

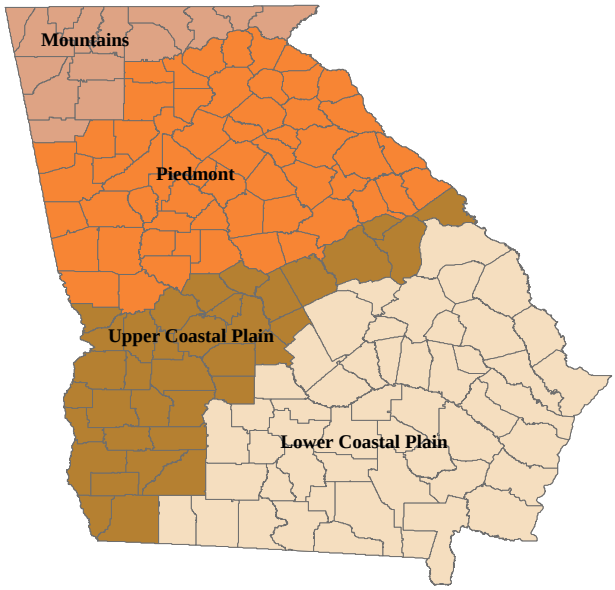

Figure 5-2 Physiographic regions in Georgia

Emission factor uncertainties

Emission factors for CO, VOC, NH_3, SO_2, PM_{10} and $PM_{2.5}$ (Table 5-7) are larger during smoldering than flaming, though their associated uncertainties are comparable in these two phases. On the contrary, the NO_X emission factor is larger during the flaming phase, with a larger uncertainty during smoldering. In addition, uncertainties in emission factors of CO, PM_{10} and $PM_{2.5}$ are much smaller than other pollutants. Emission factors and their uncertainties of CO, VOC, NO_X, PM_{10}, and $PM_{2.5}$ agree well with aggregated emissions factors during both combustion phases for extra-tropical forests (Table 5-7) (Andreae and Merlet, 2001), though emission factors for NH_3 and SO_2 used here are much lower. As they are largely determined by nitrogen and sulfur content in the fuel, values used in this study are more representative of forests in Georgia.

Table 5-7 Emission Factors (lbs/ton of fuel consumed) and their uncertainties[1] based on literature review and field measurements of prescribed fires in Georgia

				Flaming		Smoldering		Andreae
	Source	Equation	cov[2]	Mode[3]	UC (factor)[4]	Mode[3]	UC (factor)[4]	(2001)
CO	Equation	1922 – 1968 * CE	10%	81.9	1.9	265	1.9	214±74
VOC	Equation	0.085 * EF(CO)	55%	7.0	2.4	22.5	2.4	11.4±9.2
NO_X	Literature			6.2	1.7	2.2	3.4	6±2.8
NH_3	Measurement			0.301	4.8	0.996	4.1	2.8±1.6
SO_2	Measurement			0.0624	4.9	0.207	4.1	2
PM_{10}	Equation	1.18 * EF($PM_{2.5}$)	10%	11.7	1.6	26.3	1.7	
$PM_{2.5}$	Equation	134.8 – 133.6 * CE	10%	9.9	1.6	22.3	1.7	26±14

[1] Log-normal distribution is assumed.
[2] cov refers to uncertainty in the parameters of empirical equations.
[3] Mode refers to the nominal value.
[4] UC refers to uncertainty range (includes 95% of data) between (Mode / Factor) and (Mode x factor).

Emission uncertainties

Emission and their associated uncertainties during flaming or smoldering of the largest prescribed fire within each physiographic region of Georgia during 2002 (Table 5-8) are first estimated. Emissions during smoldering contribute about 66% of CO, 66% of VOC, 20% of NO_X, 66% of NH_3, 66% of SO_2, 58% of PM_{10}, and 58% of $PM_{2.5}$ total emissions. Uncertainties in emissions during each combustion phase are similar, except for NO_X emissions with much larger uncertainties during smoldering. Sensitivities of uncertainties in total emissions during both combustion phases for Thomas County during March to correlations (i.e. cor_F_{af}&F_{as} and cor_E_{ff}&E_{fs}) indicate that emission estimates for most pollutants are not very sensitive to cor_F_{af}&F_{as} and cor_E_{ff}&E_{fs}, except NH_3 and SO_2. For example, uncertainties in total $PM_{2.5}$ emissions during both combustion phases range from 0.21 to 0.25 (as cov) with different correlations. Given the small amount of NH_3 and SO_2 emissions, this study assumes rank correlation coefficients for cor_F_{af}&F_{as} and cor_E_{ff}&E_{fs} are 0 for the following analysis. Total emissions during both combustion phases have smaller uncertainties than those during each combustion

phase. Generally, prescribed forest fires in the mountain and piedmont regions are smaller than those in the coastal regions, while the associated uncertainties are opposite due to the large uncertainties in the fuel consumption. Similar to the uncertainties in emission factors, CO, PM_{10} and $PM_{2.5}$ emissions have relative smaller uncertainties compared to other pollutants, especially NH_3 and SO_2. In addition, area itself, alone, does not govern emission strength due to variability of fuel consumption. For example, the same area burned in the lower coastal region has larger emissions than in the piedmont region.

Table 5-8 Uncertainties in individual emission estimate (tons) from each physiographic region within Georgia

Source	Combustion Phase[5]	CO		VOC		NO_X		NH_3		SO_2		PM_{10}		$PM_{2.5}$	
		mean	cov[4]	mean	cov[4]	mean	cov[4]	mean	cov[4]	mean	cov[4]	mean	cov[4]	mean	cov[4]
Floyd_3[1]	F	120	0.49	11	0.61	9	0.45	0.6	1.09	0.12	1.02	17	0.40	15	0.40
1258[2]	S	250	0.47	22	0.57	2	0.80	1.1	0.96	0.25	0.94	24	0.45	21	0.45
Mountain[3]	A	370	0.39	33	0.48	12	0.42	1.8	0.76	0.37	0.78	42	0.35	36	0.35
Jones_2[1]	F	910	0.42	81	0.54	68	0.38	4.3	1.00	0.9	0.96	120	0.33	100	0.33
7279[2]	S	1800	0.42	160	0.54	17	0.70	8.1	0.86	1.7	0.84	170	0.37	150	0.37
Piedmont[3]	A	2700	0.34	240	0.44	84	0.37	12	0.73	2.5	0.71	300	0.29	250	0.29
Baker_3[1]	F	4400	0.39	400	0.51	330	0.33	21	0.96	4.4	0.98	610	0.28	520	0.28
27555[2]	S	8500	0.36	750	0.48	82	0.69	39	0.85	8.1	0.84	840	0.33	710	0.33
Upper Coast[3]	A	13000	0.31	1200	0.41	410	0.34	60	0.69	13	0.69	1500	0.25	1200	0.25
Thomas_3[1]	F	18000	0.36	1600	0.49	1300	0.32	85	0.95	17	0.96	2500	0.26	2100	0.26
65632[2]	S	35000	0.35	3100	0.48	340	0.69	160	0.82	33	0.81	3500	0.31	2900	0.31
Lower Coast[3]	A	53000	0.30	4700	0.40	1700	0.32	250	0.70	51	0.69	5900	0.24	5000	0.24

[1] A county with largest prescribed forest fires in each physiographic region within Georgia is chosen. Source name is composed by the county name and the month when the county has the largest prescribed forest fires. For example, Thomas_3 refers to forest fires in Thomas County, Georgia during March.
[2] The number is the burned area of the prescribed forest fires in acres.
[3] It is the physiographic region that each source is located in.
[4] cov: coefficient of variance, which equals to the standard deviation divided by the mean.
[5] Emissions and their associated uncertainties are given by combustion phases. F: flaming; S: residual smoldering combustion; A: both phases.

Uncertainties in monthly total emission estimates for all counties in Georgia during March 2002 are estimated by different methods (Table 5-9), with same mean of emissions. Uncertainties calculated by EQN are comparable to those by IND, and uncertainties by DEP are much larger. Both EQN and IND ignore the correlation between each fire, which leads to a smaller uncertainty. Uncertainties estimated by DEP are comparable to those in individual fires since ideal correlation between each fire is assumed. Actual uncertainties in emission estimates should be somewhere between the estimates by IND and DEP. Uncertainties estimated with various rank correlation coefficients indicate that the uncertainties are not sensitive to the correlations of A, intra-region F_a, inter-region F_a and E_f between individual estimates, though larger effects on NH_3 and SO_2 emission estimates are observed (They are ignored due to their low contributions.). For example, uncertainties in total $PM_{2.5}$ emissions in Georgia during March range from 0.15 to 0.20 (as cov) with the coefficients mentioned above. Therefore, 0.1, 0.7, 0.1 and 0.7 are chosen for rank correlation coefficients of A, intra-region F_a, inter-region F_a, and E_f respectively. These values are then used to estimate uncertainties in other monthly or annual total emissions in Georgia or by regions. Relative uncertainties in total emissions within Georgia during March 2002 are 22% for CO, 30% for VOC, 25% for NO_X, 52% for NH_3, 52% for SO_2, 18% for PM_{10} and 18% for $PM_{2.5}$ (Table 5-10). Similar results have been observed for uncertainties in total emissions during other months, and are not included here for brevity. Monthly total $PM_{2.5}$ emissions during each month in 2002 (Figure 5-1) show similar trends as the burned area, peaking in March (95% confidential intervals are also shown.). Difference in uncertainties by pollutants or combustion phases is same as the individual estimate.

Table 5-9 Uncertainties in monthly total emission estimates for all counties in Georgia during March 2002

	Rank Correlation Coefficient				CO	VOC	NO_X	NH_3	SO_2	PM_{10}	$PM_{2.5}$
	Area	F_a Intra-region	F_a Inter-region	E_f							
					Mean (10^3 tons)						
					210	19	6.6	1.0	0.20	24	20
					Uncertainties (cov)						
EQN					0.08	0.11	0.09	0.19	0.19	0.06	0.06
IND	0.0	0.0	0.0	0.0	0.08	0.11	0.09	0.19	0.19	0.06	0.06
DEP	1.0	1.0	1.0	1.0	0.27	0.36	0.30	0.62	0.62	0.22	0.22
COR	0.1	0.7	0.1	0.7	0.22	0.30	0.25	0.52	0.52	0.18	0.18

In total, it is estimated that 48 ± 8.2 (mean ± standard deviation) thousand tons of $PM_{2.5}$ are emitted by prescribed forest fires in Georgia during 2002. These emission estimates and their associated uncertainties are also compared with estimates using state-average fuel consumption and emission factors (Table 5-2, Figure 5-3). CO, PM_{10} and $PM_{2.5}$ emission estimates from EPA tend to be significantly overestimated, while VISTAS estimates reside within the 95% confidential interval. VOC and NO_X emissions estimates from both EPA and VISTAS are closely enough inside the 95% confidential interval of emissions estimates. Great discrepancies in various NH_3 and SO_2 emission estimates have been observed. This probably reflects current emission inventory status for all sources: better quality for ozone precursor (NO_X and VOC) emissions, fair quality for CO and PM emissions, and worse quality for NH_3 and SO_2 emissions, which is also consistent with the amount of effort that has been put into emissions inventory development. In addition, three EPA emission inventories and VISTAS inventory approach to the updated emission estimates in this study using more detailed data (e.g. physiographic region-specific fuel consumption and separate fuel consumption and emissions factors during flaming and smoldering) by the respective time for their development, though difference in the development methods is still large. For example, VISTAS used larger emission factors and smaller fuel consumption than the updated

emission estimates in this study. More field measurements are required for further improvements in emission inventory.

Table 5-10 Uncertainties in March and annual total emission estimates (10^3 tons) for Georgia or physiographic regions during 2002

		CO		VOC		NO_X		NH_3		SO_2		PM_{10}		$PM_{2.5}$	
		mean	cov	mean	cov	mean	cov	mean	cov	mean	cov	mean	cov	mean	cov
Annual															
	F	170	0.30	15	0.41	13	0.26	0.79	0.77	0.16	0.77	23	0.21	20	0.21
GA	S	330	0.29	30	0.39	3.2	0.56	1.5	0.66	0.32	0.66	33	0.25	28	0.25
	A	500	0.22	45	0.29	16	0.24	2.3	0.50	0.48	0.50	56	0.17	48	0.17
March															
	F	71	0.31	6.4	0.42	5.3	0.27	0.34	0.79	0.07	0.79	9.9	0.22	8.3	0.22
GA	S	140	0.29	13	0.40	1.3	0.57	0.65	0.67	0.14	0.67	14	0.26	12	0.26
	A	210	0.22	19	0.30	6.6	0.25	0.99	0.52	0.20	0.52	24	0.18	20	0.18
	F	0.27	0.44	0.024	0.53	0.02	0.40	0.0013	0.92	0.00027	0.92	0.038	0.37	0.032	0.37
Mountain	S	0.54	0.42	0.048	0.51	0.01	0.67	0.0025	0.77	0.00052	0.77	0.053	0.39	0.045	0.39
	A	0.82	0.32	0.073	0.39	0.03	0.35	0.0038	0.60	0.00079	0.60	0.091	0.28	0.077	0.28
	F	3.2	0.36	0.29	0.45	0.24	0.32	0.015	0.81	0.0031	0.82	0.45	0.28	0.38	0.28
Piedmont	S	6.4	0.35	0.57	0.45	0.06	0.61	0.029	0.71	0.0061	0.71	0.63	0.32	0.53	0.28
	A	9.7	0.26	0.86	0.33	0.3	0.29	0.045	0.54	0.0092	0.54	1.1	0.22	0.91	0.22
	F	28	0.33	2.5	0.43	2.1	0.29	0.14	0.81	0.028	0.81	3.9	0.24	3.3	0.24
Upper Coastal	S	55	0.32	4.9	0.43	0.52	0.60	0.25	0.71	0.052	0.71	5.4	0.28	4.6	0.28
	A	83	0.24	7.4	0.32	2.6	0.26	0.39	0.54	0.08	0.54	9.3	0.19	7.9	0.19
	F	39	0.32	3.5	0.43	2.9	0.28	0.18	0.80	0.038	0.80	5.4	0.23	4.6	0.23
Lower Coastal	S	77	0.31	6.9	0.42	0.74	0.60	0.36	0.72	0.074	0.72	7.6	0.27	6.4	0.27
	A	120	0.23	10	0.32	3.6	0.25	0.54	0.55	0.11	0.55	13	0.19	11	0.19

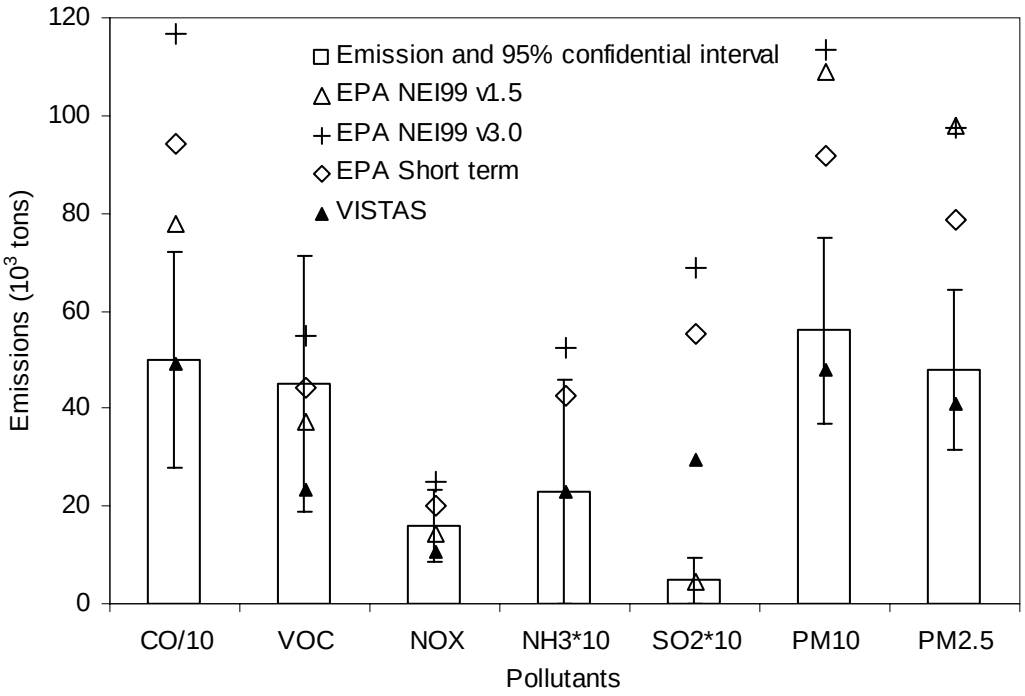

Figure 5-3 Total emissions of prescribed forest fires in Georgia during 2002 CO emission is divided by 10, and NH_3 and SO_2 emissions are multiplied by 10 for better visual effect. Error bars refer to 95% confidence interval.

Impact on air quality

Prescribed forest fires emissions concentrate on the southwest of GA, with peak emissions of 23.6 tons/day (tpd). These emissions have large local impact and significant impact in $PM_{2.5}$ non-attainment area (Figure 5-4), coinciding with elevated $PM_{2.5}$ concentrations. PM2.5 sensitivities refer to the difference between simulations with and without forest fire emissions. Specifically, prescribed forest fires contribute 7.7 $\mu g/m^3$ $PM_{2.5}$ to Georgia during March 2002, when $PM_{2.5}$ concentration is 19 $\mu g/m^3$. Their contributions within $PM_{2.5}$ non-attainment area are much smaller (2.1 $\mu g/m^3$) due to the long distance to emissions. It is kept same for Jefferson street (JST), an SEARCH station inside of central Atlanta. Meanwhile, 2.5 $\mu g/m^3$ $PM_{2.5}$ out of 12 $\mu g/m^3$ can be attributed to forest fire emissions at Okeefeenookee swamp (OKEF), an IMPROVE station located

in class I area. Therefore, air quality impact from prescribed forest fires should be addressed in effective air quality management.

$PM_{2.5}$ emissions are underestimated by 15% in the VISTAS forest fire emission inventory, roughly leading to underestimation of $PM_{2.5}$ by 1.1, 0.32, 0.30, and 0.38 $\mu g/m^3$ respectively for GA, non-attainment area, JST and OKEF, using the $PM_{2.5}$ sensitivities above. Since $PM_{2.5}$ caused by forest fire emissions are mainly determined by $PM_{2.5}$ emissions, the relation between $PM_{2.5}$ and emissions are more linear and can be used to directly interpolate $PM_{2.5}$ concentrations at different level of emissions. $PM_{2.5}$ using the EPA emission inventories is overestimated by at least 60%. Great care should be taken when using these emission inventories. Detailed uncertainty analysis reveals uncertainties in the updated forest fire emission inventory (18% for $PM_{2.5}$ as of cov), resulting in the uncertainties of $PM_{2.5}$ concentrations with 1.4 (3.7%), 0.39 (1.8%), 0.36 (2.4%), and 0.45 (7.3%) $\mu g/m^3$ respectively for GA, non-attainment area, JST and OKEF.

Table 5-11 Monthly average daily $PM_{2.5}$ concentrations ($\mu g/m^3$), their sensitivities to prescribed forest fires emissions ($\mu g/m^3$), and associated uncertainties during March 2002

	Concentrations	Sensitivity	Uncertainties (std)	Uncertainties (cov)
OKEF	12	2.5	0.45	0.037
JST	20	2.0	0.36	0.018
Non-attainment	16	2.1	0.39	0.024
GA	19	7.7	1.4	0.073

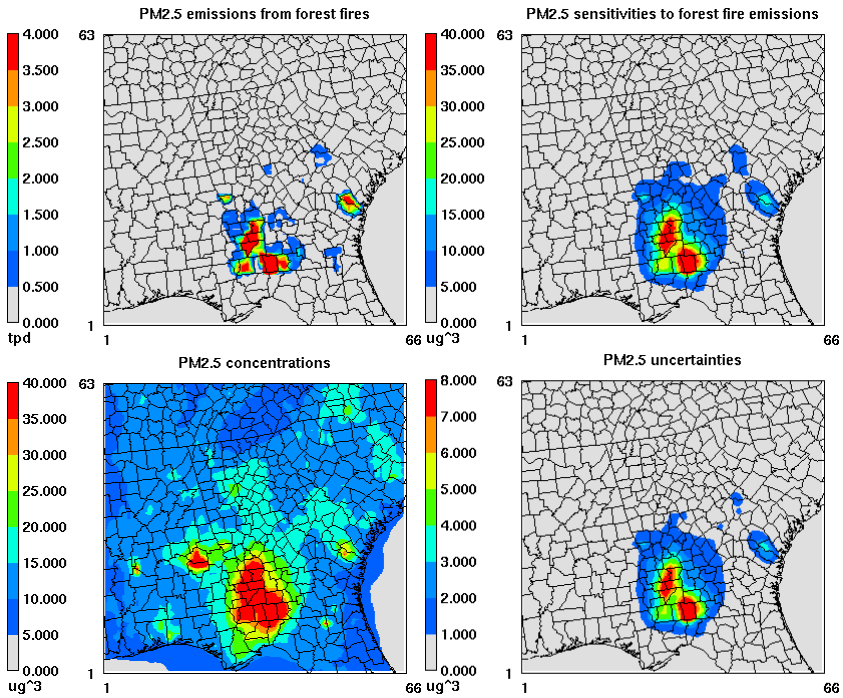

Figure 5-4 Monthly average daily $PM_{2.5}$ emissions from forest fires, concentrations, their sensitivities to prescribed forest fires emissions, and associated uncertainties as in standard deviation (μg/m^3) during March 2002

Conclusion

Various fire behavior models and methods have been used to estimate prescribed forest fire emissions and their associated uncertainties. Fuel consumption estimates vary from 4.2 to 11.8 tons/acre in Georgia, with the largest uncertainties in the mountain region. Emission factors during smoldering are larger than those during flaming, with similar uncertainties for both phases, except for NO_X. CO, PM_{10}, and $PM_{2.5}$ emissions factors are less uncertain than other pollutants. Emission strength is determined by both the size of fire and fuel consumption. Forest fires emissions in the mountain region are smaller than those in coastal area, while having large uncertainties. 58% of $PM_{2.5}$ emissions are emitted during smoldering, though only 38% of fuels are consumed during smoldering. Total emissions during both phases have smaller uncertainties than those associated emissions during each combustion phase. Uncertainties in total emissions for Georgia or by physiographic regions change with correlations between individual

estimates. In total, it is estimated that 48 ± 8.2 thousand tons of $PM_{2.5}$ are emitted by prescribed forest fires in Georgia during 2002. Monthly total emissions within Georgia peak in March, with same uncertainty factor (18% for $PM_{2.5}$ as cov). Estimates from the VISTAS emission inventory fall inside the 95% confidential interval of the updated emission estimates in this study, though different data and method are used. Prescribed forest fire emissions concentrate in the southwest of Georgia during March 2002, coinciding with the elevated $PM_{2.5}$ concentrations. These emissions contribute 7.7 $\mu g/m^3$ of $PM_{2.5}$ to Georgia and 2.1 $\mu g/m^3$ of $PM_{2.5}$ to non-attainment area. The uncertainties in prescribed forest fire emissions lead to 7.3% uncertainties (as cov) in simulated $PM_{2.5}$ concentrations within Georgia and 2.4% for non-attainment area. Even though uncertainties in fuel consumption and emissions factors are significantly large, the total uncertainties in air quality modeling results caused by forest fire emissions are small.

References

Anderson, G. K., Sandberg, D. V., and Norheim, R. A. (2004). "Fire Emission Production Simulator (FEPS) User's Guide v1.0."

Andreae, M. O., and Merlet, P. (2001). Emission of trace gases and aerosols from biomass burning. Global Biogeochemical Cycles 15, 955-966.

Barnard, W. R., and Brewer, P. (2004). Development of Managed Burning and Wildland Fire Emission Estiamtes for VISTAS. In "13th International Emission Inventory Conference "Working for Clean Air in Clearwater"", Clearwater, FL.

Battye, W., and Battye, R. (2002). "Development of Emissions Inventory Methods for Wildland Fires. Final Report prepared for U.S. EPA.." EC/R Incorporated, Research Triangle Park, NC.

Bertschi, I., Yokelson, R. J., Ward, D. E., Babbitt, R. E., Susott, R. A., Goode, J. G., and Hao, W. M. (2003). Trace gas and particle emissions from fires in large diameter and belowground biomass fuels. J. Geophys. Res. 108.

Brown, J. K., and Smith, J. K. (2000). "Wildland Fire in Ecosystems: Effects of Fire on Flora," Rep. No. General Technical Report RMRS-GTR-42-volume 2. United States Department of Agriculture, Forest Service, Rocky Mountain Research Station, Ogden, UT.

Carter, M. C., and Foster, C. D. (2004). Prescribed burning and productivity in southern pine forests: a review. Forest Ecology and Management 191, 93-109.

GCVTC (1996). "Recommendations for Improving Western Vistas." Grand Canyon Visibility Transport Commission, Western Governors' Association, Denver, CO.

GFC (2005). Mainly Burned Forest Types. Georgia Forestry Commission, Macon, GA.

Hardy, C. C., Ottmar, R. D., Peterson, J. L., Core, J. E., and Seamon, P. (2001). "SMOKE Management Guide for Prescribed and Wildland Fire: 2001 Edition," Rep. No. PMS 420-2. NFES 1279. . National Wildfire Coodination Group, Boise, ID.

Heinselman, M. L. (1978). "Fire in Wilderness ecosystems." USDA Forest Service, Misc. Pub. 1365.

Houyoux, M. R., Vukovich, J. M., Jr., C. J. W., Wheeler, N. J. M., and Kasibhatla, P. (2000). Emission inventory development and processing for the seasonal model for regional air quality. J. Geophys. Res. 105, 9079-9090.

Kendall, M. G. (1987). "Kendall's advanced theory of statistics," Oxford University Press, New York

Lee, S., Baumann, K., Schauer, J. J., Sheesley, R. J., Naeher, L. P., Blake, D. R., Edgerton, E. S., Russell, A. G., and Clements, M. (2005). Gaseous and Particulate Emissions from Prescribed Burning in Georgia. Environmental Science & Technology (submitted).

McNab, W. H., and Edwards, M. B. (1976). Estimating Forest Fuel Buildup. Forest Farmer 35, 6-7.

McNab, W. H., Edwards, M. B., and Hough, W. A. (1978). Estimating Fuel Weights in Slash Pine-Palmetto Stands. Forest Science 24, 345-358.

Morgan, M. G., and Henrion, M. (1990). "Uncertainty: A Guide to Dealing with Uncertainty in Quantitative Risk and Policy Analysis," Cambridge University Press.

NIFC (2005). Fire Statistics. pp. http://www.nifc.gov/stats/. Accessed in May 2005.

NWCG (1998). "Managing Wildland Fire: Balancing America's Natural Heritage and the Public Interest."

Ottmar, R. (2005). Fuel Characteristic Classification System.

Phuleria, H. C., Fine, P. M., Zhu, Y. F., and Sioutas, C. (2005). Air quality impacts of the October 2003 Southern California wildfires. Journal of Geophysical Research-Atmospheres 110.

Reinhardt, E. (2004). Using FOFEM 5.0 to Estimate Tree Motality, Fuel Consumption, Smoke Production and Soil Heating From Wildland Fire. http://fire.org/fofem/download/FOFEM5Using.pdf.

Sandberg, D., and Dost, F. N. (1990). "Effects of Prescribed Fire on Air Quality and Human Health," Oregon State Universtiy Press.

Sandberg, D., Ottmar, R., Peterson, J., and Core, J. (2002). "Wildland Fire in Ecosystems: Effects of Fire on Air," Rep. No. General Technical Report RMRS-GTR-42-volume 5. United States Department of Agriculture, Forest Service, Rocky Mountain Research Station, Ogden, UT.

Sapkota, A., Symons, J. M., Kleissl, J., Wang, L., Parlange, M. B., Ondov, J., Breysse, P. N., Diette, G. B., Eggleston, P. A., and Buckley, T. J. (2005). Impact of the 2002 Canadian forest fires on particulate matter air quality in Baltimore City. Environmental Science & Technology 39, 24-32.

Schoch, P., and Binkley, D. (1986). Prescribed Burning Increased Availability in a Mature Loblolly Pine Stand. Forest Ecology and Management 14, 13-22.

Tian, D., Hu, Y., Wang, Y., and Russell, A. (2006). Impacts of Biomass Burning Emissions on Ambient PM2.5 in the Southeastern United States using CMAQ. In preparation.

USEPA (1998). Interim Air Quality Policy on Wildland and Prescribed Fires.

USEPA (2002). "National Emissions Inventory Version 1.5 Criteria Air Pollutant Methodologies for Miscellaneous Area Sources." U.S. Environmental Protection Agency.

USEPA (2003a). "Ducumentation for the Final 1999 National Emissions Inventory (Version 3.0) for Criteria Air Pollutants and Ammonia." U.S. Environmental Protection Agency.

USEPA (2003b). "Date Needs and Availability for Wildland Fire Emission Inventories - Short-term Improvements to the Wildland Fire Component of the National Emission Inventory." U.S. Environmental Protection Agency, Research Triangle Park, NC.

USFS (1976). "Southern Forestry Smoke Management Guidebook by Southern Forest Fire Laboratory Staff," Rep. No. General Technical Report SE-10. United States Department of Agriculture, Forest Service, Southeast Forest Experiment Station, Asheville, N.C.

Ward, D. E., Peterson, J., and Hao, W. M. (1993). An inventory of particulate matter and air toxic emissions from prescribed fires in the USA for 1989. In "Air and Waste Management Association's 86th Annual Meeting and Exposition". Air and Waste Management Association, Denver, Colorado, USA.

CHAPTER 6 CONCLUSION

Major Findings

Uncertainties in simulated ozone concentrations and emission control responses caused by emission uncertainties

Impacts of emission inventory uncertainties on ozone formation and emission control response using future year 2007 emissions with three historical meteorological conditions have been estimated using high-order sensitivities calculated by CMAQ-HDDM-3D. Large emission inventory uncertainties, e.g. a factor of 2 for all emissions except a factor of 1.5 for of stationary point NO_X emission, lead to less than 10% uncertainties (as cov) in ozone concentrations.

Elevated ozone concentrations in Atlanta are impacted by NO_X emissions from Atlanta mobile sources, point sources inside and outside Atlanta, and Atlanta anthropogenic VOC emissions in a decreasing order, with anthropogenic VOC emissions having their primary impacts in the downtown Atlanta area. Linear regression analysis indicates a strong positive correlation between ozone concentrations with source contributions from Atlanta mobile NO_X emissions and anthropogenic VOC emissions. Correlations between ozone concentrations and point NO_X emissions vary significantly from year to year and the responses decrease with increasing ozone concentrations. Uncertainties in Atlanta mobile NO_X emissions have the largest impact on uncertainties in ozone concentrations, with similar impacts of uncertainties in emissions from other source categories at a smaller scale. A large variance in the impacts of emission inventory uncertainties is found within an episode, while the variance between episodes is small.

Modeling uncertainty analysis indicates that reducing NO_X emissions from Atlanta mobile sources provides the greatest response using the nominal values, followed

by reducing point NO_X emissions inside and outside of Atlanta and Atlanta anthropogenic VOC emissions. Mean emission control responses after consideration of emission inventory uncertainties, indicate similar rankings. Uncertainties in emissions from Atlanta mobile sources suggest that negative emission control responses, i.e. ozone concentrations increase with emission reduction are possible. Better understanding of emissions in Atlanta is required for a reliable control strategy development for Atlanta area.

Policy-making based on air quality modeling requires understanding impacts of emission inventory uncertainties on such modeling. In addition, methods proposed in this paper greatly reduce the computational cost for similar uncertainty analyses, which requires running air quality models hundreds of times, if not more. Such methods can also be applied to other modeling systems, when high-order sensitivities are available.

Uncertainties in biomass burning emissions and seasonal $PM_{2.5}$ source contributions from biomass burning

Total and speciated $PM_{2.5}$ are simulated for January, March, May and July 2002 over the southeastern US. Impacts of uncertainties in emissions, including total amount, temporal and spatial characteristics, and speciation on air quality modeling during January are investigated. Though model performance evaluated by observations is similar with different emission inventories, significant different spatial distributions of $PM_{2.5}$ emissions and resulted $PM_{2.5}$ concentrations have been observed. Simulations with updated speciation profiles lead to increased POA and decreased EC emissions and concentrations. Model performance for EC is improved, along with deteriorated OM performance. Estimated source contributions are further compared with CMB results, suggesting a 90% reduction of emissions from wood burning in fireplaces and woodstoves.

About 83% of $PM_{2.5}$ caused by biomass burning is POA and EC, and the rest is secondary in origin (e.g. SOA, NH_4^+ and NO_3^-). SOA formed from biomass burning emissions is mainly due to a shift in the gas-aerosol phase partitioning from increased POA emissions. Both primary and secondary impacts are limited to areas in close proximity of emissions. Seasonal source contributions from biomass burning using the updated emissions have large temporal and spatial variations, higher in winter (January) and spring (March), and lower in summer (May and July).

Biomass burning influences much of the modeling domain and peaks in the southwestern Georgia (a more rural area). Prescribed burning is has the largest air quality impacts among biomass burning sources, peaking in March and the southwestern Georgia. Overall impacts from wildfires are much smaller in spite of a sever local impact and peak in May. Emissions from other biomass burning have significant air quality impacts during January and March at much smaller magnitudes, and negligible impacts during May and July. In the Atlanta $PM_{2.5}$ non-attainment area prescribed burning is always the largest biomass burning source, followed by land clearing and wood burning in fireplaces and woodstoves.

Air quality impacts from forest fires under different forest management practices

Air quality impacts from forest fires when employing different forest management practices, including changing burning season and fire-return intervals (FRIs), and controlling emissions during smoldering, are investigated using source-oriented air quality modeling. The identical forest fire emissions lead to different air quality impacts when released in different seasons, with 2.0 $\mu g/m^3$ of $PM_{2.5}$ in January, 1.9 $\mu g/m^3$ in March 1.3 $\mu g/m^3$ in May and 0.9 $\mu g/m^3$ in July for the Atlanta $PM_{2.5}$ non-attainment area. The reduced impacts in summer is due to stronger removal processes and greater ventilation in the summer period. Such emissions can also cause violating the posposed future daily $PM_{2.5}$ standard (35 $\mu g/m^3$) when emitted during January. On the other hand,

the impacts on daily maximum 8-hr O_3 averaged within a month are highest in July, followed by May, March and January, consistent with the order of O_3 formation potentials between seasons. However, these forest fire emissions cause the highest increase in peak O_3 concentrations in May, with 2.5 ppbv for Atlanta area. Slightly negative O_3 source contributions from forest fire emissions in January have also been found.

Fuel consumptions ($F_a s$) with 2-, 3-, 4- and 5-year FRIs are respectively 2.9, 3.8, 4.3, and 5.0 tons/acre. Therefore, emissions from an individual forest fire with a 5-year FRI are approximately 72% larger than those with a 2-year FRI. For forest fires in Georgia, however, average annual emissions with a 5-year FRI are 32% less than those if a 2-year FRI is employed as less forest area is burned each year.

The calculated fraction of emissions coming from smoldering depends on the approach used. If time periods for smoldering are used, 30% of the burn emissions come from smoldering. Alternatively, if separate $F_a s$ and emission factors are used, 55% is calculated to be from the smoldering stage. This has significantly consequences on the predicted air quality impacts. The emission fraction of 30% during the smoldering contributes 53% of $PM_{2.5}$ source contributions from forest fires for the Atlanta $PM_{2.5}$ non-attainment area, while the emission fraction of 55% leading to 76% of $PM_{2.5}$ source contributions. A larger fraction of emissions during the smoldering stage also cause increased total $PM_{2.5}$ source contributions from forest fires in spite of the same amount of total $PM_{2.5}$ emissions, with 1.8 µg/m3 more $PM_{2.5}$ for the entire Georgia and 0.6 µg/m3 for the Atlanta $PM_{2.5}$ non-attainment area. It is likely due to the fact that daytime flaming emissions disperse more effectively than those during smoldering. In addition, emissions during flaming possibly impact a more distant area, while emissions during smoldering impact more locally.

Understanding air quality impacts from forest fires using different forest management practices is important for effective air quality and ecosystem management. Such information also illustrates potential uncertainties in current air quality modeling, which neglects the impacts from different forest management practices. Air quality impacts from other forest management practices can also be investigated using the methods proposed in this paper.

Uncertainties in prescribed forest fire emission inventories

Various fire behavior models and methods have been used to estimate prescribed forest fire emissions and their associated uncertainties. Fuel consumption estimates vary from 4.2 to 11.8 tons/acre in Georgia, with the largest uncertainties in the mountain region. Emission factors during smoldering are larger than those during flaming, with similar uncertainties for both phases, except for NO_X. CO, PM_{10}, and $PM_{2.5}$ emissions factors are less uncertain than other pollutants. Emission strength is determined by both the size of fire and fuel consumption. Forest fires emissions in the mountain region are smaller than those in coastal area, while having large uncertainties. 58% of $PM_{2.5}$ emissions are emitted during smoldering, though only 38% of fuels are consumed during smoldering. Total emissions during both phases have smaller uncertainties than those associated emissions during each combustion phase. Uncertainties in total emissions for GA or by physiographic regions change with correlations between individual estimates. In total, it is estimated that 48 ± 8.2 thousand tons of $PM_{2.5}$ are emitted by prescribed forest fires in Georgia during 2002. Monthly total emissions within GA peak in March, with same uncertainty factor (18% for $PM_{2.5}$ as cov). Estimates from the VISTAS emission inventory fall inside the 95% confidential interval of the updated emission estimates in this study, though different data and method are used. Prescribed forest fire emissions concentrate in the southwest of GA during March 2002, coinciding with the elevated $PM_{2.5}$ concentrations. These emissions contribute 7.7 $\mu g/m^3$ of $PM_{2.5}$ to GA and

2.1 μg/m^3 of $PM_{2.5}$ to non-attainment area. The uncertainties in prescribed forest fire emissions lead to 7.3% uncertainties (as cov) in simulated $PM_{2.5}$ concentrations within GA and 2.4% for non-attainment area. The uncertainties caused by forest fire emissions are small, though uncertainties in fuel consumption and emissions factors are significantly large.

Integration of different chapters

Each chapter in this dissertation has focused on different perspectives of impacts of emission uncertainties on air quality modeling results. Chapter 2 evaluates how uncertainties in emissions from different regions and source categories affect ozone simulations and ozone responses of various emission controls. It is a top-down evaluation and its results identify the emission sources with the largest impacts on air quality modeling. Chapters 3 to 5 are bottom-up evaluations, concentrating on how uncertainties in emissions from biomass burning impact air quality modeling. Improving biomass burning emissions used in current air quality modeling shows how better understanding of such emissions impact on air quality modeling (shown in Chapter 3). In addition, emissions from forest fires are also impacted by different human activities and should be addressed in air quality modeling (shown in Chapter 4). However, no matter how emission inputs are improved, uncertainties in emissions will always exist. Such uncertainties should be quantified to evaluate their impacts on air quality modeling (shown in Chapter 5). All in all, this dissertation shows how to systematically address the impacts of emission uncertainties on air quality modeling. The order of the four chapters also indicates the requirements from practice. Since there are so many interested emission sources at the same time, a top-down method should always be first used to prioritize detailed research addressing different source categories. For the specific source selected, emissions should then be improved using state-of-the-art science. Finally, remaining

uncertainties should be quantified for the future analysis using the top-down method, forming a circle to improve the emissions and respectively air quality modeling results.

Recommendation for Future Research

Application of the simplified ozone air quality model to data assimilation

Data assimilation adjusts emission inputs according to the differences between simulated and observed concentrations using sensitivity coefficients. However, sensitivity coefficients in a non-linear system are not constant and multiple iterations are usually required to obtain a convergence in data assimilation. Instead of running the original air quality models multiple times, model concentrations and sensitivities in different iterations can be updated using the simplified ozone air quality model based on high-order sensitivity coefficients (as in Chapter 2). This method can greatly reduce the computational time required to iterate to an approximate solution, followed by final tuning using a final application of the air quality model.

Improvement of emission inventories for wood burning in fireplaces and woodstoves.

Though the amount of emissions from wood burning in fireplaces and woodstoves is much less than the other biomass burning emissions, such emissions from fireplaces and woodstoves have the largest impacts on ambient $PM_{2.5}$ among all biomass burning sources in the Atlanta $PM_{2.5}$ non-attainment area according to currently available emission inventories. It is likely due to that numbers of single family homes are usually used to spatially allocate the total emissions at a national level. The allocation method ignores the difference of living habits in different regions and tends to overestimate $PM_{2.5}$ emissions in the urban area. Such emissions appear to lead to overestimated $PM_{2.5}$

concentrations during heating seasons in the Atlanta $PM_{2.5}$ non-attainment area as shown through source apportionment assessment in Chapter 3. It is likely a fact for other $PM_{2.5}$ non-attainment areas due to the same estimation method used. Since air quality impacts from such emissions are limited to an area in close proximity of emissions, a survey of wood consumption for fireplaces and woodstoves in selected counties is recommended. It is better that there are observation stations in these counties. Such observational data can be used to assess the improved emission inventories for wood burning in fireplaces and woodstoves and corresponding simulations from air quality modeling. In cases without available observational data, a short-term field measurement campaign is recommended.

Uncertainty analysis of emissions from other primary organic matter (OM) sources and their impacts on secondary organic aerosols (SOA) simulations

Underestimation of OM is common in the current CMAQ model, and it is widely regarded as a result of underestimation of SOA formation. SOA underestimation is usually attributed to a low aerosol yield or missing aerosol precursor emissions. However, results in chapter 3 indicate that large impacts of primary OM may be missed and there is a likely underestimation of primary OM due to the low primary OM fractions used in current speciation methods. In addition, larger primary OM can also lead to larger SOA formation by changing the gas-particle phase equilibrium.

A preliminary sensitivity test by increasing current primary OM emissions by 50% is suggested for a summer episode, when OM underestimation in the current CMAQ model is significant. These results indicate how both primary and secondary OM changes with primary OM emissions. Increased primary and secondary OM concentrations are expected for the simulations. Furthermore, major sources for primary OM emissions should be identified for the desired regions based on current emission inventories, and then their primary OM fractions should be updated according to the most recent measurement results.

Biomass burning in other regions

Biomass burning emissions in different regions have different air quality impacts due to different types of biomass fuel burned, fuel and meteorological conditions. Different ecosystems might not share the same dependences on fires, which are further complicated by human activities. For example, prescribed forest fires are rarely used in remote areas. Compared with prescribed forest fires, difference between wildfires is even larger and thus respective air quality impacts should be individually quantified with consideration of exact locations and time, fuel and meteorological conditions for a wildfire. Wildfires in the western US are of particular interest since both their occurrence and extent has increased recently. In addition, recent studies have shown that wildfires are exacerbated by climate change. Current air quality managements assume wildfires and most prescribed fires as natural processes and thus no emission controls are required. However, air quality impacts from burning during different seasons and frequencies are different. Such impacts also change with application of various smoke control techniques. Policies are wanted to address all these issues.

Uncertainty analysis of emissions of different pollutants from different source categories

Major source categories, whose emission uncertainties have large impacts on air quality modeling uncertainties, should be identified through detailed uncertainty analysis (e.g. the method proposed in Chapter 2). Different sources can be addressed for different pollutants. For example, biomass burning is a major source for $PM_{2.5}$. However, it appears to be only a significant, but not major contributor to O_3 fromation. For major sources, both different measurement methods and emission models should be employed. Advancement in measurement technologies, including satellite, aircraft and ambient

measurements, will improve future understanding of emission characteristics and their associated uncertainties.

Specifically, Atlanta mobile emissions are the largest contributor to ozone non-attainment in Atlanta area and recommended for further investigation. Uncertainties in such emissions can lead to negative benefits of emission reduction calculated using CMAQ (shown in Chapter 2). These uncertainties are large and hard to quantify due to the complex emission processes. Evaluation of uncertainties in emissions estimated by Mobile 6 is suggested, as well as different measurement methods such as mobile laboratories, onboard sensors, roadway tunnel, and road-side measurements. Discrepancies in estimates by different methods provide additional insights in emission uncertainties.

Closing remarks

In summary, this thesis has provided important insights regarding emission uncertainties and their impacts on air quality modeling. Its findings can be directly used to improve current air quality modeling. They can also guide future research and efforts to reduce the impacts from emission uncertainties. Methods developed and employed in this thesis can be applied to other sources, regions, and episodes. However, there is still much to be done to improve the performance of air quality modeling. Such work is a foundation for development of efficient and effective control strategies and policy-making.